1993

Connexin Trafficking And The Control Of Gap Junction Assembly In The Mouse Preimplantation Embryo

Sousa Paul De

CONNEXIN TRAFFICKING AND THE CONTROL OF GAP JUNCTION ASSEMBLY IN THE MOUSE PREIMPLANTATION EMBRYO

by

Paul A. De Sousa

Department of Zoology

Submitted in partial fulfilment
of the requirements for the degree of
Doctor of Philosophy

Faculty of Graduate Studies
The University of Western Ontario
London, Ontario
July, 1993

ISBN 0-315-83929-5

Abstract

Gap junction assembly in the preimplantation mouse embryo is a temporally regulated event, beginning a few hours after the third cleavage during the morphogenetic event known as compaction. The purpose of the present study was to determine which connexins contribute to gap junctions in the preimplantation mouse embryo and how their assembly into gap junctions at compaction is regulated. Using antibodies raised against different synthetic C-terminal peptides of connexin43 (Cx43), this protein was shown to assemble into gap junction-like plaques beginning with compaction. Prior to this time no Cx43 can be detected in the plasma membrane. Cell fractionation and reverse transcription-polymerase chain reaction (RT-PCR) were employed to show that Cx43 mRNA is in polyribosomes at the 4-cell stage, suggesting that synthesis of Cx43 begins at least one cell cycle in advance of when gap junctions first form. The fate of nascent Cx43 was followed throughout preimplantation development by means of immunofluorescence in conjunction with confocal laser scanning microscopy. In morulae and blastocysts Cx43 becomes differentially distributed in the apposed plasma membranes: a zonular distribution predominates between outside blastomeres and trophectoderm cells whereas plaque-like localizations predominate between inside blastomeres and cells of the inner cell mass. The cytoplasmic immunoreactivity in morulae was deemed to be nascent connexin *en route* to the plasma membrane since it could be abolished by treatment with cycloheximide, and redistributed by treatment with monensin or brefeldin-A, known inhibitors of

protein trafficking. These latter two drugs were shown to cause specific alterations in the structure and distribution of a variety of organelles in morulae, especially those involved in protein trafficking and degradation.

No conclusive evidence for the contribution of connexin32 (Cx32) to gap junctions in morulae could be found. However, using immunogold electron microscopy, the contribution of Cx43 was confirmed. Cx43 was also found to contribute to gap junctions in cumulus-oocyte complexes (COCs), both between cumulus granulosa cells and these cells and the oocyte. Although 100% of gap junctions between cumulus cells were labeled with Cx43 specific antisera, over 30% of gap junctions in morulae were not. Thus other members of the connexin gene family may yet be found to contribute to gap junctions at this stage. Treatment of uncompacted 8-cell embryos with either monensin or brefeldin-A inhibited the appearance of gap junction-like structures containing Cx43 and the onset of gap junctional coupling in a reversible manner. These data demonstrate that the onset of gap junction assembly during compaction is regulated post-translationally and involves mobilization of connexin43 and possibly other members of the connexin gene family through trafficking organelles to plasma membranes.

Acknowledgements

This thesis would not be complete without acknowledging the influence and support of several people who contributed to the development of the person that I am today, and who have made the journey worthwhile. First and foremost I wish to thank my parents, Antonio and Maria De Sousa, whose Love and encouragement instilled in me a desire to explore my potential and become the most that I could be. Whatever successes or failures await me in the future, you have taught me that it is only through the act of trying that we grow as individuals. To my wife Dina, I will always be grateful for your Love and perseverance, and for reminding me that it is possible to enjoy a life outside of work. I also thank you for enriching my life with Christopher.

To my advisor Gerry Kidder, I will always look fondly on the time spent in your lab. Your enthusiasm, clearness of thought, and devotedness to truth were exemplary and often inspiring. You are a true scholar Gerry, and I will always be proud of what we accomplished together and the scientific values you have instilled me with.

During my time here it has been my good fortune to work with many good people, whose spirit and thoughtfulness have touched my life. This includes Andy Watson, Gunnar Valdimarsson, Daniel Macphee, Cindy Pape, Dagaung Zhu and Ying Zhu. My years at Western have been filled with a strong sense of belonging and

community. For that I must thank all the staff, faculty and students whose friendships have made the years so enjoyable. I am especially grateful to Richard Harris, Ian Craig, Ron Smith, Harry Leung, Mary Martin, Jane Sexsmith, and Drs. Stan Caveney and Richard Shivers for their assistance and guidance over the years. To all of you, I wish you every success in the future and I sincerely hope our paths cross again.

Table of Contents

List of Figures

List of Tables

List of Abbreviations

BFA	.....	Brefeldin-A
cDNA	.....	Copy DNA
CHX	.....	Cycloheximide
COC	.....	Cumulus-oocyte complex
Cx	.....	Connexin
FM	.....	Flushing medium
hCG	.....	Human chorionic gonadotropin
hr	.....	Hour/hours
ICM	.....	Inner cell mass
min	.....	Minute/minutes
mRNA	.....	Messenger RNA
PCR	.....	Polymerase chain reaction
PMSF	.....	Pregnant mare's serum gonadotropin
RT-PCR	.....	Reverse transcription-PCR
sec	.....	Second/seconds
TE	.....	Trophectoderm

Chapter 1

Introduction

1.1 Intercellular communication via gap junctions.

Gap junctions are aggregations of aqueous intramembranous channels, which connect the cytoplasm of adjacent cells by permitting the direct passage of small, water soluble molecules up to 1000 Daltons in size (Schwarzmann *et al.*, 1981). Although most protein and nucleic acids are excluded, gap junctions are permeant to the cytoplasmic pool of ions and second messengers (Lawrence *et al.*, 1978; Saez *et al.*, 1989), and many small metabolites including nucleotides, sugars, glycolytic substrates, amino acids and small peptides (Subak-Sharpe *et al.*, 1969; Rieske *et al.*, 1975; Kohen *et al.*, 1979; Johnson and Sheridan, 1971; Simpson *et al.*, 1977). As a result, gap junctions permit electrotonic and metabolic coupling between adjacent cells, as well as synchronization of cellular behaviour (Gilula *et al.*, 1972; Fishman, 1992).

Due to the broad range of molecules which may traverse gap junction channels, these structures have been implicated in numerous cell processes. In electrically excitable tissues, such as neurons, smooth muscle, and cardiac myocytes, gap junctions have been shown to allow direct transmission of action potentials (Furshpan and Potter, 1959; Garfield *et al.*, 1977; Fishman, 1992). Gap junctions are also generally believed to play a role in the regulation of cell growth. The

uncontrolled growth of many cancer cell lines is correlated with a reduced capacity for intercellular communication (Loewenstein, 1981). Similarly, cultured tumor cells treated with growth-reducing agents show reappearance of gap junctions and intercellular communication (Flagg-Newton *et al.*, 1981). A strong direct link between gap junctional communication and growth regulation has also been shown recently, by studies involving the transfection of communication-deficient tumor cell lines with cDNA for the protein subunits of gap junctions. In these studies, the resulting increase in gap junctional communication is accompanied by reduced cellular proliferation (Zhu *et al.*, 1991, 1992; Eghbali *et al.*, 1990; Naus *et al.*, 1992)

During development, regulation of intercellular communication across gap junctions is believed to play a role in the creation of developmental fields or compartments which function semiautonomously and give rise to different structures (Caveney, 1985). This is exemplified in the mouse where after implantation there is no gap junctional communication between regions of the embryo derived from the inner cell mass (embryonic compartment) and those from the trophectoderm lineage (extraembryonic compartment; Kalimi and Lo, 1988; 1989). Furthermore, within the inner cell mass-derived embryonic compartment, gap junctional communication is further subdivided between germ layers (Kalimi and Lo; 1988). Gap junctions have also been reported in communication compartments in the development of the mouse limb bud (Laird *et al.*, 1992), the imaginal disc of *Drosophila* (Weir and Lo, 1984), and in the postembryonic epidermis of insects (reviewed by Caveney, 1985).

Communication via gap junctions is also believed to play a developmental role in mediating the direct exchange of morphogenetic signals. In amphibian development, injection of antibodies against gap junction proteins into a presumptive dorsal cell of an 8-cell embryo, reduces intercellular communication between the progeny of that cell and results in tadpoles with misplaced or even absent structures (*e.g.* eye, forebrain; Warner *et al.*, 1984). These same antibodies have been reported to interfere with morphogenetic signals involved in the patterning of the *Hydra* and the chick limb bud. In tissue grafting experiments in *Hydra*, blockage of gap junctional communication in the donor tissue interfered with the ability of the host tissue to suppress duplication of body structures in the graft (Fraser *et al.*, 1987). In the developing limb bud, pattern formation along the anteroposterior axis is influenced by a posterior margin of mesenchyme known as the polarizing region (Saunders and Gasseling, 1968). This tissue is believed to produce a morphogen, possibly retinoic acid, which specifies digit character by its local concentration (Tickle *et al.*, 1982). In grafting experiments, simultaneous blockage of gap junctional communication within donor polarizing regions and host anterior mesenchyme, decreased the ability of the former to induce digit specification (Allen *et al.*, 1990).

1.2 Gap junction structure.

Initially, gap junctions were characterized by their appearance in thin-section electron micrographs as a pair of membranes of variable area separated by a 2-nm "gap" (Robertson, 1963; Revel and Karnovsky, 1967). Analysis of freeze fracture

replicas, revealed that these structures consisted of dense plaque-shaped aggregations of intramembranous particles (Goodenough and Revel, 1970). With the molecular characterization of the subunit components of gap junctions, a generally accepted terminology has also been developed (Caspar *et al.*, 1977; Makowski *et al.*, 1977; Fig. 1.1). Gap junction channels in each cell are referred to individually as connexons. Connexons in one membrane join with connexons in the membrane of an adjacent cell to form a functional channel. Connexons consist of a hexamer of integral membrane proteins termed connexins, which constitute a large multigene family of highly related proteins. Connexins are commonly identified according to their molecular mass as predicted from their cDNA (Beyer *et al.*, 1987). Thus, connexin26 (Cx26) is 26 kD, connexin31 (Cx31) is 31 kD (etc.). A second, Greek nomenclature, emphasizing genetic origin and both nucleotide and amino acid sequence similarities, has also been introduced (Risek *et al.*, 1990). According to this nomenclature, connexins have been subdivided into 2 groups, α and ß, based on their similarity to two of the originally identified connexins, Cx43 and Cx32, respectively (Risek *et al.*, 1990; Haefliger *et al.*, 1992). This alternative nomenclature has been largely overlooked, except by its original proponents.

To date at least twelve members of the connexin gene family have been identified in mice, although when this study was first begun only four were known, these being Cx26, 32, 43, and 46. The first connexin to be identified was Cx32, whose cDNA was isolated from a rat liver expression library using an antibody raised against isolated junctions (Paul, 1986). Screening of a cDNA library by hybridization

at low stringency led to identification of two additional distinct cDNAs; from rat heart, Cx43, and lens, Cx46 (Beyer *et al.*, 1987, 1989; Paul *et al.*, 1991). Shortly after this, cDNA encoding Cx26 was found with an oligonucleotide probe based on the partial sequence of a second presumptive gap junction protein, isolated from hepatocytes (Nicholson *et al.*, 1987; Zhang and Nicholson, 1989). In recent years, an additional eight novel members of the connexin gene family have been reported, predominantly in the rat and mouse. These include Cx30.3, 31, 31.1, 33, 37, 40, 45, and 50 (Hennemann, Dahl, and Willecke, unpublished; Hoh *et al.*, 1991; Hennemann *et al.*, 1992a,b; Haefliger *et al.*, 1992; Willecke *et al.*, 1991a,b; Beyer *et al.*, 1992; White *et al.*, 1992). Novel connexins have also been identified in other vertebrates, including Cx30 and 38 in *Xenopus* (Gimlich *et al.*, 1988; Ebihara *et al.*, 1989), and Cx42 in the chick, which also expresses the avian homolog to Cx45 (Beyer, 1990).

Hydropathy analysis in conjunction with epitope mapping experiments performed on crude membrane preparations containing isolated gap junctions has shown the various connexins to possess similar structural features. All members of the connexin family possess four transmembrane, two extracellular, and three cytoplasmic domains (Fig. 1.1). The extracellular, transmembrane, and N-terminal cytoplasmic domains are highly conserved among different members of the family, whereas the middle and C-terminal cytoplasmic domains are variable in both size and sequence (reviewed in Bennett *et al.*, 1991; Willecke *et al.*, 1991a).

Figure 1.1. A model depicting gap junction structure and the membrane topology of the connexins. Gap junctions consist of aggregations of intramembranous channels, termed connexons, which pair with connexons in an adjacent membrane to form functional channels. Each connexon is composed of a hexamer of integral membrane proteins termed connexins. Members of the connexin gene family generally are believed to possess four transmembrane, two extracellular, and two cytoplasmic domains. Both the amino- (NH_2) and carboxy- (COOH) terminal ends of connexin proteins lie on the cytoplasmic side of the unit membrane.

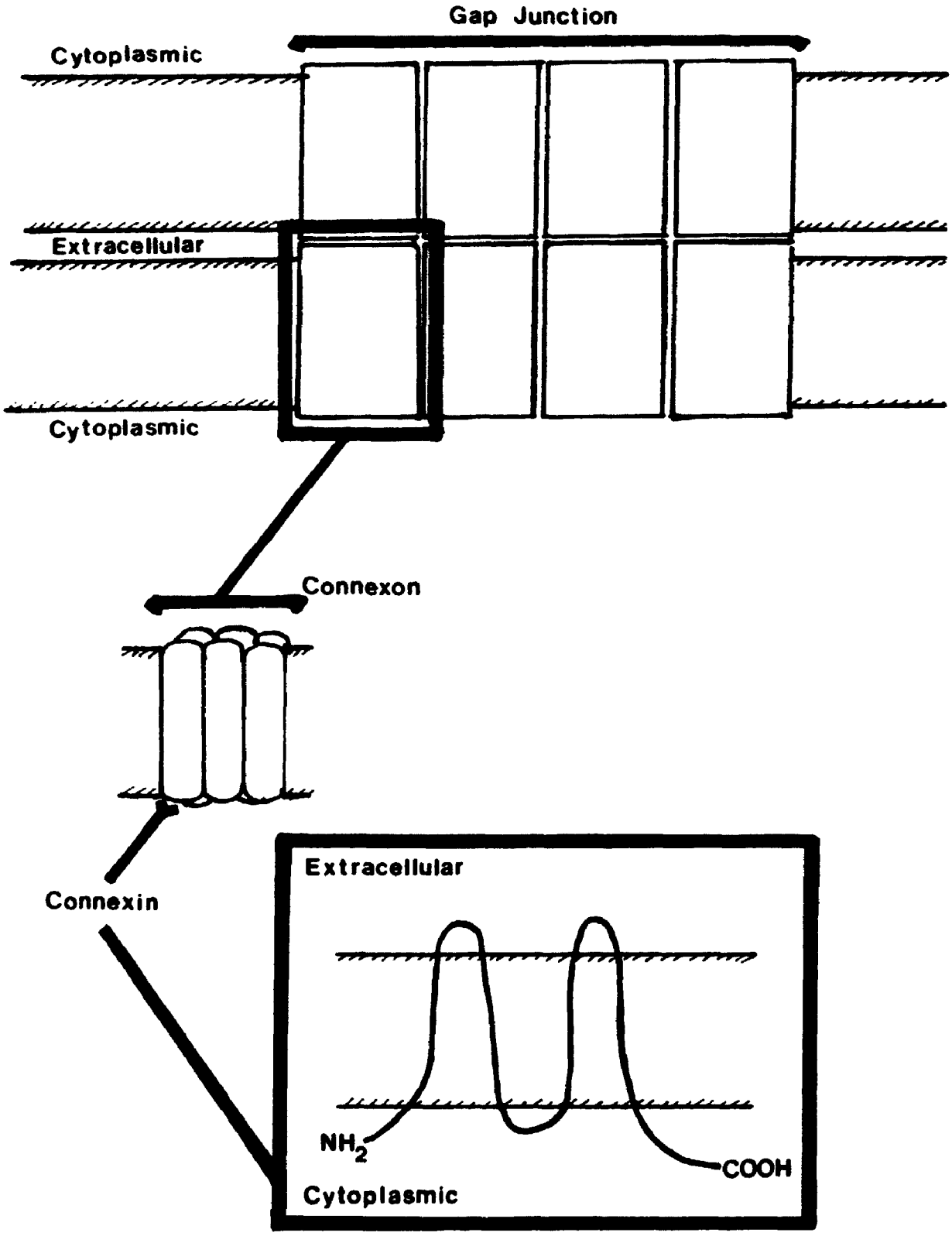
Gap Junction
Cytoplasmic
Extracellular
Cytoplasmic
Connexon
Connexin
Extracellular
NH2
COOH
Cytoplasmic

In both adult and embryonic tissues, connexins are expressed in overlapping patterns with specific connexins exhibiting either relatively broad (Cx43; found in heart, brain, kidney, ovary, testes,) or highly restricted (Cx31; found in skin) distributions (Haefliger *et al.*, 1992). An individual cell may also locate two connexins in the same junctional plaque (Cx32/26 in hepatocytes; Nicholson *et al.*, 1987; Traub *et al.*, 1989; Cx43/26 in decidual cells adjacent to an invading trophoblast; Winterhager *et al.*, 1993). Connexins also display varying abilities to interact with one another. Cx43, for example, has been shown to form heterotypic channels with some (Cx32) but not all (Cx40) members of the connexin gene family (Swenson *et al.*, 1989; Bruzzone *et al.*, 1992). Selectivity among connexins may represent the molecular mechanism underlying the establishment of "communication compartments", where cells communicate within, but not between, groups. These compartments, which are present in both developing and adult organisms (Kalimi and Lo, 1988; Laird *et al.*, 1992; Chanson *et al.*, 1991), could result from the inability of different connexins to interact functionally. To date however, the biological significance of both overlapping patterns of connexin expression and their differential capacities to interact with one another, remains largely unknown.

1.3 Modulation of gap junctional communication.

Modulation of intercellular communication via gap junctions may be achieved by one or both, of two mechanisms: the first by gating of existing channels, and the second, by the regulation of gap junction formation and disassembly. Given the focus

of the present study on the latter, the former will be reviewed only briefly. Two factors commonly cited for their ability to modulate gap junction channel permeability are Ca^{2+}, and H^+ ions (Spray *et al.*, 1982). Elevated concentrations of both have been found to reduce channel permeability, and there is evidence that this effect is mediated through the direct physical interaction of the Ca^{2+}-modulating protein calmodulin with either gap junctions or connexins (Peracchia, 1989; Zimmer *et al.*, 1987). Phosphorylation of connexins has also been implicated in both the up- and down-regulation of channel permeability. For example, in hepatocytes, gap junctional communication can be increased by treatment with cAMP, or decreased by treatment with tumor promoting phorbol esters or diacylglycerol, both of which activate protein kinase C (reviewed by Murray and Gainer, 1989). These divergent effects on gap junctional communication are believed to be mediated by the phosphorylation of unique serine and/or threonine residues on Cx32 (Saez *et al.*, 1990). Gap junction permeability is also known to be regulated through the direct activity of the tyrosine-specific protein kinase $p60^{v\text{-}src}$, or its corresponding cellular proto-oncogene product $p60^{c\text{-}src}$ (Atkinson *et al.*, 1981; Azarnia *et al.*, 1988). Cx43 is a substrate for $p60^{v\text{-}src}$, and phosphorylation of tyrosine residue 265 by this kinase abolishes Cx43-induced intercellular coupling between paired *Xenopus* oocytes (Swenson *et al.*, 1990). However, gap junctional communication may also be disrupted indirectly by activation of other tyrosine kinases. In a rat liver epithelial cell line, ligand induced activation of Epidermal Growth Factor (EGF) receptor kinase activity, results in down-regulation of coupling and phosphorylation of Cx43 serine residues, presumably through the activation of serine protein kinases (Lau *et al.*, 1992).

1.4 Control of gap junction formation and disassembly.

Communication via gap junctions may also be modulated by factors affecting the synthesis, trafficking and degradation of connexins. In addition to its effects on channel permeability, cAMP also increases communication in cells expressing a basal level of Cx43 mRNA, by dramatically increasing the rate of transcription of this message, and the subsequent formation of Cx43 bearing plaques (Mehta *et al.*, 1992). Similarly, Basic Fibroblast Growth Factor (bFGF) increases junctional communication in endothelial cells by an apparent increase in Cx43 expression (Pepper and Meda, 1992). In contrast, down-regulation of intercellular communication in keratinocytes, in response to transformation with the *ras*-oncogene or treatment with tumor promoting phorbol esters, is accompanied by serine phosphorylation of Cx43 and its reduced expression (Brissette *et al.*, 1991).

Very little is understood about the regulation of nascent connexin trafficking and membrane insertion. Although connexins appear to lack cleaved leader or signal sequences at their NH_2 terminus (Paul, 1986), newly synthesized membrane proteins lacking any obvious sorting signals are still efficiently transported from the endoplasmic reticulum (ER) to the Golgi complex and from there to the cell surface (Pelham, 1991). Confirmation of passage of connexins through the Golgi was recently provided immunocytochemically *in situ* by Hendrix *et al.* (1992), and in membrane fractions by Rahman *et al.* (1993). Cx32 detected in liver membrane fractions is not

glycosylated, and can be detected in both lateral and sinusoidal membranes although the precise point of insertion, or the cellular location at which connexins oligomerize into connexon hemichannels, remains unknown (Rahman *et al.*, 1993).

Once in the plasma membrane, the manner by which connexins/connexons assemble into gap junction plaques also remains unknown. In some cells, such as in Novikoff cells in culture and granulosa cells *in vivo*, the assembly of recognizable gap junctions is preceded by the appearance of "formation plaques" (reviewed by Johnson *et al.*, 1989). These structures, apparent in freeze fracture replicas of cell surfaces, are defined as flattened areas of plasma membrane containing clusters of loosely arranged 9-11 nm intramembranous particles. These particles, presumed to be individual connexons, then spontaneously self-assemble into tighter clusters representative of gap junction plaques, at which point each particle diminishes in size to about 8 nm. Plaques then grow either through the amalgamation of smaller plaques or the accretion of individual particles to the periphery of an existing plaque. In *Xenopus* oocytes, the distribution of exogenous connexins within the plasma membrane is apparently determined by the net charge in their cytoplasmic domains (Levine *et al.*, 1993).

In formation plaques, the interaction of connexons between apposed membranes is hypothesized to form functional channels and bring apposing membranes together. Support for this model was recently provided by studies on reaggregating Novikoff cells which found that incubation with antibodies to the extracellular domains of Cx32 and Cx43 prevented the assembly of formation plaques and gap

junctions, as well as adherens type junctions (Meyer *et al.*, 1992). Similar effects on both coupling and cell adhesion were also observed using an antibody to a calcium-dependent cell adhesion molecule (A-CAM/N-cadherin). The dependence of gap junctional communication on cell adhesion has also been observed in communication-deficient NRK cell lines which, when transfected with cDNA for the cell adhesion molecule L-CAM, phosphorylate Cx43 and incorporate it into functional plaques (Musil *et al.*, 1990).

Gap junction disassembly may be achieved through either plaque disaggregation, via the lateral diffusion of components in the plane of the membrane, or endocytosis, wherein plaques are internalized whole or in part by one of the cells in a neighbouring pair. This latter mechanism is typified by the removal of the gap junctions between neighbouring granulosa cells in response to an ovulatory stimulus, and results in cytoplasmic gap junction vesicles, which ultimately are believed to be degraded after fusion with lysosomes (Larsen *et al.* 1988). In support of this, clathrin-coated invaginating gap junctions, coated and uncoated annular gap junctions, and lysosomal like structures, were all found to label positively for Cx43 in cultured glioma cells transfected with Cx43 cDNA (Naus *et al.*, 1993).

1.5 Preimplantation development in the mouse.

Preimplantation development in the mouse culminates 4 1/2 to 5 days after fertilization with the differentiation of a blastocyst consisting of two divergent cell lines: an inner cell mass (ICM), which eventually gives rise to the embryo proper, and the trophectoderm, a polarized transporting epithelium from which much of the foetal contribution to the placenta is derived (reviewed by Rossant, 1986). Although the morphogenetic processes leading to this stage are dependent on the expression of embryonic genes (see below), like most species the initiation of embryogenesis is believed to be dependent on maternally derived gene transcripts and translation products stockpiled in the growing oocyte (reviewed by Schultz, 1986). This is exemplified by the activation of embryonic transcription.

General activation of embryonic transcription begins in the mouse in the 2-cell stage. The transition from oogenetic to embryonic control of development is characterized by a sharp decline in oogenetic mRNA content (Taylor and Piko, 1987; Schultz, 1986), the accumulation of embryonic gene transcripts (reviewed by Kidder, 1992), a shift in polypeptide synthesis (Latham *et al.*, 1991), and the onset of sensitivity to the transcriptional inhibitor α-amanitin (Braude *et al.*, 1979). Once activated, most genes continue to transcribe throughout preimplantation development (Kidder, 1992, 1993). Although a small amount of transcription is detectable in late 1-cell zygotes, which acquire a transcriptionally permissive state (Latham *et al.*, 1992), development to the 2-cell stage is not inhibited by treatment with α-amanitin (Braude

et al., 1979). Transcriptional activation is also independent of DNA synthesis, cell division, or nucleocytoplasmic ratio (Howlett, 1986; Petzoldt, 1984; Petzoldt and Muggleton-Harris, 1987). However, treatment with inhibitors of cAMP-dependent protein kinase (PK-A), inhibits the synthesis at the 2-cell stage of transcription dependent products (Poueymirou and Schultz, 1989; Manejwala *et al.*, 1991). Thus, general activation of embryonic transcription is likely regulated post-translationally in the 1-cell zygote, and may involve phosphorylation of maternally derived protein.

Two morphogenetic events are responsible for the differentiation of a blastocyst: compaction and cavitation. Compaction occurs in the 8-cell stage, and is characterized by the flattening of blastomeres against one another. As a result, individual cell boundaries become less distinct and the embryo becomes referred to as a morula. Compaction also results in the definition of apical (free) and basolateral (apposed) membrane domains for each cell. The onset of compaction also appears to be regulated post-translationally. Cell flattening at compaction is dependent on the Ca^{2+}-dependent cell-cell adhesion glycoprotein, E-cadherin (Shirayoshi *et al.*, 1983). During compaction E-cadherin is phosphorylated and redistributed from a global to a basolaterally restricted arrangement in the plasma membrane (Sefton *et al.*, 1992; Vestweber *et al.*, 1987). Although compaction is dependent on embryonic gene expression, the transcriptional requirements for this event are completed by the mid 4-cell stage, approximately 10 hours prior to the onset of cell flattening, whilst the requirement for translation is completed 4-5 hours in advance (Kidder and McLachlin, 1985). Consistent with this, E-cadherin mRNA and protein begin to accumulate by the

4-cell stage (Kidder and Blaschuk, unpublished results; Sefton *et al.*, 1992).

Cell flattening at compaction is accompanied by blastomere polarization and the assembly of tight and gap junctions (Ducibella and Anderson, 1975). Cell polarity is manifested at all levels by the asymmetric distribution of cytoplasmic organelles, the cytoskeleton, and surface features (reviewed by Johnson and Maro, 1986). Divergence of the inner cell mass and trophectoderm cell lineages is believed to stem from the differentiative cleavage of polarized blastomeres at this time. This occurs by the formation of a cleavage furrow running parallel to the apical surface. The inheritance of the apical surface by one of the resulting daughter cells of such a division is associated with trophectoderm formation (Wiley *et al.*, 1990).

Cavitation, the formation of a blastocoel cavity, is dependent on the polarized distribution of at least one protein, Na^+,K^+-ATPase, to the basolateral domain of the outer blastomeres (trophectoderm). The asymmetric distribution of this enzyme, combined with its active transport of osmotically active Na^+ into basolateral extracellular spaces, results in the accumulation of extracellular fluid between blastomeres. This process is dependent upon the maintenance of E-cadherin-mediated cell adhesion, and is facilitated by the expansion of focal tight junctions between trophectoderm cells (Watson and Kidder, 1988; Watson *et al.*, 1990). With continued enzyme activity, blastocoel expansion occurs which contributes to hatching of the differentiated embryo from its mucopolysaccharide coating, the zona pellucida. Unlike compaction, the gene expression requirements for cavitation are more immediate. The

onset of cavitation is dependent on concomitant protein synthesis and transcription in late morulae until 5 hours preceding the event (Kidder and McLachlin, 1985). Once cavitation has begun however, this requirement is substantially reduced, such that hatching from the zona can occur in blastocysts cultured for at least 14 hours in α-amanitin (Kidder and McLachlin, 1985).

1.6 Gap junctions in the preimplantation mouse embryo.

As mentioned, gap junctions are first detected structurally, by freeze fracture and thin section electron microscopy (Ducibella and Anderson, 1975; Magnuson *et al.*, 1977), and physiologically, by ionic and dye coupling of blastomeres (Lo and Gilula, 1979; McLachlin *et al.*, 1983), beginning in the 8-cell stage. The assembly of gap junctions at this time can be described as a *de novo* event relative to the absence of gap junctions during the early cleavage stages of zygotic development. However, this terminology does not preclude the possibility that stored as well as nascent connexins may be utilized in the formation of these initial channels. Although correlated with compaction, gap junction assembly is independent of the cell flattening which occurs at this time. Incubation of embryos in the presence of antibodies against E-cadherin does not prevent the establishment of intercellular coupling (Goodall, 1986). Similarly, the onset of coupling is unaffected by the disruption of cell flattening, as well as cytokinesis, resulting from the disruption of microfilaments with cytochalasins. An intact microtubule network also does not appear to be required (Kidder *et al.*, 1987). With development, the number of gap junctions between

blastomeres increases (Magnuson *et al.*, 1977; McLachlin and Kidder, 1986). Coupling of blastomeres via established gap junctions also does not require the maintenance of extensive cell apposition (Goodall, 1986; Kidder *et al.*, 1987).

Gap junctional communication in the preimplantation embryo appears to be an essential requirement for maintaining the compacted state and by extension, further development to the blastocyst stage. Injection of antibodies or antisense RNA against connexins into mouse blastomeres results in decompaction and extrusion of injected cells (Lee *et al.*, 1987; Bevilacqua *et al.*, 1989). A similar phenotype is observed in embryos derived from crosses between female DDK mice and males from a different strain (Buehr *et al.*, 1987). These zygotes exhibit reduced dye coupling and spontaneously begin to extrude cells at the late 16-cell stage, with 95% of embryos dying by the blastocyst stage. Treatment of these embryos with a weak base to raise intracellular pH, increases dye transfer between cells and rescues them to the blastocyst stage.

Prior to the *de novo* assembly of gap junctions it is unlikely that gap junction precursors are present at the surfaces of blastomeres. Although communication competent, compacted embryos can be induced to form interembryonic gap junctions when aggregated together, as assessed by their ability to transfer dye, no dye transfer is observed when one or both of the embryos paired has yet to undergo compaction and become coupled (McLachlin *et al.*, 1983; Kidder *et al.*, 1987). Inhibition of transcription or translation from the 4-cell stage onward inhibits the acquisition of dye

coupling although a residual amount of ionic coupling, the more sensitive measure of intercellular communication, can still be detected (McLachlin and Kidder, 1986). Thus, there are sufficient junctional components prior to the time of gap junction assembly to permit at least some intercellular channels to form. Although the establishment of normal coupling is dependent on continued embryonic gene expression, these experiments suggest that both the mobilization and assembly of preexisting gap junctional components in the preimplantation embryo is under precise temporal control.

1.7 Objectives of study.

Given that gap junctions in the preimplantation mouse embryo assemble *de novo* during a precise window in time, the early embryo provides a unique opportunity to explore both the regulation of gap junction assembly as well as to further examine the importance of gap junctional communication during embryonic development. In the present study there were two principle objectives. The first was to determine which members of the connexin gene family contribute to gap junctions in the early embryo. Chapter 2 of this thesis documents experiments wherein immunological probes directed against two members of the connexin gene family, Cx32 and Cx43, characterize the distribution of these proteins in preimplantation embryos. The distribution of Cx43 in the cumulus oocyte complexes (COCs) from which the embryos were derived, was also examined.

The second objective of this study was to determine how the *de novo* assembly of connexins, namely Cx43, into gap junctions might be regulated. To address this I first examined the nature of Cx43 distribution patterns in the embryo using the protein synthesis inhibitor, cycloheximide, and the trafficking inhibitors monensin and brefeldin-A. In chapter 3, the effects of these agents on nascent Cx43 in the cytoplasm of morulae is presented. This information, combined with that obtained in chapter 2 on the cytoplasmic distribution of Cx43 prior to gap junction assembly, was used in chapter 4 to examine the timing of Cx43 translation and trafficking in relation to the acquisition of functional gap junctional channels in the preimplantation embryo.

Chapter 2

Connexin distribution and contribution to gap junctions during preimplantation development in the mouse

2.1 Introduction.

During preimplantation development, mRNA for Cx43 is detectable as early as the 4-cell stage, and accumulates steadily thereafter (Valdimarsson *et al.*, 1991; Nishi *et al.*, 1991). Likewise, Cx43 protein is found by Western blotting to accumulate from the 4-cell stage onward (Valdimarsson *et al.*, 1991). This pattern of increasing mRNA and protein abundance beginning prior to when gap junctions first become detectable at the 8-cell stage confirms the interpretation of inhibitor studies that gap junction precursors are present prior to compaction. In addition, these results have made Cx43 a likely constituent of gap junctions in the early embryo.

Although protein with antigenic and size similarity to Cx32 can be detected in approximately equal abundance throughout preimplantation development by Western blot analysis, no Cx32 mRNA can be detected at any preimplantation stage by Northern blotting or the more sensitive technique of RT-PCR (Barron *et al.*, 1989; Kidder, unpublished). However, Cx32 and Cx43 mRNA can both be detected in ovarian oocytes, where the abundance of Cx32 transcripts is rapidly down-regulated within hours of hormonal (hCG) stimulation of (PMSG)-primed ovaries (Valdimarsson *et al.*, 1993). These results suggest, therefore, that Cx32 resides in the

preimplantation embryo as a persistent oogenetic product not augmented by zygotic transcription. Previous attempts to immunofluorescently localize this protein in embryos have met with failure, leaving unresolved the role of this protein in development (Barron and Kidder, unpublished; Nishi *et al.*, 1991).

Of the remaining ten members of the connexin gene family expressed in mammalian tissues, no mRNA for Cx26 or Cx46 has been detected throughout preimplantation development (Valdimarsson *et al.*, 1991; Valdimarsson and Kidder, unpublished). Determination of the putative contribution of the more recently discovered remaining eight connexins awaits the availability of both cDNA and immunospecific probes.

In the present chapter my intent was to examine the distribution of Cx32 and Cx43 during early development which, based on the data summarized above, seemed the most likely constituents of gap junctions during this period. To this end I utilized the technique of wholemount immunofluorescence in conjunction with both conventional epifluorescence and confocal laser scanning microscopy. Immunoelectron microscopy was also used.

2.2 Materials and methods.

2.21 Embryo isolation.

Embryos were flushed from the reproductive tracts of CF1 female mice (Charles River Canada Ltd., St. Constant, Québec) which had been superovulated with 5 IU pregnant mare serum gonadotropin (PMSG) followed 46 hr later with 5 IU human chorionic gonadotropin (hCG), and then mated with $CB6F_1/J$ males (The Jackson Laboratory, Bar Harbor, ME). Embryos up to the late morula stage were flushed and sorted at room temperature in flushing medium-I (FM-I), whilst blastocysts were flushed in flushing medium-II (FM-II; Spindle 1980). Stage specific collections were carried out at the following times (hr post-hCG): 1- to 2-cell, 24 hr; uncompacted 4- to 8-cell, 58-67 hr; 8- to 16-cell compacted morulae, 74-76 hr; late morulae (up to 32 cells), 80 hr; blastocysts, 90-92 hr.

2.22 Wholemount immunofluorescence microscopy.

Prior to fixation, embryos were washed by passage through at least five changes of Ca^{2+}- and Mg^{2+}-free phosphate buffered saline (CMF-PBS) containing 0.3% polyvinylpyrrolidone (PVP), followed by one change of PHEM buffer (Schliwa and Van Blerkom, 1981; 60 mM PIPES, 25 mM HEPES, 10 mM EGTA, and 1 mM $MgCl_2$, pH 6.9). All overnight steps were carried out at 4°C. All remaining steps were conducted on ice or at room temperature with no appreciable difference in the

results. Embryos were fixed for at least 1 hr to overnight in freshly prepared 1% paraformaldehyde in PHEM. Fix was removed by passage of embryos through four changes of PHEM, and embryos were permeabilized for 20 min with 0.1% Tween-20 in PHEM followed by another 20 min in 0.1% Tween-20 in CMF-PBS. Embryos were blocked in CMF-PBS containing 1% BSA and 0.1% Tween-20 for at least 30 min and then incubated in the primary antiserum in blocking solution overnight. Treatment with primary antisera from 1 to 3 hr was found to be insufficient. Following passage through at least six changes of CMF-PBS containing 0.1% Tween-20, the last for at least 5 hr, embryos were labeled for at least 1 hr with a fluorochrome conjugated species specific secondary antibody in blocking solution. Occasionally 5 μg/ml DAPI stain (Polysciences Inc., Warrington, PA) was added to the secondary antibody mix to visualize the nuclei of immunostained embryos. The secondary antibody solution was removed as described for the primary antibody except that the last wash lasted overnight. Immunofluorescence on blastocysts required the substitution of 0.1 % Triton X-100 for Tween-20 in the protocol. Higher concentrations of Tween-20 up to 0.5% were insufficient to permeabilize blastocysts, whilst no noticeable improvement in permeabilization was observed with higher concentrations of Triton X-100 up to 0.5%.

Immunofluorescence was also performed on cryosections (10 μm thick) of fresh frozen mouse liver collected using a Kryostat 1720 (Leitz). Cryosections were fixed with paraformaldehyde and extracted with Tween-20 as described for embryos. Immunostained tissues were wholemounted in FITC-Guard (Testog Inc., Chicago, IL)

and viewed either with a Zeiss Photomicroscope I equipped with epifluorescence optics or a Bio-Rad MRC 600 confocal laser scanning microscope (CLSM).

2.23 Conventional and immunogold electron microscopy.

Optimal structural preservation of embryos for conventional electron microscopy was obtained by embedding tissue in Epon-Araldite (J.B.E.M, Dorval, Que.). All steps were performed at room temperature using filtered solutions. Embryos were fixed in 2% glutaraldehyde in 0.1 M phosphate buffer (pH 7.3), containing 2% w/v sucrose (fix buffer) for 1 hr. Glutaraldehyde fixation in phosphate buffer lacking sucrose resulted in the disruption of cell and organelle structure presumably as a result of osmotic pressure differences between the fixation buffer and embryos. All subsequent steps leading to tissue infiltration were performed on a Fisher clinical horizontal rotator set at a slow speed. Fix was removed with three 10 min changes of fix buffer, after which embryos were preembedded in molten 2% agar which was then trimmed to a 1-2 mm^3 block. To enhance the subsequent preservation and visibility of organelles, embryos were post-fixed for 1 hr with 2% OsO_4 in fix buffer. Post-fixation with 1-2% OsO_4 for 15 min was insufficient to visualize organelles. Following passage through three more 10 min changes of fix buffer, embryos were next washed through four changes of sterile double distilled water (ddH_2O) and left overnight in the last wash at room temperature. The next day embryos were *en bloc* stained with saturated aqueous (5%) uranyl acetate for 2.5 hr, which was then removed with three 20 min changes of ddH_2O. Embryos were

dehydrated by 10 min exposures to an ascending series of 20%, 50%, 70%, and 90% acetone. Dehydration was completed by two 30 min exposures to 100% acetone. Embryos were infiltrated by end-over-end rotation (0.5 revolutions per minute) for 1 hr intervals through a graded series of acetone:resin, wherein the proportion of acetone was decreased from 3:1 to 1:1 to 1:3 acetone:resin. This was followed by overnight infiltration at room temperature in pure resin, and 3-4 hr infiltration and encapsulation in fresh resin. Resin was polymerized for 40 hr at 60°C. Epon-Araldite resin was formulated as follows; 4.5 ml Epon (812), 3.5 ml Araldite (502), 18 ml dodecenyl succinic anhydride (DDSA), and 0.67 ml 2,4,6-tri- (dimethylaminomethyl) phenol (DMP-30). DMP-30 was only added after mixing the epoxy components.

Immunogold electron microscopy was performed on mouse embryos, liver, and COCs isolated from secondary (antral) follicles either 46 hr post-PMSG or 34 hr post-hCG. Flushed embryos were transferred directly into fix from flushing medium. Excised liver and ovaries were transferred directly into fixative wherein tissues were minced, and in the case of the latter, COCs isolated.

Tissues primarily intended for immunoelectron microscopy were embedded in LR White (Polysciences Inc.) essentially as described for Epon-Araldite with the following exceptions: Choice of fixatives, their concentration and the duration of their use were determined by the antigenic requirements of each antisera used. Fixatives were prepared in the same fix buffer as for Epon-Araldite and ranged from 1 to 2 hr in 1% paraformaldehyde or 1.6% glutaraldehyde, with or without a brief 15 min

exposure to 1% OsO_4. Given the brevity of osmication, an overnight wash in ddH_2O prior to *en bloc* staining with uranyl acetate was normally omitted. Tissues were dehydrated by 10 min exposures to an ascending gradient of 50%, 70%, and 95% ethanol. Tissues were infiltrated first for 1 hr in 50% LR White in absolute ethanol, and next for overnight (14 hr) in LR White. Infiltrations were performed in light tight (foil wrapped) and air tight (rubber stoppered) glass vials. Tissues were embedded in fresh LR White resin polymerized at 60°C for 24 hr. Both Epon-Araldite and LR-White embedded tissues were polymerized in gelatin capsules (size 00, Polysciences).

Silver and silver/gold sections of Epon-Araldite or LR White sections were cut with glass knives on a Reichert-Jung Ultracut E ultramicrotome. Epon-Araldite sections were collected on 200 hexagonal mesh copper grids. LR White sections were collected on 200, 300, and 400 hexagonal mesh nickel grids. Grids were immunostained as described below in moisture chambers prepared from 3 inch plastic petri dishes by placing a square of parafilm in the base of each dish and lining the inside edge with a tissue soaked in ddH_2O. Dishes were kept covered at all times to prevent drying of microdrops of treatment solutions.

Prior to immunostaining, sections were etched on one side to expose antigenic sites by treatment with oxidizing agents such as 5% H_2O_2 or saturated aqueous sodium metaperiodate ($NaIO_4$). Etching was necessary to expose antigenic sites embedded in resin. Etching with 5% H_2O_2 tended to be harsher leading to increased section

instability under the electron beam, and normally did not exceed 5 min. Etching with $NaIO_4$ was performed at room temperature or at 37°C with supersaturated $NaIO_4$ normally for 1 hr. Highly osmicated material required longer periods of etching with $NaIO_4$, up to 3 hr. Once etched, grids were washed with ddH_2O, blotted dry with filter paper, and blocked for 30 to 45 min with 3% BSA in CMF-PBS before treatment with primary antibody preparations in CMF-PBS for 3 hr at room temperature. Grids were washed free of primary antibody by passage through at least four changes of CMF-PBS in microdrops in moisture chambers placed onto magnetic stirrers set at low speed. Secondary antibody treatment, also in CMF-PBS, was normally for 90 min at room temperature, and followed by renewed washing as described following primary antibody treatment. Lastly, grids were rinsed in ddH_2O for up to 1 min before being dried on filter paper. Grids were counterstained by treatment for 1 hr with saturated aqueous uranyl acetate at 37°C, followed by washing with ddH_2O, and 10 min with lead citrate in a CO_2-free environment created in a petri-dish by the placement of 2-3 potassium hydroxide pellets. Lead staining was removed by washing with freshly boiled (CO_2-free) ddH_2O. Shorter periods of uranyl acetate treatment (5-20 min), and lead citrate (2-3 min) at room temperature produced inferior counterstaining results. Uranyl acetate prepared in 70% ethanol was found to precipitate on sections. Lead citrate stain was prepared by dissolving approximately 35 mg of lead citrate in 10 ml of freshly boiled ddH_2O, to which 3 drops of 10 N NaOH was added to dissolve the lead. Undissolved lead was pelleted by centrifugation at 2,000 rpm before use. Sections were viewed with either a Phillips EM 201 or a Phillips CM10 transmission electron microscope at 60 KV.

2.24 Antisera.

Primary antisera used in the present study as immunological probes for Cx32 and Cx43 are summarized in Table 2.4. In the present study three polyclonal rabbit antisera were used as immunological probes for Cx43, each directed against a different synthetic peptide corresponding to a carboxy-terminal cytoplasmic domain unique to this protein, as determined from the cDNA for rat Cx43. Although each of these antisera possessed a given name (see brackets below), for the sake of clarity in this thesis each is referenced by the name of the protein recognized and the number of the first amino acid residue encoded by the synthetic peptide. Thus, anti-Cx43/252 (Petunia), anti-Cx43/302 (Rebecca), and anti-Cx43/360 (CT-360) were directed against amino acids (a.a.) 252-271, 302-319, 360-382 of rat Cx43, respectively (Fig. 2.1). Although the first of these was provided as an unfractionated serum by Dr. David Paul (Harvard Medical School, Boston, Ma), the latter two, provided by Drs. Bruce Nicholson (SUNY, Buffalo, NY), and Dale Laird (McGill, Montreal, Que), respectively, were obtained as affinity-purified preparations. A search of *SwissProt*, *PIR*, and *GenPept* peptide sequence databases using *GCG* sequence analysis software (Genetics Computer Group Inc., Wisconsin) revealed that the peptide sequences recognized by anti-Cx43/252, -Cx43/302, and -Cx43/360 were 100%, 94%, and 100%, identical to corresponding mouse sequences, respectively.

The specificity of the immunostaining patterns obtained with all Cx43 antibodies was tested using preimmune sera or by omission of the primary antibody

Figure 2.1. Single lettercode amino acid sequence of rat Cx43 through a single junctional membrane, showing peptide sequences recognized by anti-Cx43 antibodies used in the present study. Cx43 is inserted into the plasma membrane as described in Fig. 1.1. Cx43 is folded here in a hypothetical manner, with smaller folds within the polypeptide chain serving only to fit the drawing in the space; no secondary structure is implied. Three peptide-specific antibodies directed against three nonoverlapping domains of rat Cx43 were used in the present study. These were anti-Cx43/252, anti-Cx43/302, and anti-Cx43/360, which were directed against amino acid sequences spanning residues 252-271 (1), 302-319 (2), and 360-382 (3), respectively. Adapted from Swenson *et al.*, 1990.

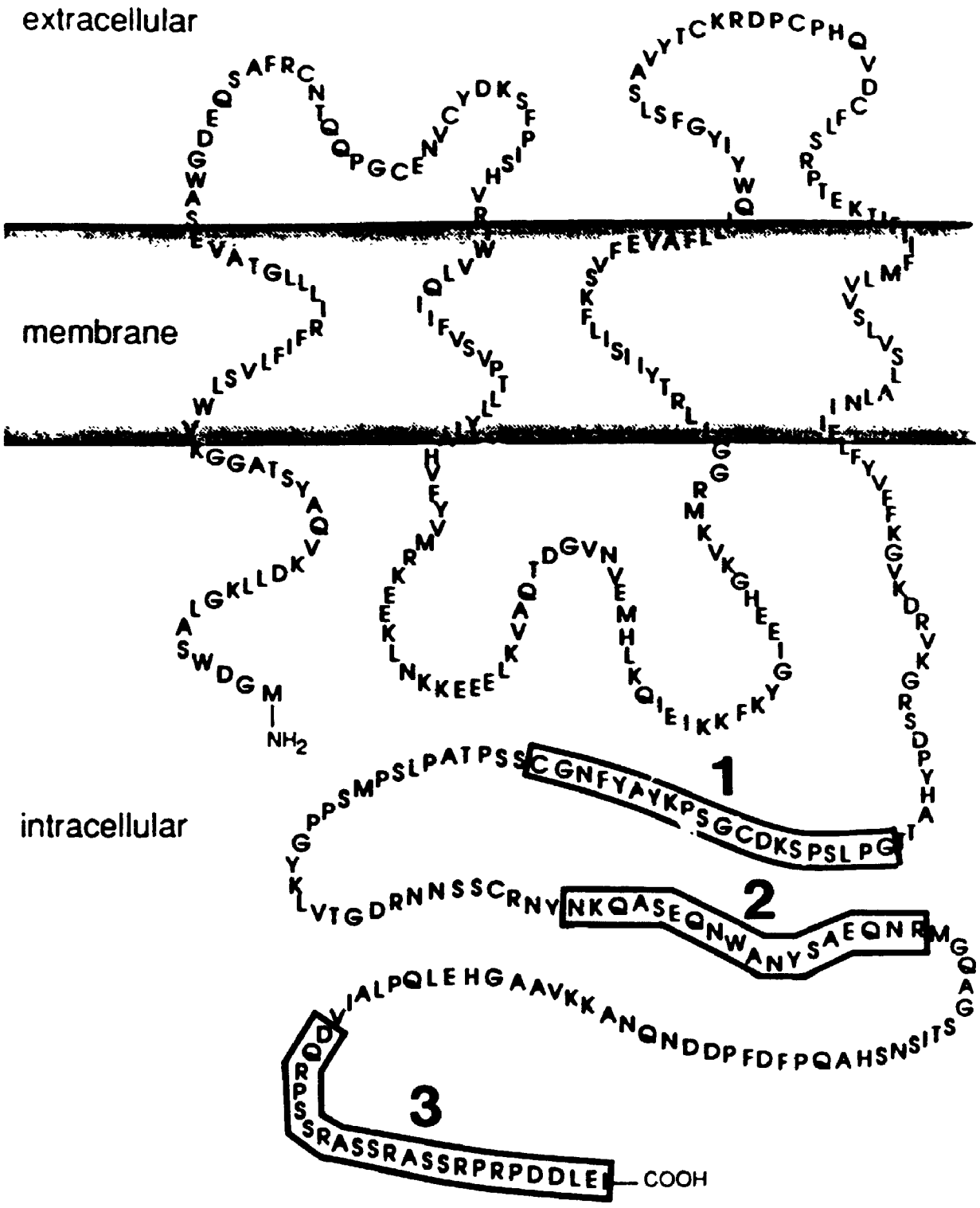
extracellular
membrane
intracellular
1
2
3
NH2
COOH

(secondary antibody control). The specificity of anti-Cx43/252 and anti-Cx43/302 were further tested by preabsorbing the antibodies with their peptide before use. Preabsorbed anti-Cx43/302 was provided by Dr. Nicholson and was used at the same concentration as the immune. Anti-Cx43/252 was preabsorbed with its corresponding peptide, donated by Dr. Paul, as follows. Peptide (0.5 mg) was first dissolved in 1.25 ml of CMF-PBS by sonication using a probe (Insonator, Ultrasonics Systems Inc., Farmingdale, NY) for 45 sec, followed by incubation at 37°C for 30 min. Tween-20 was added to a final concentration of 0.1%. One μl of immune serum was then added to 250 μl of the dissolved peptide, and mixed end over end for 1 hr at 4°C before use. For immunofluorescence anti-Cx43/252 was used at dilutions of 1:250 to 1:1000. Anti-Cx43/302 was used at a concentration of 8-9 μg/ml. Anti-Cx43/360 was used at a dilution of 1:250 to 1:500. For immunoelectron microscopy anti-Cx43/302 was used at a concentration of 5 μg/ml, whilst anti-Cx43/360 was used at a dilution of 1:500. Preimmune sera for each antibody were used at the same final dilution/concentration, respectively.

Cx32 was recognized by one peptide-specific polyclonal antiserum and one monoclonal antibody. M12.13 is a mouse monoclonal antibody provided by Dr. Paul that recognizes the 27 kD major protein (*i.e.* Cx32) in hepatocyte gap junctions, as well as the cytoplasmic surface of isolated rat liver gap junctions (Goodenough *et al.*, 1988). Affinity-purified rabbit polyclonal antiserum against a synthetic peptide corresponding to a.a. 223-244 of rat Cx32, anti-Cx32/223 (Teresa), was provided by Dr. Nicholson. A search of peptide sequence databases found this peptide sequence to

be 90% identical to that found in mouse. For immunofluorescence, M12.13 was used at a dilution of 1:10 whilst anti-Cx32/223 was used for immunofluorescence and immunogold electron microscopy at a concentration of 8.6 μg/ml. The specificity of immunostaining patterns observed with anti-Cx32/223 was tested by using preimmune serum at the same concentration.

For immunofluorescence, primary antibodies derived from rabbit antisera were detected using a fluorescein isothiocyanate-conjugated goat anti-rabbit IgG (ICN Biomedicals Canada Ltd., St. Laurent, Que.) diluted 1:50. Mouse primary antibodies were detected with a rhodamine-conjugated goat anti-mouse IgG (ICN) diluted 1:10. Goat anti-rabbit IgG conjugated to 10 nm gold (BioCell, Cedarlane Laboratories Ltd., Hornby, Ont.) was used at a dilution of 1:20 to 1:35, for immunoelectron microscopy.

2.3 Results.

2.31 Connexin32 does not contribute to gap junctions in morulae.

To facilitate the immunolocalization of Cx32 in early embryos, the CLSM was used. Precompaction embryos (1-cell zygotes to uncompacted 8-cell), 8- to 32-cell morulae, blastocysts, as well as cryosections of mouse liver, were fixed with 1% paraformaldehyde and immunostained with either a monoclonal antibody (M12.13) against a 27 kD rat liver gap junction protein, a peptide-specific antibody against amino acids (a.a.) 223-244 of rat Cx32 (anti-Cx32/223), or preimmune serum for the latter. Although M12.13 was previously found by Western blot analysis to detect protein with antigenic and size similarity to Cx32 in approximately equal abundance throughout preimplantation development, no immunoreactivity above a diffuse background was observed in any of the precompaction embryos (n = 16), or morulae (n = 25), stained with this antibody (Fig. 2.2). Neither were there any immunostaining patterns in precompaction embryos (n = 25), morulae (n = 57), or blastocysts (n = 18), reacted with anti-Cx32/223, despite the fact that the rat peptide sequence recognized by this antibody is 90% identical to the corresponding mouse sequence. In contrast to the lack of staining seen in early embryos, both M12.13 and anti-Cx32/223 detected gap junction-like plaques in cryosections of mouse liver fixed and processed in a similar manner (Fig. 2.2). Such staining was never observed in liver, precompaction embryos (n = 12), morulae (n = 28), or blastocysts (n = 14) using preimmune serum, or when using secondary antibody alone.

Figure 2.2. Cx32 cannot be detected in gap junction-like structures in pre- or postcompaction embryos. Confocal z-series projections (4 μm thick) of precompaction (A, B) and postcompaction (C,D) embryos and liver cryosections (E,F) stained with anti-Cx32 antibodies, M12.13 (A,C,E) or anti-Cx32/223 (B,D,F).

Scale bars = 25 μm.

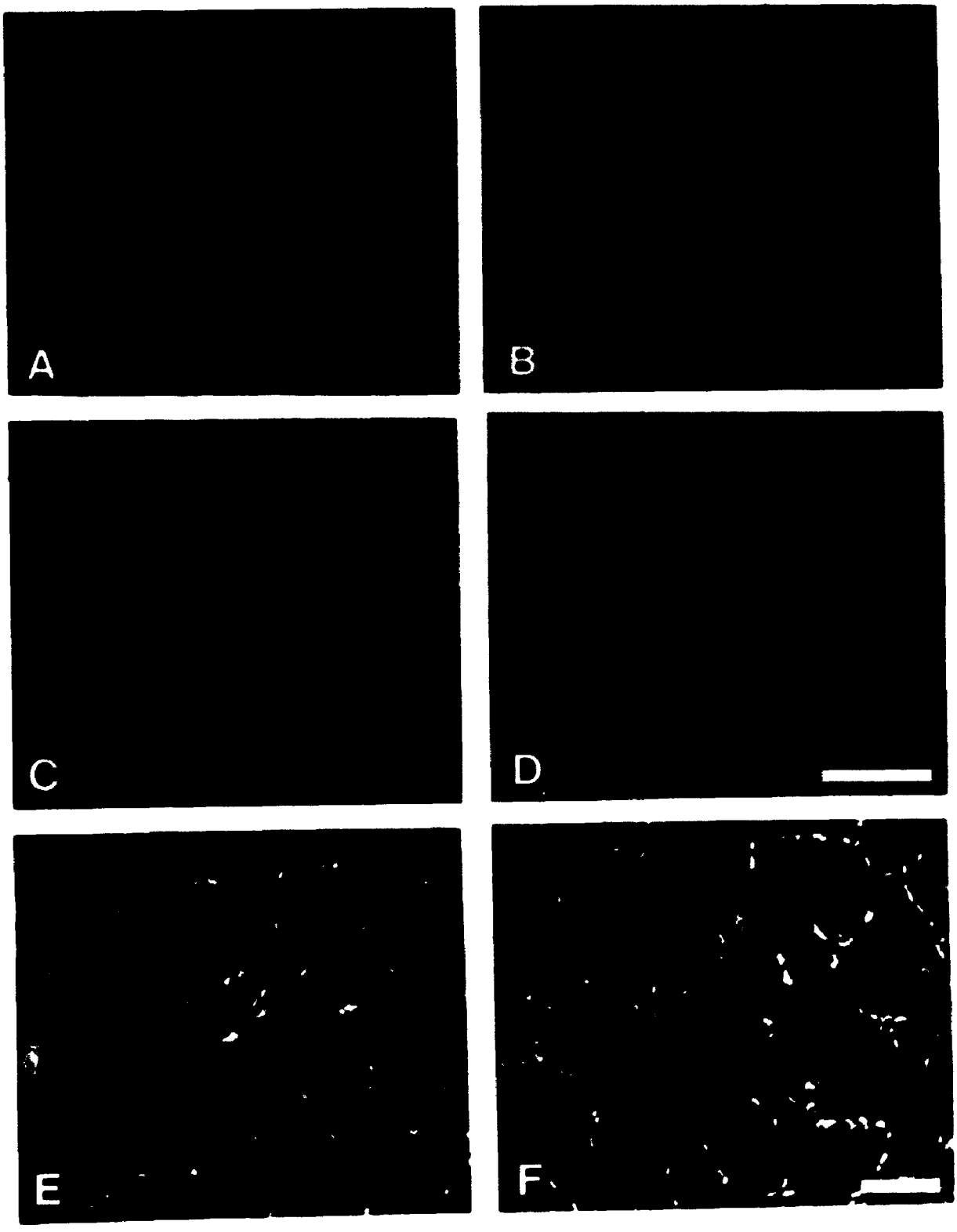
A
B
C
D
E
F

To demonstrate the specificity of anti-Cx32/223 for gap junctions containing Cx32, mouse liver fixed with 1% paraformaldehyde, as for immunofluorescence, was embedded in LR White for immunogold electron microscopy. Although tissue fixed in a such a manner was poorly preserved, gap junctions between hepatocytes remained visible and could be specifically labeled with anti-Cx32/223 (n=9) but not preimmune serum (n=11; Fig. 2.3 A,B). Attempts to improve tissue preservation by post-fixation with OsO_4 (Fig. 2.3 C), or fixation with glutaraldehyde, abolished anti-Cx32/223 antigenicity.

2.32 Cx43 distribution changes throughout preimplantation development.

The distribution of Cx43 throughout preimplantation development was also examined by immunofluorescence. Initial studies, conducted prior to the arrival of the CLSM, were performed on a Zeiss Photomicroscope I equipped with epifluorescence optics. In these studies Cx43 was localized with anti-Cx43/252, a polyclonal antiserum against a synthetic peptide unique to the C-terminal cytoplasmic domain of Cx43. Although the sequence specified by this peptide (a.a. 252-271) was based on a rat cDNA, it was also identical to the corresponding mouse sequence.

Cx43 distribution, as depicted by labeling with anti-Cx43/252, was variable throughout preimplantation development. In 2-cell, 4-cell, and 8-cell uncompacted embryos Cx43 was only detected in the cytoplasm of blastomeres, mostly in large irregular patches (Fig. 2.4 A,B, 2.5 A). All precompaction embryos labeled with

Figure 2.3. Immunogold detection of Cx32 in mouse liver gap junctions (arrows). Anti-Cx32/223 specifically labels gap junctions in liver fixed with 1% paraformaldehyde (A), whereas no labeling was seen with preimmune serum (B). Post-fixation of paraformaldehyde fixed liver with OsO_4 (C), abolished anti-Cx32/223 antigenicity which could not be recovered by etching sections with H_2O_2, or $NaIO_4$. Scale bars 250 nm.

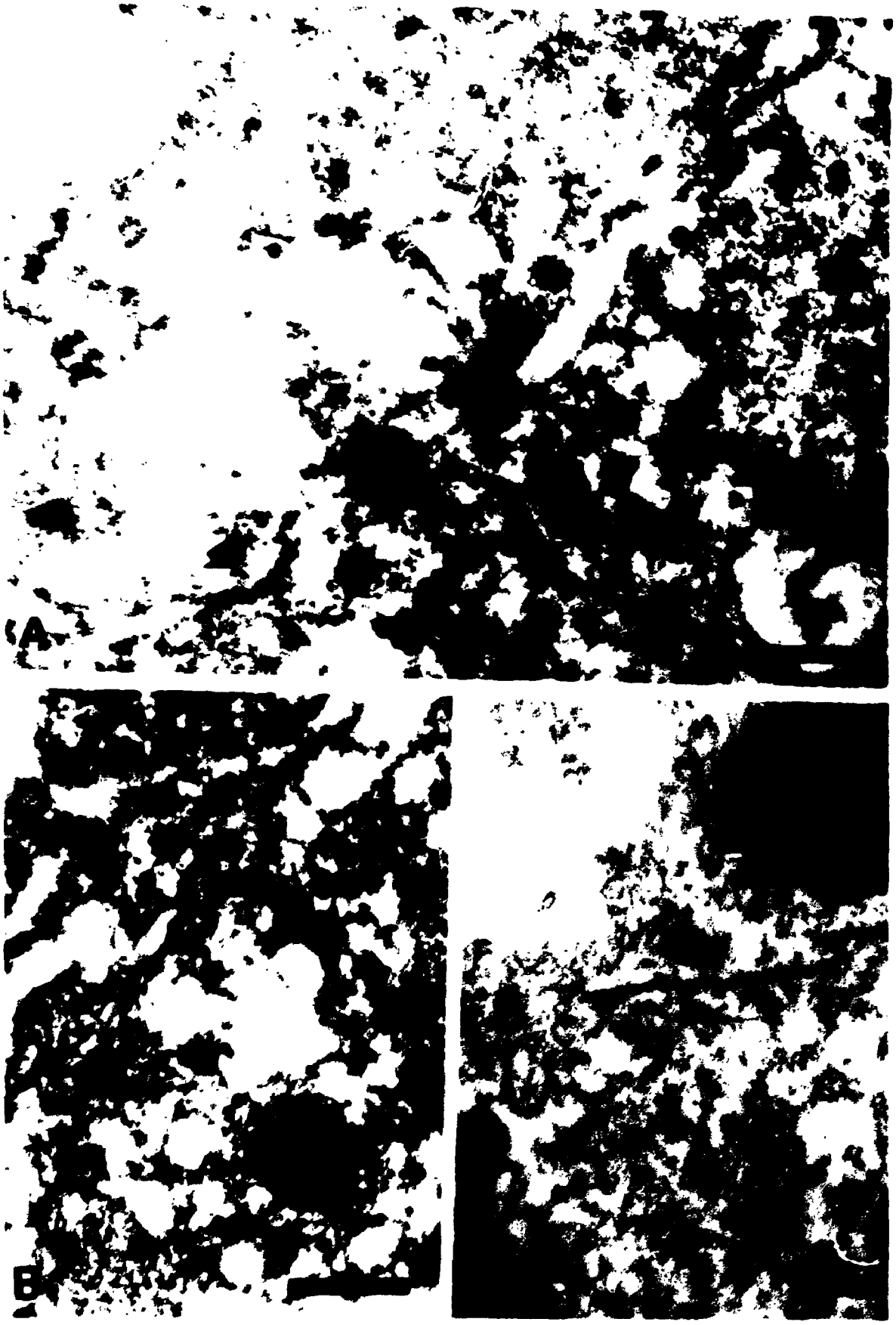
A
B

Figure 2.4. Pattern and specificity of Cx43 in precompaction embryos depicted by anti Cx43/252. Immunofluorescently stained embryos were wholemounted and viewed using conventional epifluorescence optics. Staining of precompaction embryos with anti Cx43/252 (A,B), revealed Cx43 in large irregular cytoplasmic patches. These structures were absent from precompaction embryos stained with preimmune serum (C). Two cell embryo (A). Four cell embryos (B,C). Scale bar 25 μm.

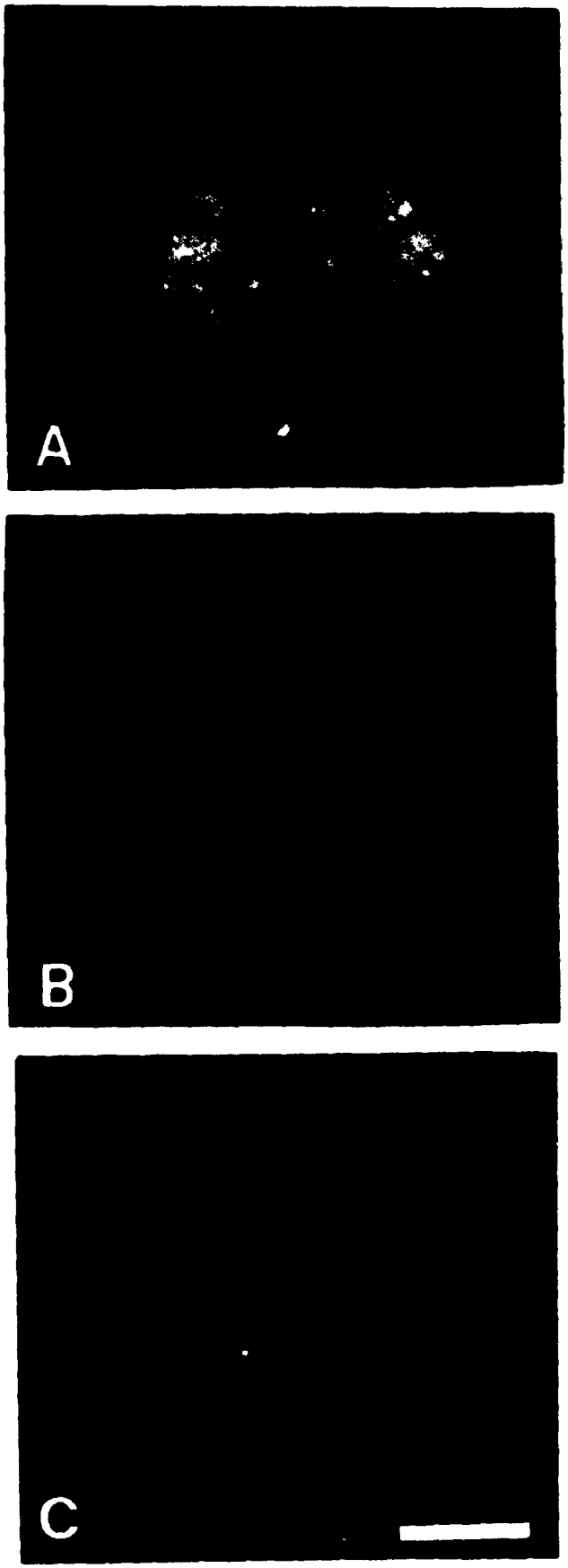
A
B
C

Figure 2.5. Pattern and specificity of Cx43 distribution in preimplantation embryos from the 8-cell stage onwards, depicted by anti-Cx43/252. Epifluorescence microscopy on wholemounted embryos revealed that prior to compaction in the 8-cell stage (A), Cx43 was mostly in large irregular cytoplasmic patches (curved arrows), although occasionally Cx43 was also seen in discrete foci near sites of cell apposition (straight arrows). Bright, punctate, intercellular staining (arrowheads), consistent with staining for gap junctions was first seen with signs of cell flattening in the 8-cell stage (B). Also at this time Cx43 was seen in the cytoplasm as evenly dispersed small diffuse foci (open arrows). With increasing cell number Cx43 was detected in morulae (C) and blastocysts (D) as continuous and discontinuous staining of apposed membrane regions. Cytoplasmic and membrane staining patterns were absent from morulae stained with peptide absorbed (E) or preimmune serum (F). Scale bar 25 μm.

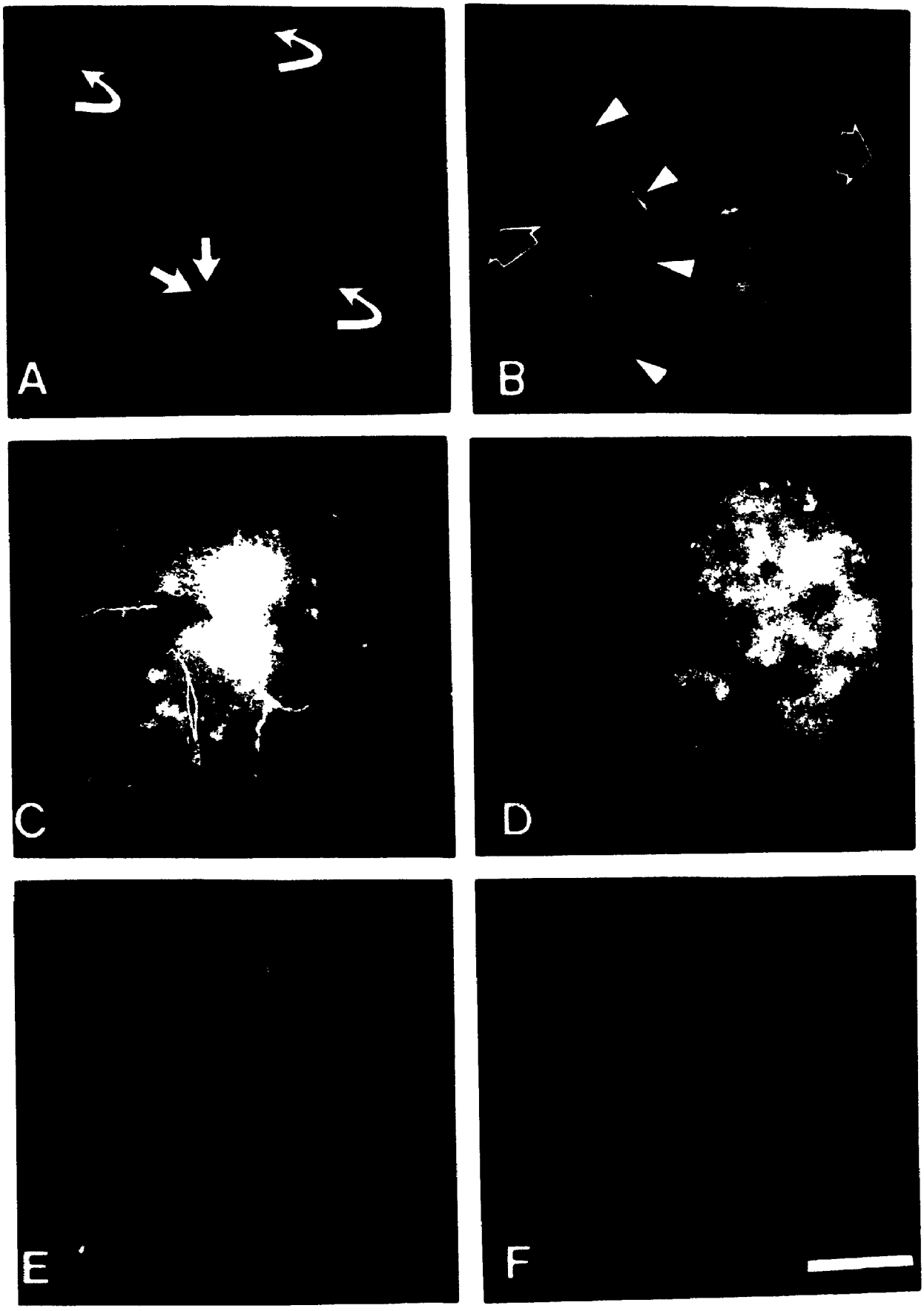
A
B
C
D
E
F

anti-Cx43/252 (n = 39), exhibited this staining pattern, although 1-cell zygotes were not examined. Occasionally, uncompacted 8-cell embryos also exhibited smaller, discrete cytoplasmic foci near sites of cell apposition (Fig. 2.5 A). No staining of apical or apposed membranes was apparent at these stages. No staining patterns, above a uniform diffuse background fluorescence, were ever observed in precompaction embryos labeled with preimmune serum (n=38; Fig. 2.4 C). Beginning with first signs of cell flattening during compaction at the 8-cell stage, bright, punctate, interblastomeric staining, consistent with staining for gap junction plaques, became evident. Also at this time, Cx43 became detectable in the cytoplasm in small discrete foci which were evenly dispersed throughout the cytoplasm and more diffuse than the punctate membrane staining (Fig. 2.5 B). With increasing cell number Cx43 was also detected in morulae and blastocysts as continuous and discontinuous zonular staining of apposed membrane regions (Fig. 2.5 C,D).

To assess the specificity of the immunostaining patterns observed in postcompaction embryos labeled with anti-Cx43/252, 8- to 16-cell morulae were scored blindly, *i.e.* their identities were revealed to the experimenter only after scoring had been completed. Diffuse cytoplasmic foci, gap junction plaque-like staining, and zonular staining of apposed membranes were detected in 100%, 61%, and 32% of morulae (n=31), respectively (Table 2.1). None of these staining patterns were ever observed using preimmune serum (n=30; Fig 2.5 E) or secondary antibody alone (n = 29), or if anti-Cx43/252 was preabsorbed with its peptide prior to use (n = 30; Fig. 2.5 F).

Table 2.1

Frequency of immunofluorescent staining patterns detected in 8-16 cell morulae labeled with anti-Cx43 antibodies[1]

Antibody	Number scored	Morulae (%)		
		Small diffuse cytoplasmic foci	Punctate plaque-like foci	Zonular apposed membrane staining
Anti-Cx43/252	31	100	61	32
Anti-Cx43/302	61	92	100	70
Anti-Cx43/360	38	87	100	0

[1] Wholemounted embryos, fixed with 1% paraformaldehyde and permeabilized with 0.1% Tween-20 before treatment with antibody, were scored using a Bio-Rad MRC 600 CLSM.

The arrival of the CLSM coincided with the arrival of a second antibody against a different synthetic peptide, also unique to the C-terminal domain of rat Cx43 (a.a. 302-319). The peptide sequence recognized by anti-Cx43/302 is 94% identical to the corresponding sequence found in the mouse. Cx43 distribution depicted by labeling with this antibody was identical to that seen with anti-Cx43/252, except in precompaction embryos. No staining patterns, above a uniform diffuse background fluorescence, were ever observed in all stages of precompaction embryos labeled with anti-Cx43/302, including 1-cell zygotes (n=33; Fig. 2.6 A,B). As described for anti-Cx43/252, Cx43 was first detected at apposed membrane regions in punctate plaque-like foci with first signs of cell flattening in the 8-cell stage (Fig. 2.6 C). Compacting and postcompaction embryos were also rich in cytoplasmic immunoreactivity, seen as small, diffuse foci (Fig. 2.6 C,D). With increasing cell number a zonular staining of apposed membranes also became apparent, which persisted through to the blastocyst stage (Fig. 2.6 D). Optical sectioning of embryos, permitted by the CLSM, revealed that this staining was confined to the basolateral domains of the outward facing cells of morulae and the trophectoderm of blastocysts, and intermittently punctuated by plaque-like structures (Fig. 2.6 D, 2.7). Gap junction plaque-like Cx43 staining was abundant between both the inner blastomeres of morulae and the inner cell mass (ICM) of blastocysts (Fig. 2.7). Visualization of Cx43 in the ICM necessitated the substitution of Triton X-100 for Tween-20 during the permeabilization step of the immunofluorescence protocol.

Figure 2.6. Pattern and specificity of Cx43 distribution depicted by anti-Cx43/302. No immunoreactivity was detected with this antibody in 1-cell zygotes (A) or uncompacted 8-cell embryos (B). Plaque-like foci at apposed membrane regions were first detected beginning with signs of cell flattening in the 8-cell stage, at which time cytoplasmic immunoreactivity also became evident (C). With increasing cell number, morulae develop a zonular pattern of intercellular staining at apposed membrane regions while still retaining plaque-like localizations (D). Cytoplasmic and membrane staining patterns were absent from morulae stained with peptide absorbed (E) or preimmune serum (F). The images are confocal z-series projections (2-2.5 μm thick). Scale bars = 25 μm.

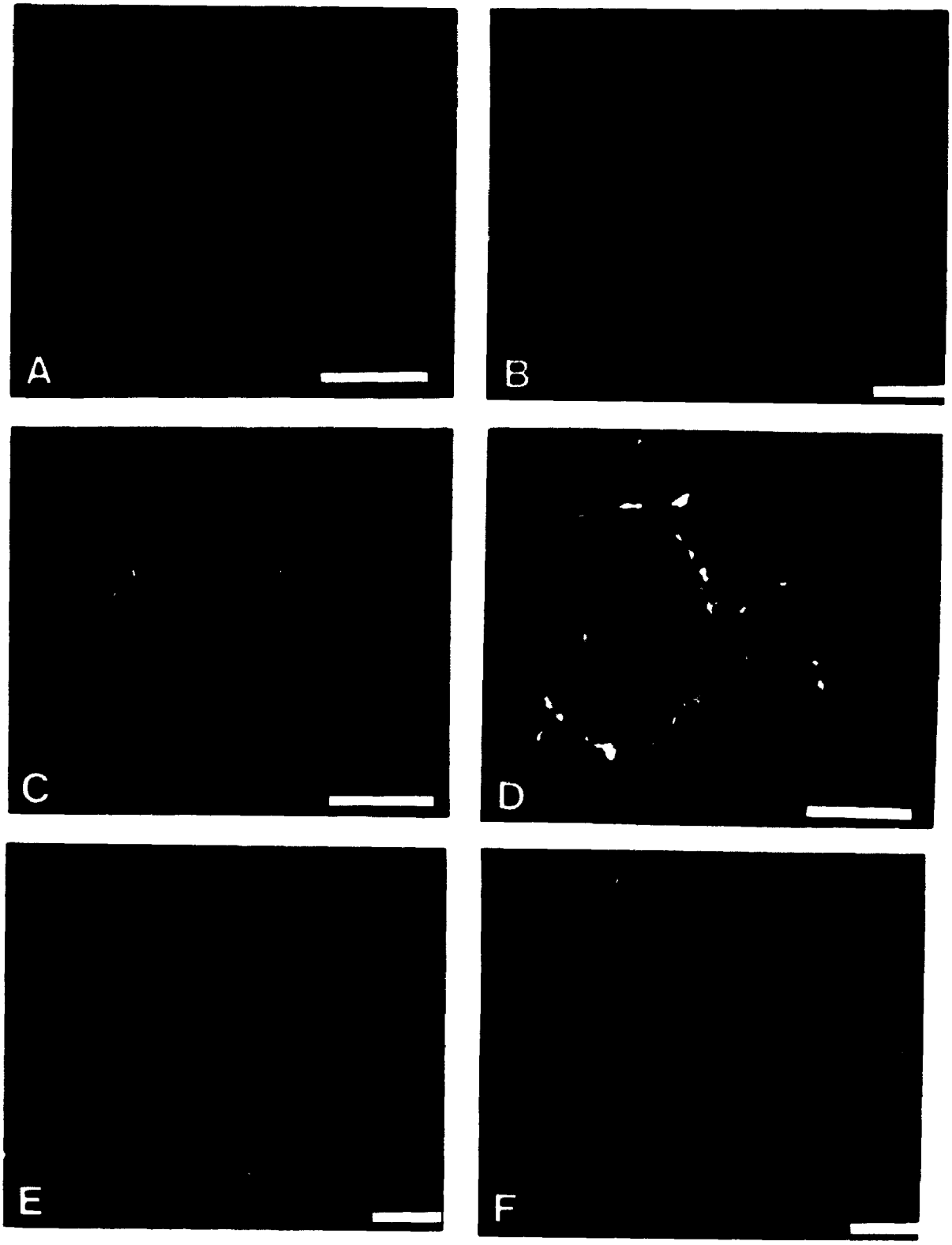
A
B
C
D
E
F

Figure 2.7. Zonular Cx43 staining at apposed membranes is confined to the outside cells of morulae and the trophectoderm of blastocysts. Each column is a through focus series of successive z-series projections (2-3 μm thick) of a morula (Ai-iv) or blastocyst (Bi-iv) stained with anti-Cx43/302. The top and bottom images in each column are superficial optical sections whereas the middle images are deeper sections. Large, plaque-like foci typical of embryonic gap junctions predominate in the ICM (Bii, iii) whereas the zonular pattern, punctuated by small, bright foci that may also represent gap junctional plaques, characterizes the trophectoderm (t) which surrounds the blastocoel (bl). Scale bar – 25 μm.

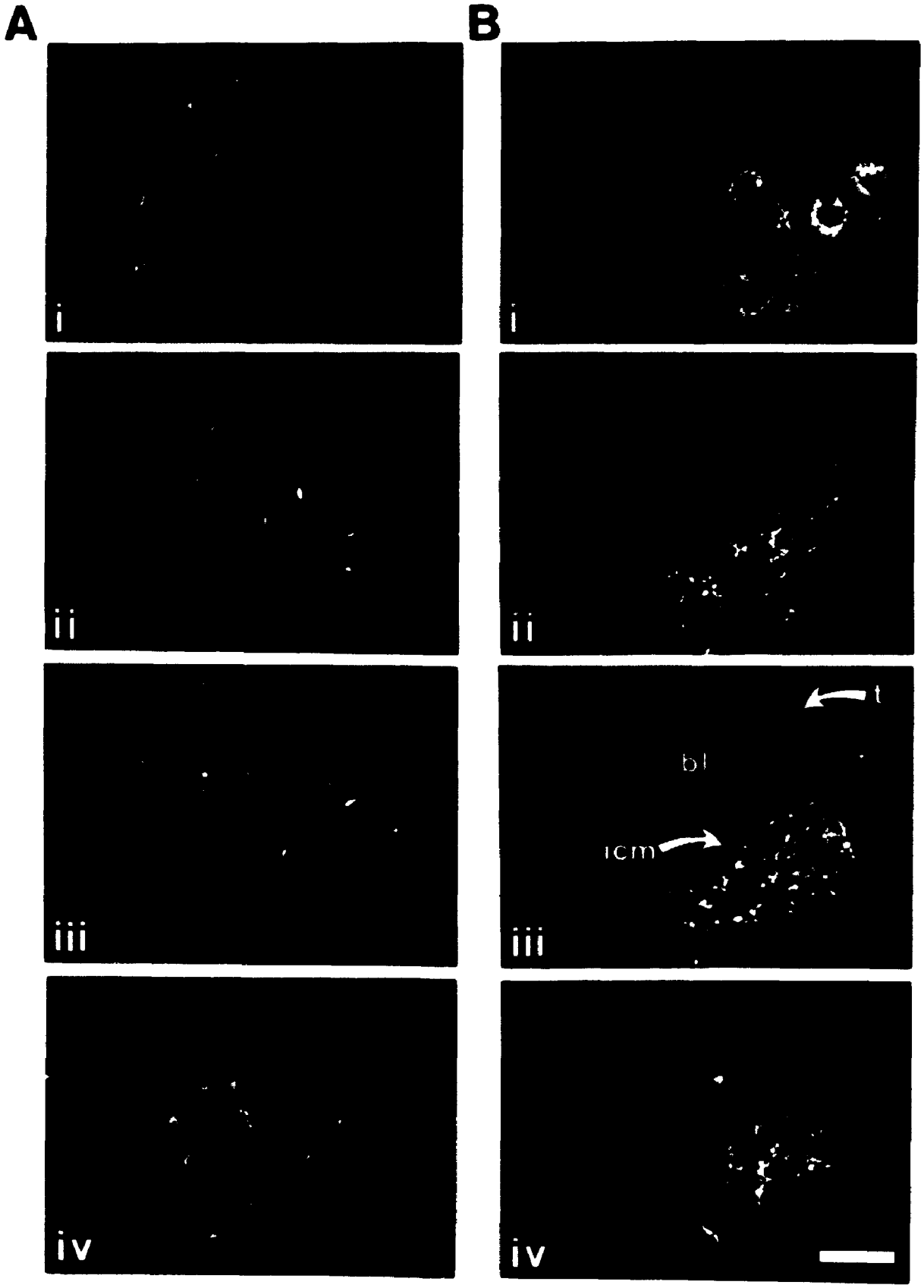
A
B
i
ii
iii
iv
i
ii
t
bl
icm
iii
iv

Occasionally both anti-Cx43/252 and anti-Cx43/302 were observed to stain the nuclei of treated embryos. Although this phenomenon was specific to the immune sera, it tended not to affect all of the embryos in a population or all of the cells within an affected embryo. Nuclear staining tended to be associated with experiments utilizing antisera which had been stored at 4°C for prolonged periods (*i.e.* one month or greater), and was accentuated by extraction with 0.1% Triton-X (Fig. 2.7 B).

To assess the specificity of anti-Cx43/302 staining patterns, 8- to 16-cell morulae were blindly scored. Small, diffuse cytoplasmic foci, punctate plaque-like foci, and zonular staining of apposed membrane regions were detected in 92%, 100%, and 70% of embryos respectively, stained with anti/Cx43/302 (n=61; Table 2.1). None of these staining patterns were ever observed using preimmune serum (n= 28) or secondary antibody alone (n=29), or if anti-Cx43/302 was preabsorbed with the peptide prior to use (n=28) (Fig. 2.6 E,F).

Given the discrepancy between the presence and absence of Cx43 in the cytoplasm of precompaction embryos as visualized with anti-Cx43/252 versus anti-Cx43/302, I sought to determine if the distribution of observed with the former antibody could be reproduced with other Cx43 specific antibodies. Using an antibody directed against a third cytoplasmic C-terminal domain (a.a. 360-382) of rat Cx43, sharing 100% amino acid sequence identity with the mouse sequence, Cx43 was detected in the cytoplasm of both pre- and post-compaction embryos, as well as in plaque-like structures in the latter (Fig. 2.8). Of 19 precompaction (4-cell) embryos,

Figure 2.8. Cx43 distribution depicted by anti-Cx43/360. Affinity-purified antibody against a third C-terminal peptide unique to Cx43 (A.A. 360-382) detects antigen in the cytoplasm of both 4-cell embryos (A) and morulae (B), as well as in gap junction-like structures (arrowheads) in the latter. Large irregular patches of fluorescent staining, consisting of tight clusters of numerous discrete foci, are detected predominantly in the cortical cytoplasm of 4-cell embryos (solid arrows). This staining pattern is qualitatively similar to that visualized with anti-Cx43/252 (Fig. 2.5), and different from the diffuse foci seen in the cytoplasm of morulae (open arrows). Images are confocal z-series projections (2 μm thick). Scale bar = 25 μm.

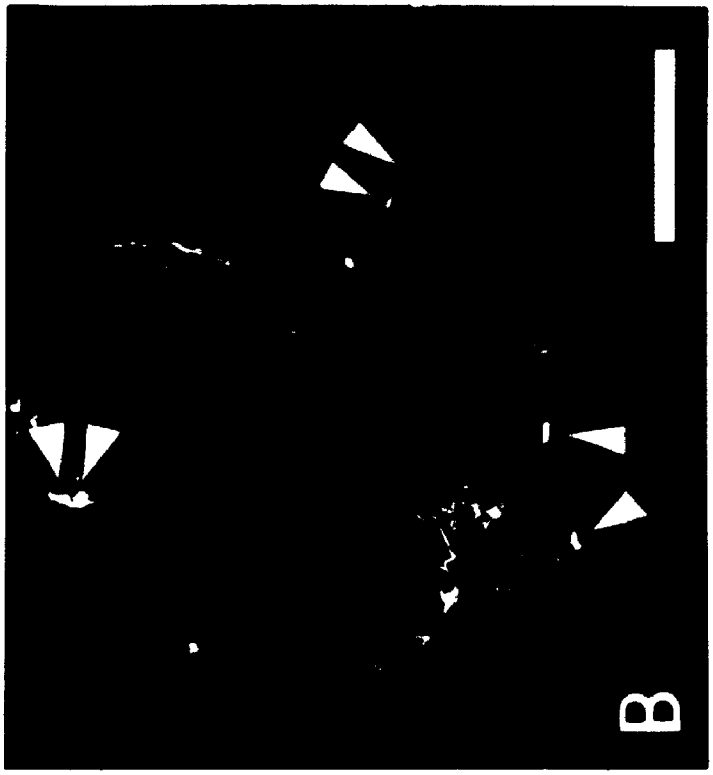
B


A

all exhibited a large irregular cytoplasmic staining pattern reminiscent of that which had been seen with anti-Cx43/252. Optical sectioning revealed that this staining pattern was localized predominantly in the cortical cytoplasm, and consisted of structures measuring up to 5 μm, composed of tight clusters of numerous discrete foci (Fig. 2.6 A). Of 38 morulae labeled with anti-Cx43/360, 87% showed the small, diffuse, cytoplasmic foci reminiscent of that seen with the other antisera at this stage, whilst 100% showed gap junction plaque-like structures. No zonular staining of apposed membranes was observed with this antibody (Table 2.1). In addition no nuclear staining was observed in any of the embryos sampled.

Lastly, during the course of the immunofluorescence experiments described above it was found that gap junction plaque-like staining for Cx43 in morulae depicted with all three antibodies was prominent at apposed membrane regions bordering both mitotic and interphase cells (Fig. 2.9).

2.33 Connexin43 contributes to gap junctions in morulae and in cumulus-oocyte complexes.

Anti-Cx43/302 and anti-Cx43/360 were tested for their ability to label gap junctions in cells known to express Cx43. For this purpose, cumulus-oocyte complexes (COCs) from secondary antral follicles isolated from the ovaries of either PMSG-primed females or females treated with PMSG as well as hCG, were embedded in LR White for immunogold electron microscopy. Gap junction plaque-like staining

Figure 2.9. Detection of Cx43 at mitotic boundaries. Postcompaction 8 cell embryo immunofluorescently stained with anti-Cx43/302 to visualize Cx43 (A), and Dapi to stain DNA (B). Cx43 is detected in bright, gap junction plaque like structures at the apposed membrane regions bordering both mitotic and interphase cells. Similar results were observed in morulae stained with both anti-Cx43/252 and anti Cx43/360. The image in (A) is a confocal z-series projection (3 μm thick). The image in (B) was obtained by conventional epifluorescence microscopy. Scale bar = 25 μm.

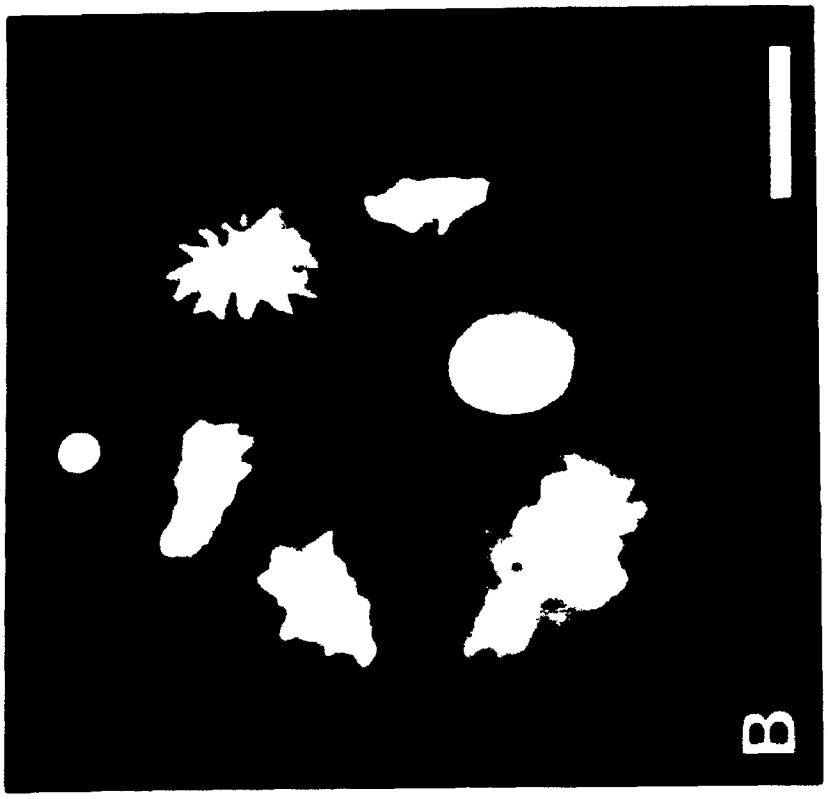
B


A

for Cx43 has previously been shown by others between cumulus cells in cryosections of whole rat ovary using two antisera specific for Cx43 [the first being anti-Cx43/252 used above (Beyer *et al.*, 1989) and the second being directed against a.a. 131-142 of rat Cx43 (Risek *et al.*, 1990)]. In addition, mRNA for Cx43 has been detected in both mouse oocytes and cumulus cells (Valdimarsson *et al.*, 1991; Nishi *et al.*, 1991). COCs were also chosen to determine whether Cx43 could be detected in gap junctions between cumulus granulosa cells and the oocyte.

Both anti-Cx43/302 and anti-Cx43/360 specifically labeled gap junctions between cumulus granulosa cells, as well as gap junctions at the oocyte surface. Labeled cumulus-cumulus (C-C) gap junctions included both those found between cell bodies (Fig. 2.10 B; 2.11 A,B), and those found between cumulus extensions traversing the zona pellucida which surrounds the oocyte (Fig. 2.10 A). Cumulus-oocyte (C-O) gap junctions reside at the surface of mammalian oocytes (Anderson and Albertini, 1976). In support of this, cumulus cell extensions, distinguishable from the oocyte and the zona pellucida by their greater electron density, occasionally were visualized to one side of gap junctions at the oocyte surface (Fig. 2.11 D). Frequently however, no associations between oocyte surface gap junctions and cumulus extensions were apparent (Fig. 2.10 D,E). Both C-C and C-O gap junctions were evenly labeled on both sides. In contrast, little or no labeling of either C-C or C-O gap junctions was apparent using the preimmune sera for either antibody (Fig. 2.10 C,E, 2.11 C,E).

Figure 2.10. Detection of Cx43 in gap junctions at the oocyte surface and between cumulus cells in non-osmicated COCs labeled with anti-Cx43/302. Secondary (antral) follicles isolated from PMSG-primed mouse ovaries were fixed with glutaraldehyde alone and embedded in LR white for immunoelectron microscopy, as described in section 2.23. Gap junctions at the oocyte surface (open arrows), between cumulus extensions traversing the zona pellucida (small solid arrows), and between cumulus cell bodies (large solid arrows), were labeled specifically with 10 nm gold particles in sections treated with anti-Cx43/302 (A, B, D). No such labeling was seen in similar sections stained with preimmune serum (C, E). Cumulus extensions (CE), Oocyte (Oo), Zona pellucida (ZP). Nuclei (N). Scale bars 400 nm.

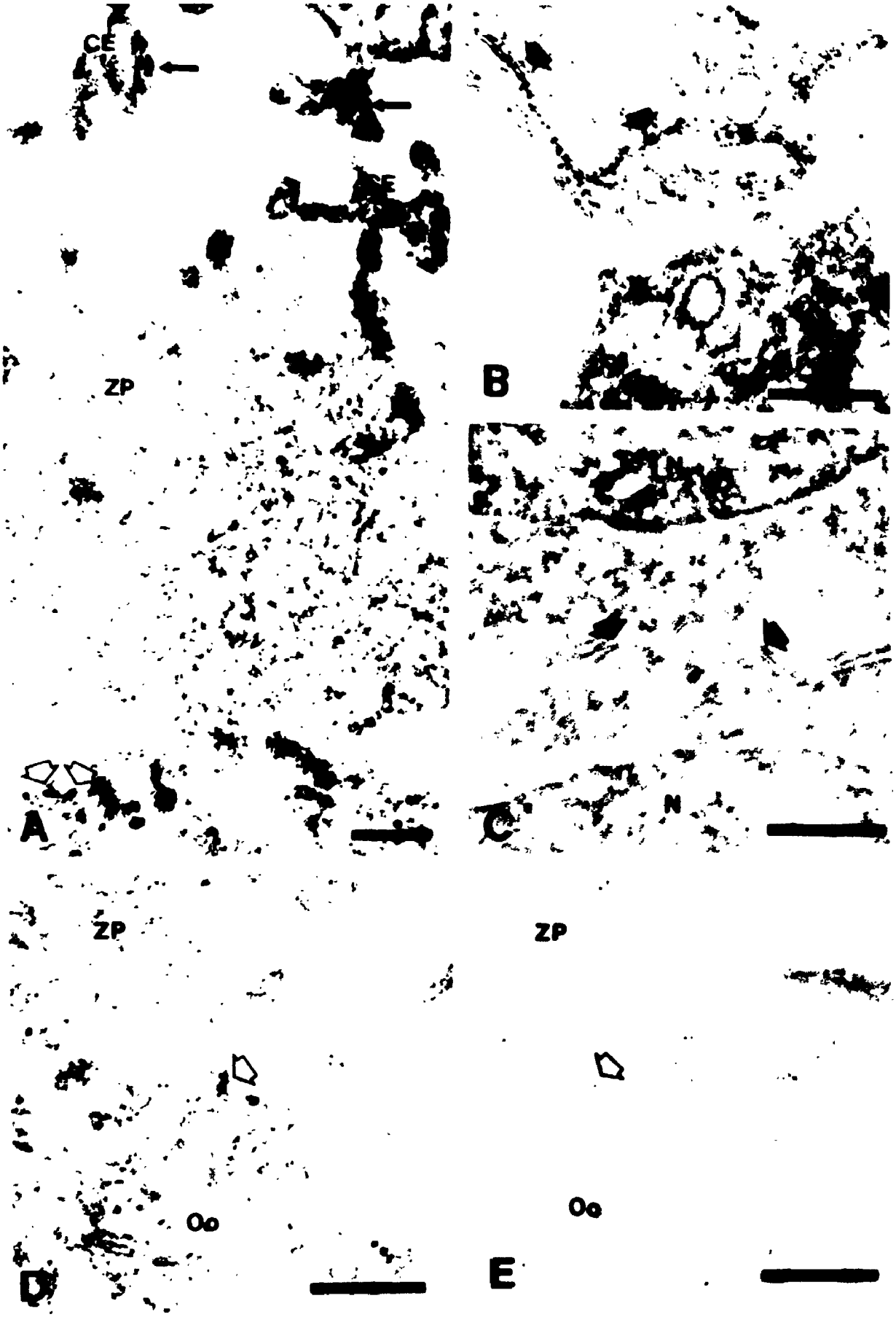
CE
ZP
A
B
N
C
ZP
ZP
Oo
D
Oo
E

Figure 2.11. Detection of Cx43 in gap junctions at the oocyte surface and between cumulus cells in osmicated COCs labeled with anti-Cx43/360. Secondary (antral) follicles isolated 34 hr post-hCG were fixed with glutaraldehyde and post-fixed briefly with OsO_4 before being embedded in LR White. Gap junctions between cumulus cells (solid arrow in A, B), and at the oocyte surface (open arrow in D), were labeled specifically with 10 nm gold particles in sections labeled with anti-Cx43/360. Occasionally, gap junctions at the oocyte (Oo) surface were found at the tips of electron dense cumulus extensions (CE), supporting that these structures represented cumulus oocyte (C-O) gap junctions. Little, if any, labeling of gap junctions between cumulus cells (C), or cumulus cells and the oocyte (E) was observed with preimmune serum. Zona pellucida (Zp). Nuclei (N). Scale bars 600 nm.

Cx32 protein in the embryo likely originates from the ovarian oocyte where it may be used in mediating communication with surrounding cumulus cells. This is discussed in section 2.44.

2.42 Connexin43 distribution in the cytoplasm of preimplantation embryos.

In the present study, Cx43 was detected by immunofluorescence in the cytoplasm of precompaction embryos, and in the cytoplasm and apposed membranes of postcompaction embryos. These results are summarized together with those for Cx32 in Table 2.4. Cx43 distribution in the cytoplasm was observed to undergo qualitative changes co-incident with the appearance of gap junction-like structures, suggesting a shift in the distribution of this protein through cytoplasmic organelles during gap junction assembly. In precompaction embryos Cx43 was distributed in large irregular patches up to 5 μm in length which, using the CLSM, were revealed to consist of numerous discrete foci, and to reside predominantly in the cortical cytoplasm. In contrast, cytoplasmic foci in compacted embryos were dispersed throughout the cytoplasm. Although it was not possible to localize Cx43 in identifiable organelles in embryos viewed at the level of the electron microscope, the clustered nature of cytoplasmic Cx43 staining and its cytocortical distribution in precompaction embryos is reminiscent of endosome clusters typically found in both pre- and postcompaction mouse embryo blastomeres (Calarco and Brown, 1969; Dvorak *et al.*, 1985; Fleming and Pickering, 1985; present study, Fig. 2.13 and 3.5 A).

Antigenicity for both anti-Cx43 antibodies was retained regardless of whether tissues were fixed in 1% paraformaldehyde or 1.6% glutaraldehyde. Anti-Cx43/302 antigenicity was irreversibly lost if tissues were briefly (15 min) post-fixed with 1% OsO_4. Although this brief osmication also reduced anti-Cx43/360 antigenicity, it could be regained by etching sections with either H_2O_2 or $NaIO_4$. There were no apparent differences in the labeling of antral follicle COC gap junctions from either PMSG primed or ovulated females.

Anti-Cx43/360 was used to confirm the contribution of Cx43 to gap junctions in the mouse embryo. To compare directly the labeling of embryos with that seen in COCs, 8-16 cell morulae were fixed, embedded, and etched exactly as for COCs (ie. fixed with 1.6% glutaraldehyde, post-fixed for 15 min with OsO_4, *en bloc* stained with saturated uranyl acetate, embedded in LR White, and etched for 1 hr with $NaIO_4$). So as not to bias interpretation of the specificity of anti-Cx43/360 labeling as opposed to that seen with preimmune serum, unequivocal gap junctions were classified as labeled if they possessed as little as one 10 nm gold particle within 10 nm of their structure. Only about 10% of C-C, C-O, or morula gap junctions stained with preimmune sera were "labeled", and this labeling tended to consist of only 1 gold particle (Fig. 2.11 C). Immune treated gap junctions were labeled more heavily with gold particles. Using a Student t-test the difference in the number of gold particles per immune-treated versus preimmune treated C-C gap junctions was significant (Table 2.2). Anti-Cx43/360 labeled 100% of C-C gap junctions, and almost 90% of C-O gap junctions. However, only 70% of the morula gap junctions seen were labeled with this

Table 2.2

Anti-Cx43/360 immunogold labeling of gap junctions in mouse COC[†] and morulae[♦]

G.J. Type	Antibody	Percentage of G.J. Labeled[§]	No. Gold Particles per Labeled G.J.[¤]
C-C[†]	anti-Cx43/360	100 (n = 47)	31.3 ± 17.5[*] (n = 12)
	preimmune	12 (n = 57)	1.6 ± 1.5[*] (n = 7)
C-O[†]	anti-Cx43/360	89 (n = 18)	3.4 ± 1.6 (n = 8)
	preimmune	9 (n = 22)	1.0 (n = 2)
Morula	anti-Cx43/360	70 (n = 20)	4.5 ± 2.1 (n = 13)
	preimmune	11 (n = 9)	1.0 (n = 1)

♦ COCs and morulae were prepared and processed identically by fixation in 1.6% glutaraldehyde, post-fixation for 15 min with OsO_4, *en bloc* with saturated aqueous UA, embedment in LR-White and etching for 1 hr with saturated aqueous $NaIO_4$.

† G.J. found between cumulus granulosa cells (C-C) and these cells and the oocyte (C-O) in cumulus-oocyte-complexes (COC) isolated from fully grown antral follicles, 34 hr post-hCG.

§ Labeled G.J. were those in which 1 or more 10 nm gold particles could be found within 10 nm of the junction.

¤ Mean ± standard deviation.

* Significant difference ($p \leq 0.005$) found by Student t-test.

antibody (Table 2.2). Unlabeled and labeled immune-treated gap junctions in morulae were frequently found together in the same embryo (Fig. 2.12 A,B), as well as side by side along the same apposed membrane region. I did not observe any immune-specific labeling of membrane outside of gap junctions that was reminiscent of the zonular staining of apposed membranes seen earlier with immunofluorescence.

C-C gap junctions labeled with anti-Cx43/360 appeared to have more gold particles associated with them, than either C-O or morula gap junctions (Table 2.2). This difference, however, could easily be attributed to the large size of C-C gap junctions compared to the others. In order to compare directly the labeling of these junctions with anti-Cx43/360, the labeling density of junctions, defined as the number of gold particles per μm of labeled gap junction, was calculated from sampled micrographs. Using a Student t-test, no significant differences were found between the labeling densities of C-C, C-O, and morula gap junctions (Table 2.3). Thus, although there were fewer C-O and morula gap junctions which contain Cx43, compared with C-C gap junctions, there was no difference in the density of Cx43 in those gap junctions which contained this protein.

In hopes of being able to localize Cx43 in the cytoplasmic organelles of embryos, 8- to 16-cell morulae fixed and embedded in Epon-Araldite, as described for conventional electron microscopy, were labeled with anti-Cx43/360. After etching sections for 3 hr with supersaturated $NaIO_4$ at 37°C, gap junctions in this well-preserved tissue could be labeled specifically with anti-Cx43/360 (Fig. 2.12 C).

Figure 2.12. Cx43 is detected in some but not all gap junctions in morulae. Morulae embedded in LR White (A,B), as described for osmicated secondary follicles, or Epon-Araldite (C,D), as described for conventional electron microscopy (section 2.23), were sectioned and immunogold labeled with anti-Cx43/360. Under conditions which labeled all gap junctions between cumulus cells (Table 2.2), both labeled (A) and unlabeled (B) gap junctions (arrows) were apparent in morulae. Similarly, both labeled (C) and unlabeled (D) gap junctions were apparent in Epon-Araldite embedded morulae, although no labeling of cytoplasmic organelles distinct from that seen with preimmune serum was seen. Mitochondria (M), Endosome (E). Scale bars 400 nm.

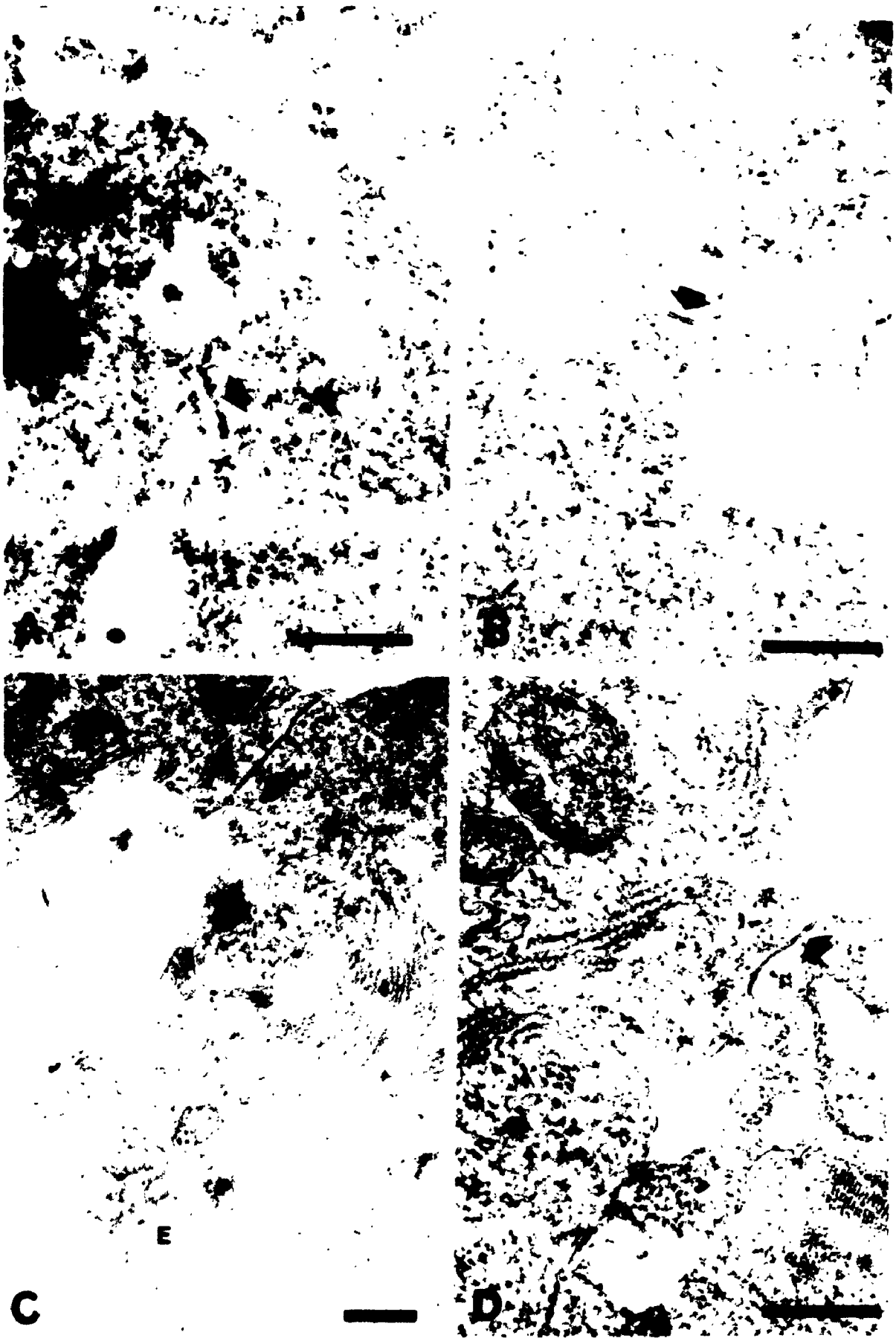
A
B
E
C
D

Table 2.3

Anti-Cx43/360 immunogold labeling density of gap junctions in mouse COC[†] and morulae

G.J Type	G.J. Length[¤] ($\times 10^{-1}\mu m$)	No. Gold Particles per μm Labeled G.J.[¤,♦]
C-C[†]	8.79 ± 3.61[a,b] (n=26)	32.4 ± 8.9[d,e] (n 12)
C-O[†]	1.06 ± 0.41[c] (n=21)	32.9 ± 17.5[f] (n 8)
Morula	1.37 ± 0.62 (n=25)	34.5 ± 13.3 (n 13)

† G.J. found between cumulus granulosa cells (C-C) and these cells and the oocyte (C-O) in cumulus-oocyte-complexes (COC) isolated from fully grown antral follicles, 34 hr post-hCG.

¤ Mean ± standard deviation.

♦ As determined from micrographs of labeled G.J. where the number of gold particles within 10 nm of a junction were counted and divided by the length of the junction.

a Significant difference ($p \leq 0.005$), compared with C-O gap junction length.

b Significant difference ($p \leq 0.005$) compared with morula gap junction length.

c No significant difference ($p \leq 0.005$), compared with morula gap junction length.

d No significant difference ($p \leq 0.005$), compared with gold particle density in C-O gap junctions.

e No significant difference ($p \leq 0.005$), compared with gold particle density in morula gap junctions.

f No significant difference ($p \leq 0.005$), compared with gold particle density in morula gap junctions.

However, even under these extreme conditions, no organelle specific labeling distinct from that seen in preimmune treated sections could be discerned. Although gap junctions in these morulae tended to be larger, presumably due to the improved fixation, unlabeled gap junctions were still apparent in these preparations (Fig. 2.12 D).

Lastly, although it was not possible to immunolocalize Cx43 in cytoplasmic organelles, 4-cell embryos were examined by conventional electron microscopy (Fig. 2.13) to identify organelles which could correspond to the large irregular cytoplasmic Cx43 staining seen in precompaction embryos by immunofluorescence. Cell and organelle structure of embryos was similar to that reported previously by others (Dvorak *et al.*, 1985). Readily identifiable organelles included mitochondria, lipid droplets, lysosomes, and Golgi complexes. Also evident were clusters up to 2 μm in diameter of electronlucent vacuoles surrounded by tubular and vesicular structures. These vacuoles have previously been identified as a prelysosomal endocytotic compartment ("endosomes") on the basis of their ability to accumulate exogenous horseradish peroxidase tracer (Reeve, 1981; Fleming and Pickering, 1985). Endosome clusters represented the largest cytoplasmic organelle complex in 4-cell embryos, whose structure was reminiscent of the Cx43 staining pattern seen at this stage. These structures were distributed throughout the cytoplasm and near the plasma membrane.

Figure 2.13. 4-cell embryo organelle structure and distribution. By conventional transmission electron microscopy a variety of readily identifiable organelles are apparent including mitochondria (M), lipid droplets (L), Golgi complexes (GC), and lysosomes (Ls). Also evident are endosome clusters (EC), up to 2 μm in diameter, consisting of electronlucent vacuoles surrounded by tubular and vesicular membranes. Box in (B) is magnified to give panel (A). Box in (A) is magnified to give panel (C). Nuclei (N). Plasma membrane (PM). Scale bars 2 μm (A), 5 μm (B), and 500 nm (C,D,E).


A
PM

2.4 Discussion.

2.41 Putative roles of connexin32 in the mouse embryo.

Using an antiserum directed against a rat Cx32 amino acid sequence (a.a. 223 244) 90% identical to that of the mouse, and the same monoclonal antibody originally found to detect Cx32 by Western blotting analysis throughout preimplantation development (Barron *et al.*, 1989), Cx32 was not localized in either the cytoplasm or plasma membrane of early embryos. However, using immunofluorescence and immunogold microscopy these same antibodies were found to recognize gap junctions in mouse liver processed in a similar manner (summarized in Table 2.4). These results add to previous unsuccessful attempts by others with two different peptide specific antibodies, the first directed against a.a. 98-124 of rat Cx32 (100% identical to the mouse sequence; Barron and Kidder, unpublished), and the second against a.a. 262-280 of human Cx32 (72% identical to the mouse sequence, and 100% identical between a.a. 267-280; Nishi *et al.*, 1991).

The failure to localize Cx32 *in situ* in embryos can be interpreted in two ways. First, it is possible that Cx32 is uniformly distributed throughout the cytoplasm and the plasma membrane of blastomeres. Under these circumstances, the putative contribution of Cx32 to any one gap junction in the embryo would be minimal, and likely to be of little significance. Alternatively, it remains possible that Cx32's contribution to gap junctions in the early embryo is masked either through post

Table 2.4

Summary of immunocytochemical results for Cx32 and Cx43 primary antibodies

Antibody	Epitope(s)	Similarity of epitope to mouse	Immunocytochemical result			
			Liver	Pre-compact. embryos	Post-compact. embryos	COCs[α]
M12.13	27 kD rat liver g.j. protein (cytoplasmic surface)	Unknown	+[b]	-	-	N.D.[◆]
Anti-Cx32/223'	Rat Cx32 a.a. 223-244	90%	+[b,B]	-	-	N.D.
Anti-Cx43/252'	Rat Cx43 a.a. 252-271	100%	N.D.	+[a]	+[a,b]	N.D.
Anti-Cx43/302'	Rat Cx43 a.a. 302-319	94%	N.D.	-	+[a,b]	+[B,•]
Anti-Cx43/360'	Rat Cx43 a.a. 360-382	100%	N.D.	+[a]	+[a,b,B]	+[B,•]

' Antibody is directed against a synthetic peptide representing a connexin specific amino acid sequence, predicted from the cDNA for that connexin.

α Cumulus-oocyte complexes.

◆ Not determined.

a Immunofluorescent cytoplasmic staining.

b Immunofluorescent gap junction plaque-like staining.

B Immunogold labeling of gap junctions.

• Immunogold labeling of both cumulus-oocyte (C-O) and cumulus-cumulus (C-C) gap junctions.

translational modifications (such as phosphorylation) or association with other proteins, or conformational changes arising from either of the previous factors making the epitopes sought to date inaccessible. Such, in fact, is believed to be the case for the amino terminus of rat liver Cx32 which does not appear to be accessible to proteases or to interaction with an antibody specific to the amino terminal region of the molecule (a.a. 7-21; Zimmer *et al.*, 1987). The inability of four different Cx32 antibodies to localize this protein in embryos, whilst localizing it in liver, would argue not only that such masking would be substantial, but also highly specific to preimplantation development. Based on the specificity of the peptide sequences recognized by three of the four antibodies tested to date, one would predict that in the preimplantation mouse embryo at least three distinct cytoplasmic domains of Cx32 spanning a.a. 98-124, 223-244, and 267-280 may be modified in such a manner that denies their accessability.

Putative masking of Cx32 may correlate with the functional regulation of Cx32 channel permeability *in vivo*. Calmodulin is one protein hypothesized to regulate gap junction channel permeability by direct interaction with channel subunits. This protein is believed to mediate the inhibitory effect of elevated Ca^{2+} and even H^+ concentrations on channel conductance (Peracchia, 1989). Calmodulin has been shown to bind to Cx32 purified from liver gap junctions in a Ca^{2+}-dependent manner (Zimmer *et al.*, 1987). Recently, this binding activity was attributed to two peptides corresponding to domains at the amino-terminus (a.a. 1-21) and carboxy-terminus (a.a. 216-230) of Cx32 (Evans *et al.*, 1992). Although the second of these overlaps

with the anti-Cx32/223 sequence recognized in liver but not embryos, the former corresponds to a region previously deemed to be inaccessible in liver (Zimmer *et al.*, 1987). Rat liver Cx32 has also been shown to possess two Ca^{2+}-independent calmodulin binding domains located in cytoplasmic regions of the protein (Zimmer *et al.*, 1987). The Ca^{2+}-independence of this interaction may be analogous to the situation in phosphorylase kinase, where calmodulin acts as an integral subunit of the enzyme in close association with its catalytic subunit (Picton *et al.*, 1980).

The functional involvement of Cx32 in gap junctional coupling in the preimplantation embryo has yet to be conclusively demonstrated. Antibodies against Cx32, isolated as a 27 kD rat liver gap junction protein, have been reported to uncouple and decompact injected 8-cell mouse blastomeres (Lee *et al.* 1987). These antibodies were also found to stain the surface membranes of morulae with a punctate pattern. However, these antibodies were previously also reported to block junctional communication in the amphibian embryo (Warner *et al.*, 1984) and *Hydra* (Fraser *et al.*, 1987), indicating that the epitopes recognized by them are highly conserved during evolution. It is now recognized that the antibodies used in these studies may detect other connexins by recognizing at least one conserved conformational epitope (Milks *et al.*, 1988). Uncoupling and decompaction of blastomeres has also been reported following microinjection of Cx32 antisense RNA (Bevilacqua *et al.*, 1989). The apparent absence of Cx32 mRNA in preimplantation embryos makes it likely however, that the antisense RNA in that experiment was cross-hybridizing with the mRNAs of other connexins transcribed in the embryo, presumably including Cx43.

Cx32 protein in the embryo likely originates from the ovarian oocyte where it may be used in mediating communication with surrounding cumulus cells. This is discussed in section 2.44.

2.42 Connexin43 distribution in the cytoplasm of preimplantation embryos.

In the present study, Cx43 was detected by immunofluorescence in the cytoplasm of precompaction embryos, and in the cytoplasm and apposed membranes of postcompaction embryos. These results are summarized together with those for Cx32 in Table 2.4. Cx43 distribution in the cytoplasm was observed to undergo qualitative changes co-incident with the appearance of gap junction-like structures, suggesting a shift in the distribution of this protein through cytoplasmic organelles during gap junction assembly. In precompaction embryos Cx43 was distributed in large irregular patches up to 5 μm in length which, using the CLSM, were revealed to consist of numerous discrete foci, and to reside predominantly in the cortical cytoplasm. In contrast, cytoplasmic foci in compacted embryos were dispersed throughout the cytoplasm. Although it was not possible to localize Cx43 in identifiable organelles in embryos viewed at the level of the electron microscope, the clustered nature of cytoplasmic Cx43 staining and its cytocortical distribution in precompaction embryos is reminiscent of endosome clusters typically found in both pre- and postcompaction mouse embryo blastomeres (Calarco and Brown, 1969; Dvorak *et al.*, 1985; Fleming and Pickering, 1985; present study, Fig. 2.13 and 3.5 A).

In well preserved specimens, fixed with glutaraldehyde and OsO_4, endosome clusters collectively measure up to 2 μm in diameter (Calarco and Brown, 1969; present study). Although this is smaller than the structures visualized by immunofluorescence with the CLSM, this discrepancy could be attributed to the poor structural preservation arising from the paraformaldehyde fixation used for the immunofluorescence procedure. Thus, Cx43 in the cytoplasm of precompaction embryos may consist predominantly of oogenetically derived protein, endocytosed from the plasma membrane where it was used to make gap junctions with surrounding cumulus cells in the ovary (see section 2.44 for discussion). Since endosomes are organelles which sort internalized components for further processing (Helenius *et al.*, 1983), it is possible that oogenetic Cx43 is also recycled to the surface for utilization in embryonic gap junctions. Such a finding would be consistent with the relative insensitivity of gap junction formation to inhibition of transcription and translation from the 4-cell stage onward (McLachlin *et al.*, 1983; McLachlin and Kidder, 1986).

2.43 Connexin43 distribution in the apposed membrane regions of postcompaction embryos.

Plaque-like Cx43 staining in compacting embryos was always confined to apposed membrane regions. Given the absence of surface staining for either Cx43 or Cx32, prior to the appearance of this staining pattern, it is unlikely that the *de novo* assembly of gap junctions at this time occurred as a result of lateral diffusion of connexons already existing in the plasma membrane. No structures reminiscent of

formation plaques have been reported in freeze fracture analysis of compacting mouse embryos (Magnuson *et al.*, 1977). Thus, *de novo* gap junction assembly in the preimplantation mouse embryo is likely achieved through the delivery of connexins/connexons to apposed membrane regions.

Although maintenance of the compacted state in embryos is dependent upon intercellular communication via gap junctions (Buehr *et al.*, 1987), it is unlikely that this requirement applies to the achievement of the compacted state. Compaction in the mouse embryo is mediated by the calcium-dependent cell adhesion molecule E-cadherin (also known as uvomorulin; Shirayoshi *et al.*, 1983). Premature induction of compaction at the 4-cell stage with activators of protein kinase C , causes a rapid shift in the localization of E-cadherin to apposed membrane regions (Winkel *et al.*, 1990), without a concomitant establishment of functional gap junctional coupling (Valdimarsson and Kidder, manuscript in preparation). Thus, it is unlikely that interaction of connexon pairs across apposed membranes in the compacting embryo plays a role in bringing these membranes together as found in reaggregating Novikoff cells (Meyer *et al.*, 1992).

In morulae, plaque-like structures were found to be equally prominent at both mitotic and interphase cell boundaries. Gap junctional coupling between blastomeres of preimplantation mouse embryos is lost or greatly reduced as they enter mitosis (Goodall and Maro, 1986). This finding demonstrates that mitotic blastomeres must down-regulate their junctional conductance through gating mechanisms rather than

plaque disassembly. Regulation of junctional activity could be mediated through cell cycle-dependent oscillations of a second messenger such as Ca^{2+}, or could involve phosphorylation of specific amino acid residues. Indeed, phosphorylation of tyrosine 265 of Cx43 by $p60^{v\text{-}src}$ abolishes Cx43-induced intercellular coupling between paired *Xenopus* oocytes (Swenson *et al.*, 1990). Furthermore, the normal cellular *src* kinase, $p60^{c\text{-}src}$, is itself subject to cell cycle regulation (its activity increases during fibroblast mitosis), and this is associated with phosphorylation by $p34^{cdc2}$, the catalytic subunit of MPF (maturation or M-phase promoting factor; Chackalaparampil and Shalloway, 1988; Shenoy *et al.*, 1989; Morgan *et al.*, 1989). Thus, a possible sequence of phosphorylations exists that could explain the mitosis-specific gating of Cx43 containing channels.

With increasing cell number following compaction, Cx43 was also detected in apposed membrane regions in zonular arrays. These arrays were confined to the basolateral domains of outer blastomeres of morulae and their descendants, the trophectoderm in blastocysts. Becker *et al.* (1992) detected a similar staining pattern in mouse morulae and blastocysts immunofluorescently stained with a different Cx43 antibody from those used in the present study. This distribution is likely related to the organization of the trophectoderm as an epithelium. In the trophectoderm, gap junction plaques and adherens type-junctions (desmosomes) lie adjacent to and interspersed along *zonula occludens* (tight) junctions (Ducibella *et al.*, 1975; Magnuson *et al.*, 1977). Zonular staining of apposed membrane regions in the trophectoderm has also been reported for components of both desmosomes

(desmoplakin 3) and tight junctions (ZO-1 and cingulin; Fleming *et al.*, 1991, 1989, 1993). Due to the intermediate intensity of the zonular staining between the brightly staining plaque-like structures and the diffuse cytoplasmic foci as seen in the CLSM, it seems likely that in the case of Cx43 this zonular pattern represents an intermediate distribution of either connexins or connexons in apposed membrane regions but outside of plaque-like aggregations. Although the ICM has also been reported to contain both adherens and occludens-type junctions, zonular arrays of the latter are confined to the trophectoderm (Magnuson *et al.*, 1977). Connexins or connexons outside of plaques may serve as a reservoir of subunits for an expansion of gap junctions later in development, or alternatively may represent channel protein prior to being internalized for degradation.

It is interesting that in morulae, no zonular staining at apposed membrane regions was observed with anti-Cx43/360. Nishi *et al.* (1991) similarly did not detect any zonular staining in the trophectoderm of blastocysts using their antibody against a similar domain. Thus the most distal C-terminal domain of Cx43 may be differentially altered once this protein is outside of gap junction plaques but still in the plasma membrane. Recognition of the peptide sequence detected by anti-Cx43/360 may correlate with the functional control of junctional permeability. Anti-Cx43/360 has been found to inhibit dye transfer in neonatal rat cardiac myocytes. Although this inhibition required that these cells be microinjected with the antibody in medium containing 0.5 to 1.0 mM calcium, such concentrations of calcium alone had no apparent effect on intercellular communication (Lal *et al.*, in press). Dye coupling

under these conditions is also inhibited with an antibody against a phylogenetically conserved amino terminal domain of Cx43 (a.a. 2-21), but not against a less conserved domain within the cytoplasmic loop of this protein (a.a. 100-122; Yancey *et al.*, 1989; Lal *et al.*, in press). Although the C-terminal domain of Cx43 is generally considered more variable in different connexins, the peptide region recognized by anti-Cx43/360 contains three potential phosphorylation sites, shared with at least one other member of the connexin gene family (Cx31.1; Hoh *et al.*, 1991). For this reason it is argued that the antibodies most effective in blocking dye coupling are those directed against conserved portions of the connexin molecule (Lal *et al.*, in press). This is in agreement with previous antibody blocking experiments directed against Cx32 (Warner *et al.*, 1984; Fraser *et al.*, 1987; Lee *et al.*, 1987), and raises the possibility that all connexins gate junctional permeability by the same mechanism.

2.44 Contribution of connexin43 to gap junctions in morulae and cumulus-oocyte complexes.

Using immunogold electron microscopy, gap junctions between cumulus granulosa cells (C-C), cumulus cells and the oocyte (C-O), and between compacted blastomeres in morulae, were labeled specifically with Cx43 antibodies. In all cases junctions were similarly labeled on both sides of their structure, suggesting in each case that these channels may have been formed by the pairing of Cx43 connexons in apposed membranes.

Gap junctions between cumulus cells were similar in size to those reported previously (Larsen *et al.*, 1981) and larger than either of the other two types of junction. Regardless of this, there was no difference in the contribution of Cx43 per unit length of junction, as assessed by labeling with anti-Cx43/360. However, under conditions which specifically labeled 100% of C-C gap junctions, at least 30% of morula gap junctions and 10% of C-O gap junctions failed to show evidence of Cx43. Based on previous discussions, the apparent Cx43-less junctions may have contained Cx43 modified in such a manner as to not be recognized by the antibody used, perhaps as a result of gating (see sections 2.41, 2.43). However, there were no apparent structural differences between labeled and nonlabeled junctions in these cells. An alternative explanation is that other members of the connexin gene family are expressed in these cells, to form heterotypic gap junctions (*i.e.* gap junctions composed of different types of connexins). In support of heterotypic gap junctions between embryonic blastomeres, preliminary results suggest that mRNA for at least five other connexins (Cx30.3, 31, 31.1, 40, and 45) can be detected throughout preimplantation development (Zhu and Kidder, personal communication). In the ovary, both C-C and C-O gap junctions may also be heterotypic. Transcripts for Cx32 mRNA have been reported in both cumulus cells and ovarian oocytes, declining precipitously in the latter following hormonal stimulation (Valdimarsson *et al.*, 1993). The same study also immunofluorescently detected both Cx32 and Cx43 in plaque-like structures between cumulus cells in preantral COCs, although no unequivocal structures resembling C-O gap junctions could be detected. Heterotypic gap junctions composed of Cx43 or Cx32 are exemplified in the developing limb of the mouse,

where these proteins can be seen immunofluorescently in the same optical section of the basal cells of the ectoderm, but in separate plaques (Laird *et al.*, 1992).

Since all C-C gap junctions observed in the present study were labeled positively for Cx43, the immunofluorescent detection of Cx32 between cumulus cells by Valdimarsson *et al.* (1993) suggests that C-C gap junctions may also be heteromolecular, wherein each gap junction is composed of more than one type of connexin. Heteromolecular gap junction plaques composed of Cx43 and Cx26 can be found in decidual cells adjacent to an invading trophoblast in the rat (Winterhager *et al.*, 1993). In the present study there was no evidence for the existence of heteromolecular Cx43/Cx32 gap junctions in preimplantation embryos, although heteromolecular plaques consisting of Cx43 and other members of the connexin gene family cannot be ruled out. Similarly the existence of heteromolecular Cx43/Cx32 C-O gap junctions cannot be discounted.

Since Cx43 is utilized by the oocyte in C-O gap junctions, and this protein is detected in endosome-like structures in the cortical cytoplasm of precompaction embryos, it is possible that oogenetic Cx43 is recycled to the plasma membrane for use in embryonic gap junctions. Based on studies in the rat, oocytes lose most if not all of their gap junctions with cumulus cells just before ovulation, although cumulus cells remain attached to the ovulated oocyte (Larsen *et al.*, 1987). Disassembly of C-O gap junctions is thought to be achieved through the lateral diffusion of their components in the plasma membrane, rather than internalization of whole plaques as

seen between cumulus cells (reviewed by Larsen and Wert, 1988). However, the lack of Cx43 staining in the plasma membrane of precompaction embryos, and the ability of ovarian oocytes and precompaction embryos to endocytose horse radish peroxidase tracer (Fleming and Pickering, 1985), suggest that, ultimately, connexins used by the oocyte in C-O gap junctions may be internalized from the cell surface.

Chapter 3

Sensitivity of nascent connexin43 and membranous organelles in the preimplantation embryo to trafficking inhibitors

3.1 Introduction.

Immunofluorescence data from chapter 2 revealed that in addition to being detected in the plasma membrane, both in and out of gap junctions, Cx43 is also extensively distributed throughout the cytoplasm of pre- and postcompaction embryos. However, since it was not possible to regain intracellular Cx43 antigenicity lost to the fixation conditions required to visualize cytoplasmic organelles, the exact intracellular location of this protein throughout preimplantation development remains unanswered.

In the present chapter my intent was to use experimental means to examine the nature of cytoplasmic anti-Cx43/302 immunoreactivity in morulae. Using cycloheximide I first determined the sensitivity of Cx43 in the cytoplasm to protein synthesis inhibition. The ability of two trafficking inhibitors, monensin and brefeldin-A (BFA), to redistribute this protein was then examined. Lastly, since the effects of monensin and BFA on preimplantation embryos have never been reported in the literature, the effects of these agents on cell and organelle structure were examined using the electron microscope.

3.2 Materials and methods.

3.21 Embryo culture and manipulation.

Morulae were flushed from the reproductive tracts of CF1 female mice, as described in section 2.21, beginning 70 hr post-hCG. Embryos were cultured in microdrops (40-50 μl) of standard egg culture medium (SECM; Spindle, 1980) under heavy paraffin oil (BDH, Toronto, Ont.), at 37°C in 5% CO_2, in the presence or absence of cycloheximide, monensin, brefeldin-A, or ethanol. Cycloheximide (Sigma Chemical Co., St. Louis, MO), was dissolved in distilled water to make a stock of 5 mg/ml, which was then diluted into culture medium to give a final concentration of 50 μg/ml (McLachlin *et al.*, 1983). Monensin (Sigma) and brefeldin-A (BFA; Epicentre Technologies, Madison, WI) were dissolved in ethanol to make a stock of 10 mg/ml, and used in culture at a concentration of 1-5 μg/ml. These concentrations were within the range reported in the literature for these agents (Donaldson *et al.*, 1990; Mollenhauer *et al.*, 1990). Ethanol was added to control cultures at the same final concentrations (0.01 to 0.05%). For immunofluorescence, embryos were fixed and processed as described in section 2.22. For conventional transmission electron microscopy, embryos were fixed and embedded in Epon-Araldite as described in section 2.23.

3.3 Results.

3.31 Cycloheximide treatment of morulae abolishes connexin43 immunoreactivity in the cytoplasm.

To determine if the Cx43-specific cytoplasmic staining detected in post-compaction embryos (chapter 2) represents nascent Cx43, 8- to 16-cell morulae were cultured for 4 hr in the presence of 50 μg/ml cycloheximide (CHX) and then immunostained with anti-Cx43/302. The frequency of immunostaining patterns was then scored blindly. Treatment of mouse embryos with cycloheximide as described above, effectively inhibits protein synthesis, causing greater than 97% inhibition of ^{35}S-methionine incorporation (McLachlin *et al.*, 1983). Cycloheximide reduced the incidence of small, diffuse cytoplasmic foci to approximately one quarter of that seen in control embryos without affecting the incidence of plaque-like foci (Table 3.1). Affected embryos were completely devoid of any cytoplasmic staining pattern above a uniform, diffuse background (Fig. 3.1).

3.32 The trafficking inhibitors monensin and brefeldin-A redistribute nascent connexin43 in the cytoplasm of morulae.

Given the likelihood that most of the Cx43-specific cytoplasmic immunoreactivity detected in morulae represents nascent connexin, the ability of protein trafficking inhibitors to redistribute this protein was next examined.

Table 3.1

Anti-Cx43/302 immunoreactivity in morulae is sensitive to inhibitors of protein synthesis and intracellular trafficking

		Morulae (%)				
		Cytoplasmic Staining			Intercellular Staining	
Treatment[1]	Number Scored	Small Diffuse Foci	Large Juxta-nuclear	Reticulated	Plaque-like foci	Zonular
Control	87	99	0	0	99	66
50 μg/ml CHX	92	26	0	0	98	55
5 μg/ml Monensin	73	100	97	0	100	69
5 μg/ml BFA	52	0	0	93	98	87

[1] Embryos were cultured for 4 hr in SECM containing either 0.05% ethanol (control) or inhibitor, prior to being fixed and processed for immunofluorescence. Culturing in the presence of 0.05% ethanol did not effect the frequency or nature of anti-Cx43/302 immunoreactivity, compared with uncultured embryos (Table 2.1). For the BFA treatment group the data are from two experiments whereas the other treatment data are from three experiments.

Figure 3.1. Cycloheximide abolishes Cx43-specific diffuse cytoplasmic foci (arrows) in morulae. Each image is a confocal *z*-series projection (1.5 μm thick) of a 16 cell morula stained with anti-Cx43/302 following 4 hr of culture in SECM with (B) or without (A) 50 μg/ml cycloheximide. Nuclei are indicated (N). Scale bars = 25 μm.

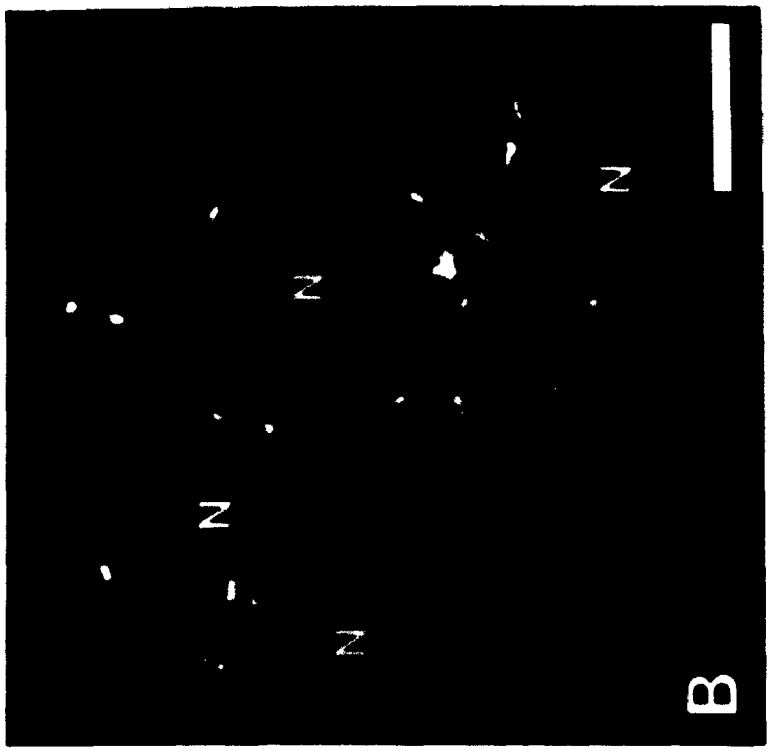
Z
Z
Z
Z
B

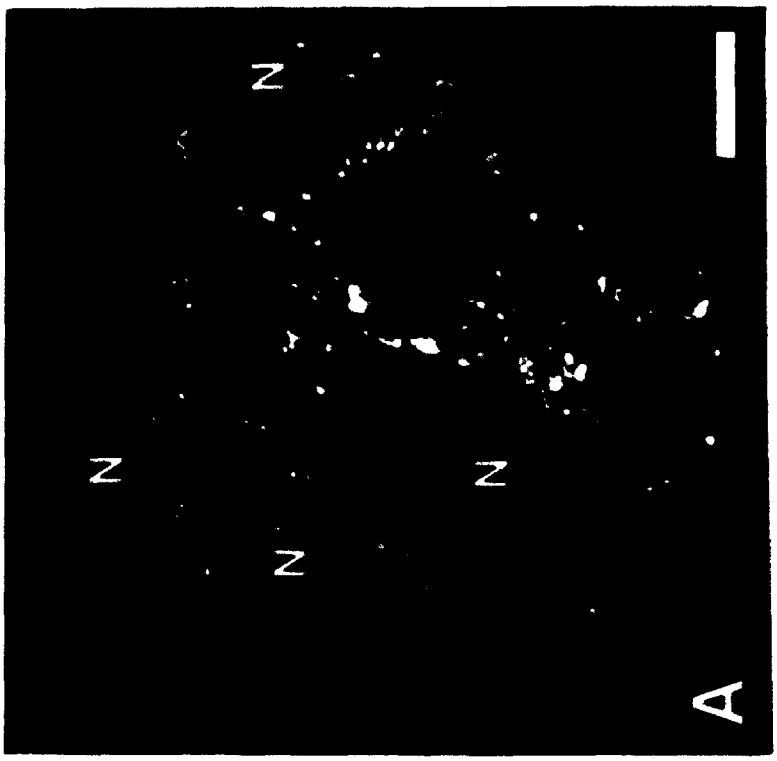
Z
Z
Z
Z
A

Postcompaction 8- to 16- cell embryos were treated for 4 hours with 5 μg/ml of either monensin or BFA and scored blindly. The duration of this treatment period was chosen to match that of cycloheximide and to ensure sufficient accumulation of nascent Cx43 in affected organelles to be detectable by immunofluorescence. Although both these agents have been shown to possess other species specific effects, monensin is a well known inhibitor of flow through the trans-Golgi network (TGN), while BFA blocks translocation of proteins from the endoplasmic reticulum to the Golgi apparatus (Mollenhauer *et al.*, 1990; Klausner *et al.*, 1992). Compacted 8-cell embryos and morulae treated with monensin acquired a new cytoplasmic staining pattern consisting of large, juxtanuclear clouds of immunoreactivity (Fig. 3.2 C,D), although the frequency of the small, diffuse foci characteristic of control embryos remained unaltered (Fig. 3.2 A,B; Table 3.1). In contrast, treatment with BFA abolished these small diffuse foci, replacing them instead with a reticulated network of immunoreactivity (Fig. 3.2 E,F). BFA-treatment over this period had the added effects of inducing decompaction and inhibiting cytokinesis, the latter evidenced by the presence of binucleate blastomeres (Fig. 3.3 B). Embryos treated for 4 hours with monensin or BFA still possessed plaque-like and zonular staining patterns in apposed membranes. Although occasionally, inhibitor-treated embryos appeared to possess fewer of these structures, this effect was not quantifiable.

Figure 3.2. Treatment for 4 hr with monensin or BFA causes redistribution of cytoplasmic Cx43 immunoreactivity in morulae. Each image is a confocal z-series projection (2 μm thick) of early (A,C,E) or late (B,D,E) morulae stained with anti-Cx43/302 following 4 hr culture in SECM containing 0.05% ethanol (A,B), 5 μg/ml monensin (C,D), or 5 μg/ml BFA (E,F). Cytoplasmic immunoreactivity in ethanol-treated embryos did not differ qualitatively from uncultured embryos (Fig.2.6) and consisted mainly of small diffuse foci. Monensin induced the formation of large juxtanuclear clouds while BFA caused the replacement of small diffuse foci with larger, reticulated structures. Scale bar = 32 μm.

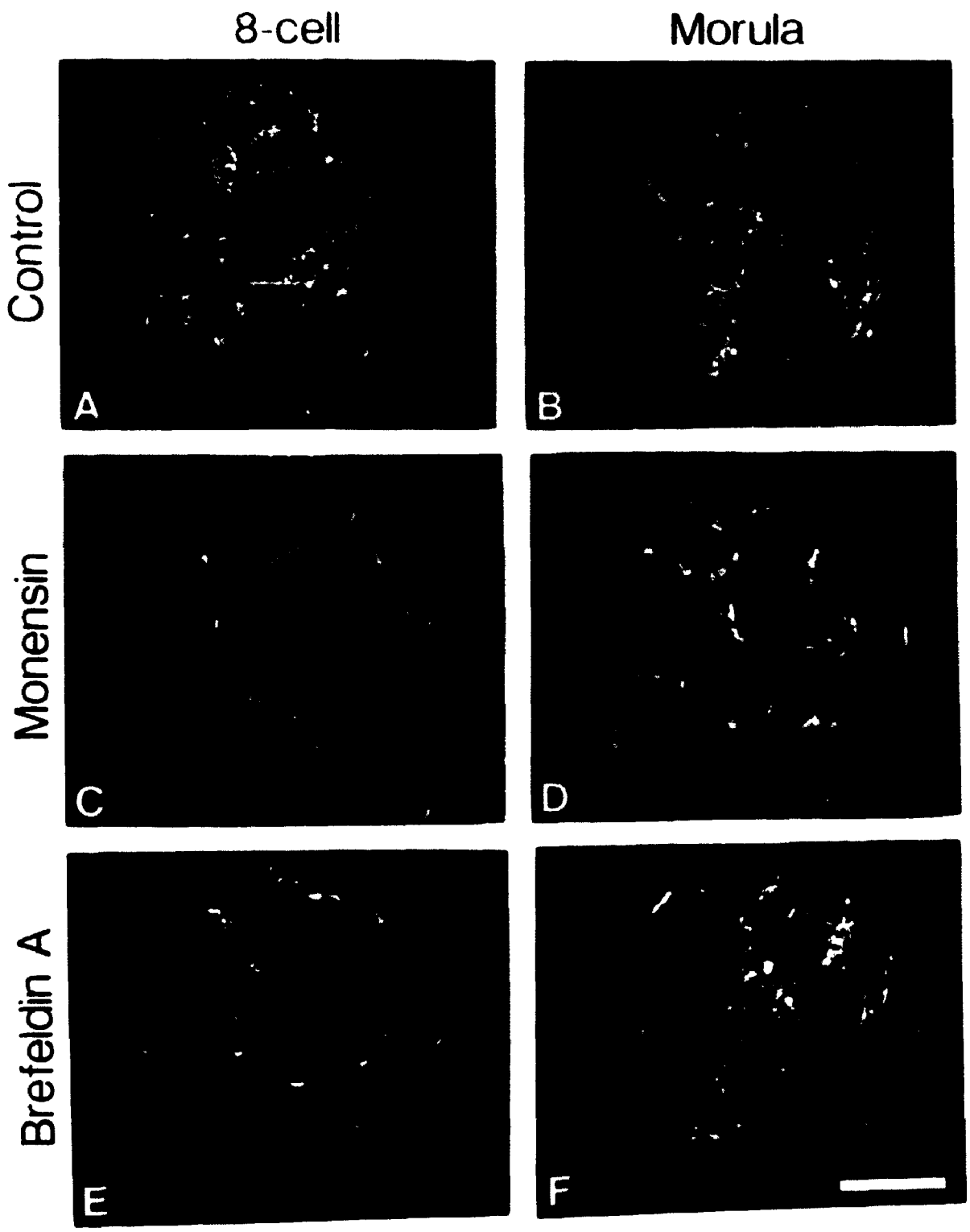
8-cell
Morula
Control
Monensin
Brefeldin A
A
B
C
D
E
F

Figure 3.3. Monensin and BFA alter the structure and distribution of membranous organelles in morulae. Morulae cultured for 4 hr in SECM (A), or SECM containing 5 μg/ml BFA (B) or 5 μg/ml monensin (C), were fixed and embedded for conventional transmission electron microscopy in Epon-Araldite. At low magnification a variety of organelles could be discerned distributed singly or in small aggregates throughout the cytoplasm of control embryos including, mitochondria (M), lipid droplets (L), lysosomes (Ls), and endosome clusters (EC). In BFA treated embryos examined under a similar magnification, cytoplasmic organelles were redistributed into large heterogeneous organelle clusters (HOC). BFA treated morulae also contained binucleate blastomeres (B, upper right blastomere). The most prominent effect of monensin visible at low magnification was disruption of the plasma membrane at apposed membrane regions (C, between arrows). Nuclei (N). Scale bars = 5 μm.

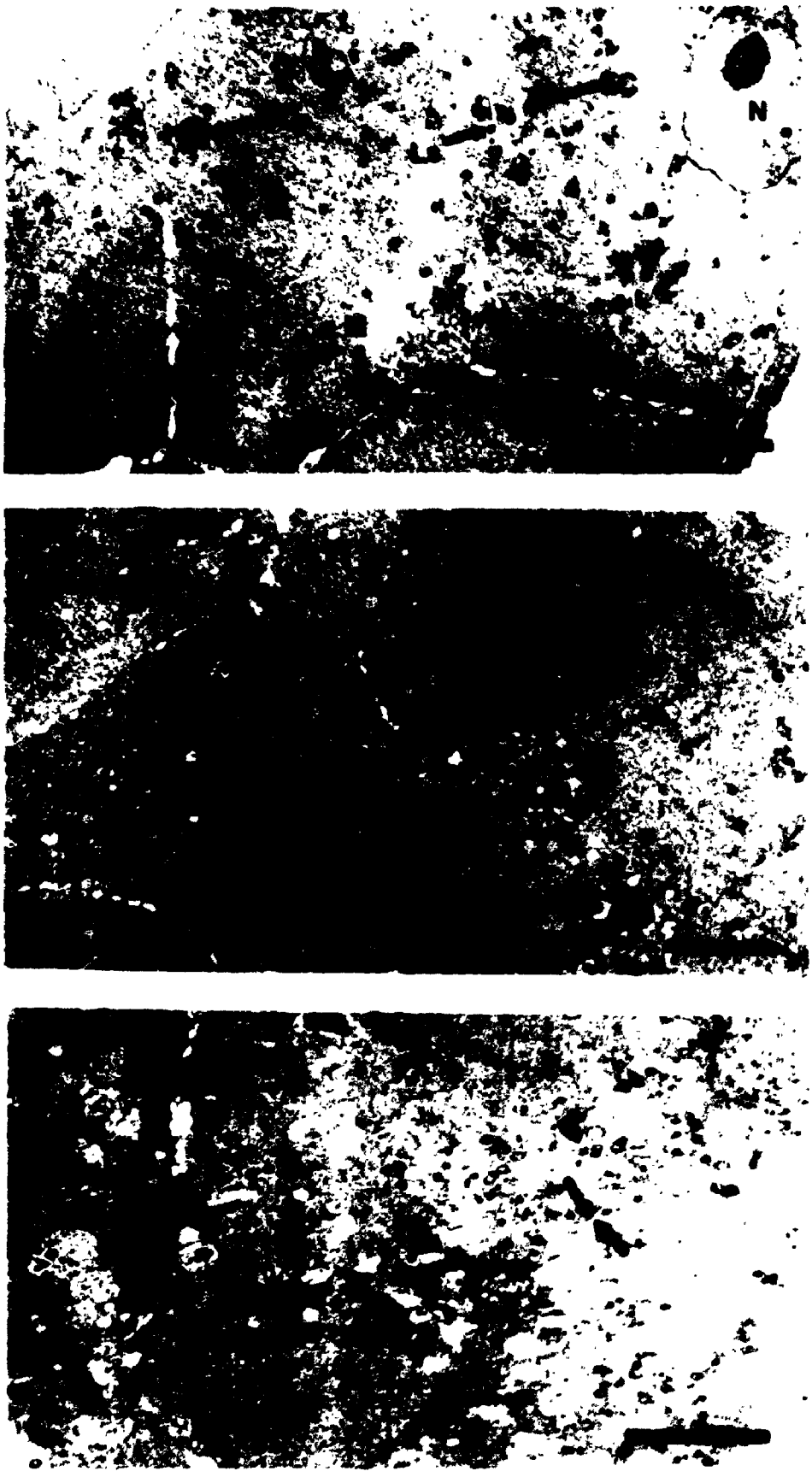
N

3.33 Monensin and brefeldin-A disrupt membranous organelles in morulae.

To investigate the effect of the trafficking inhibitors on cell and organelle structure, 8- to 16- cell morulae treated as described above for immunofluorescence were embedded in Epon-Araldite for conventional electron microscopy. Under the fixation conditions used, only slight shrinkage of cells was evident which helped to identify regions of high membrane adhesiveness (Fig. 3.3 A). For each treatment condition, three separate blocs of embryos were sectioned and viewed. Sections from 13, 10, and 11 embryos cultured in control medium, monensin, and BFA, respectively, were examined.

Cell and organelle structure in control cultured embryos was similar to that reported previously by others (Calarco and Brown, 1969; Dvorak *et al.*, 1985; Fleming and Pickering, 1985). At low magnification, certain cytoplasmic organelles could be discerned singly or aggregated in small areas with other organelles (Fig. 3.3 A). These included: mitochondria, which were either vacuolated, ovoid structures with small numbers of cristae (Fig. 3.7 D), or non-vacuolated ovoid or elongated structures with traversely oriented cristae (Fig. 3.4 D); lipid droplets, which appeared as spherical structures of medium electron density, with an approximate diameter of 0.5 μm; and degradative vacuoles or lysosomes, which were up to 1.5 μm in diameter and contained electron dense material. The lysosomal nature of these structures has previously been confirmed cytochemically by the detection of acid hydrolase activity, specifically trimetaphosphatase (Fleming and Pickering, 1985). In addition, endosome

Figure 3.4. Distribution of Golgi complexes in untreated morulae. Golgi complexes (GC) in SECM cultured morulae appeared predominantly in the cortical cytoplasm near apical (A) and basolateral (C,D) membranes, although occasionally they were also seen near nuclei (B). Most Golgi consisted of only 4-6 flattened cisternae, although some also possessed a network of tubular and vesicular membranes at one of their ends reminiscent of trans-Golgi network cisternae (D). Also evident at this magnification were mitochondria (M), lipid droplets (L), and crystalloid inclusions (CI). Nuclei (N). Apical plasma membrane (APM). Zona pellucida (ZP).
Scale bars = 250 nm.

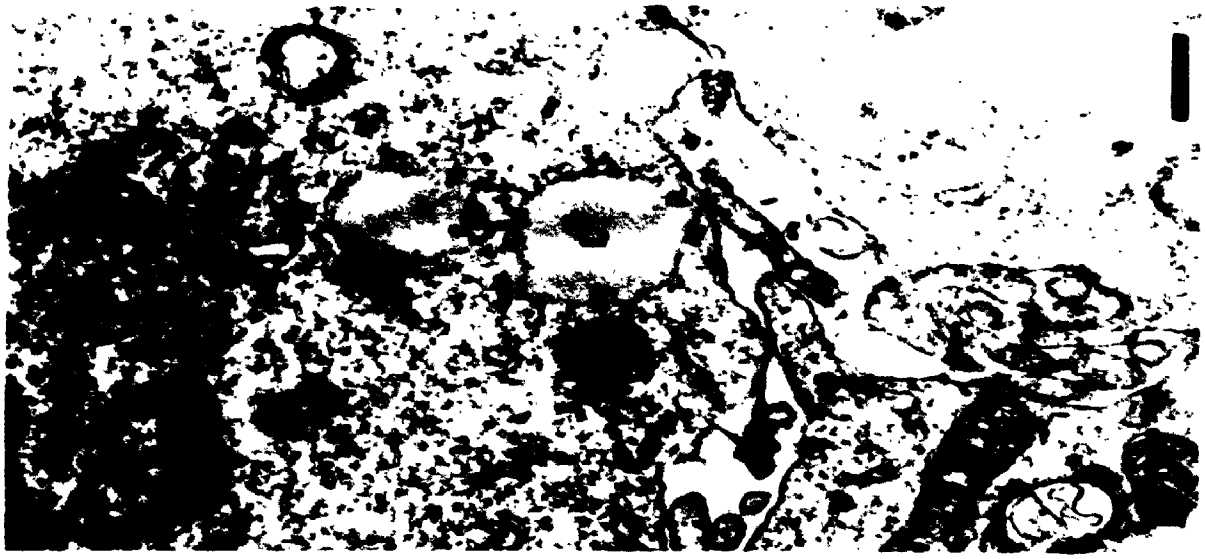

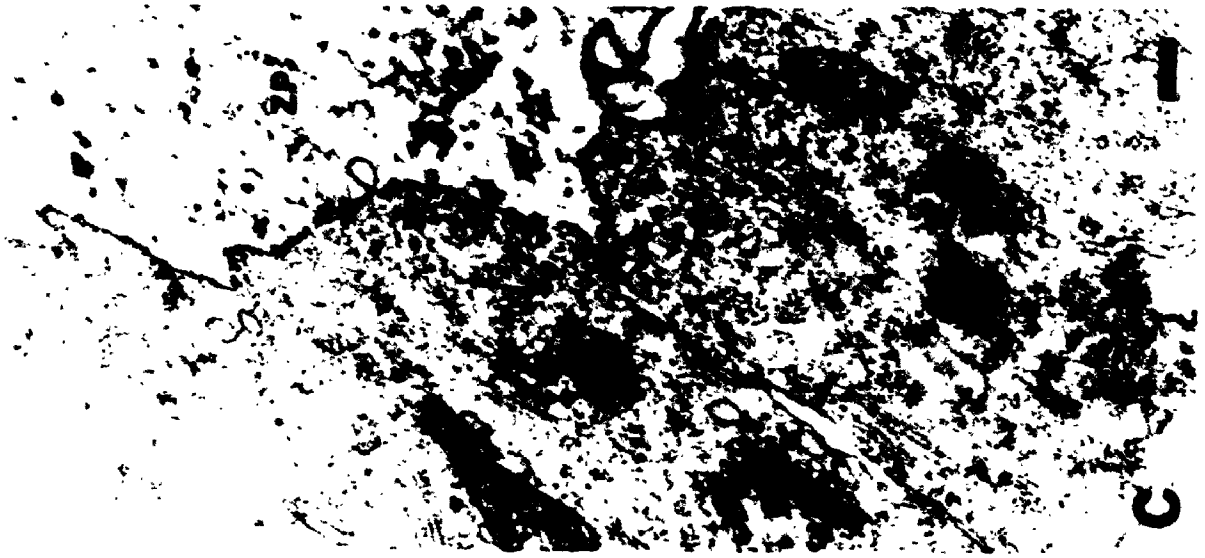

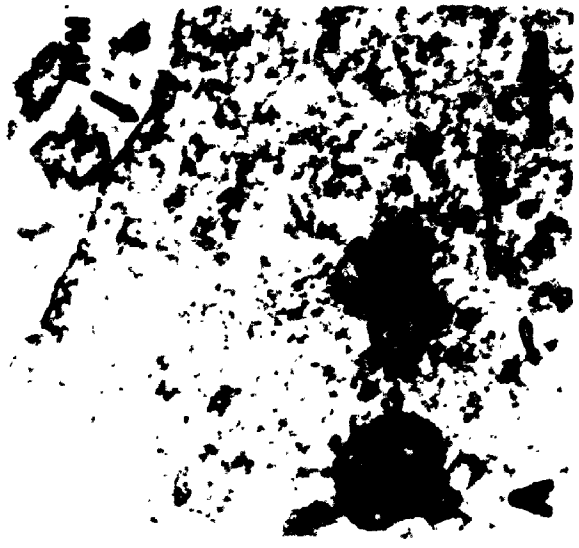

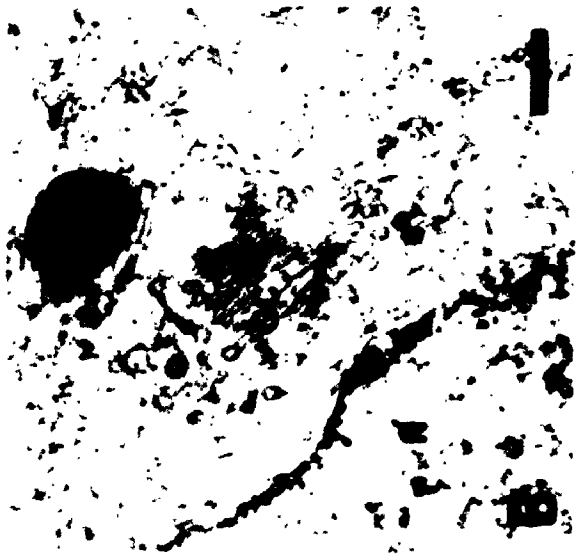

clusters, up to 2 μm in diameter, were evident. As described in 4-cell embryos (section 2.33, Fig. 2.13), endosomes at higher magnification appeared as vacuoles surrounded by vesicular structures (Fig. 3.5 A, 3.7 E). Also evident at higher magnification in the ground cytoplasm were fibrillar bodies. These structures were irregularly distributed throughout the cytoplasm, and consisted of loose bundles of 3-6 fibrous strands (Fig. 3.5 A).

In control morulae, Golgi complexes were evident predominantly in the cortical cytoplasm near apical and basolateral membranes. However, occasionally Golgi were evident near the nucleus. All Golgi seen consisted of several (4-6) flattened cisternae slightly dilated at their end parts at which minute vesicles were situated (Fig. 3.4). Individual Golgi cisternae measured up to 0.5 μm across, whilst stacks were approximately 0.125 μm in depth. Thirty six percent of the Golgi observed (n=11) possessed a network of tubular and vesicular membranes at one of their ends, reminiscent of typical trans-Golgi network cisternae (Fig. 3.4 D). Structures resembling rough endoplasmic reticulum (RER) consisted mostly of single, short, flattened cisternae studded with electron dense particles. These structures were normally found in association with mitochondria (Fig. 3.6 B). Also evident were clusters of smooth tubular and vesicular membrane independent of endosomes, which appeared either singly or near mitochondria (Fig. 3.5 A; 3.6 A,B).

One nucleus was apparent per blastomere of control morulae. Nuclei, normally containing 1-2 nucleoli were generally located centrally and in sections appeared

Figure 3.5. Morulae treated with BFA form large heterogeneous clusters of tubular and vesicular membranes. Membranous organelles in the cytoplasm of control morulae, cultured in SECM (A), were dispersed throughout the cytoplasm. These included lysosomes (Ls), smooth tubular and vesicular membranes (SM), and endosome clusters (EC). In BFA-treated morulae (B) membranous tubular and vesicular structures tended to be aggregated into large heterogenous complexes (Arrow). Also evident in the ground cytoplasm of both treated and untreated morulae were fibrillar bodies (FB). Although in the present figure these structures appear to be more condensed in the BFA-treated morula, this was not a consistent feature of all treated embryos. Nuclei (N). Scale bar = 500 nm.

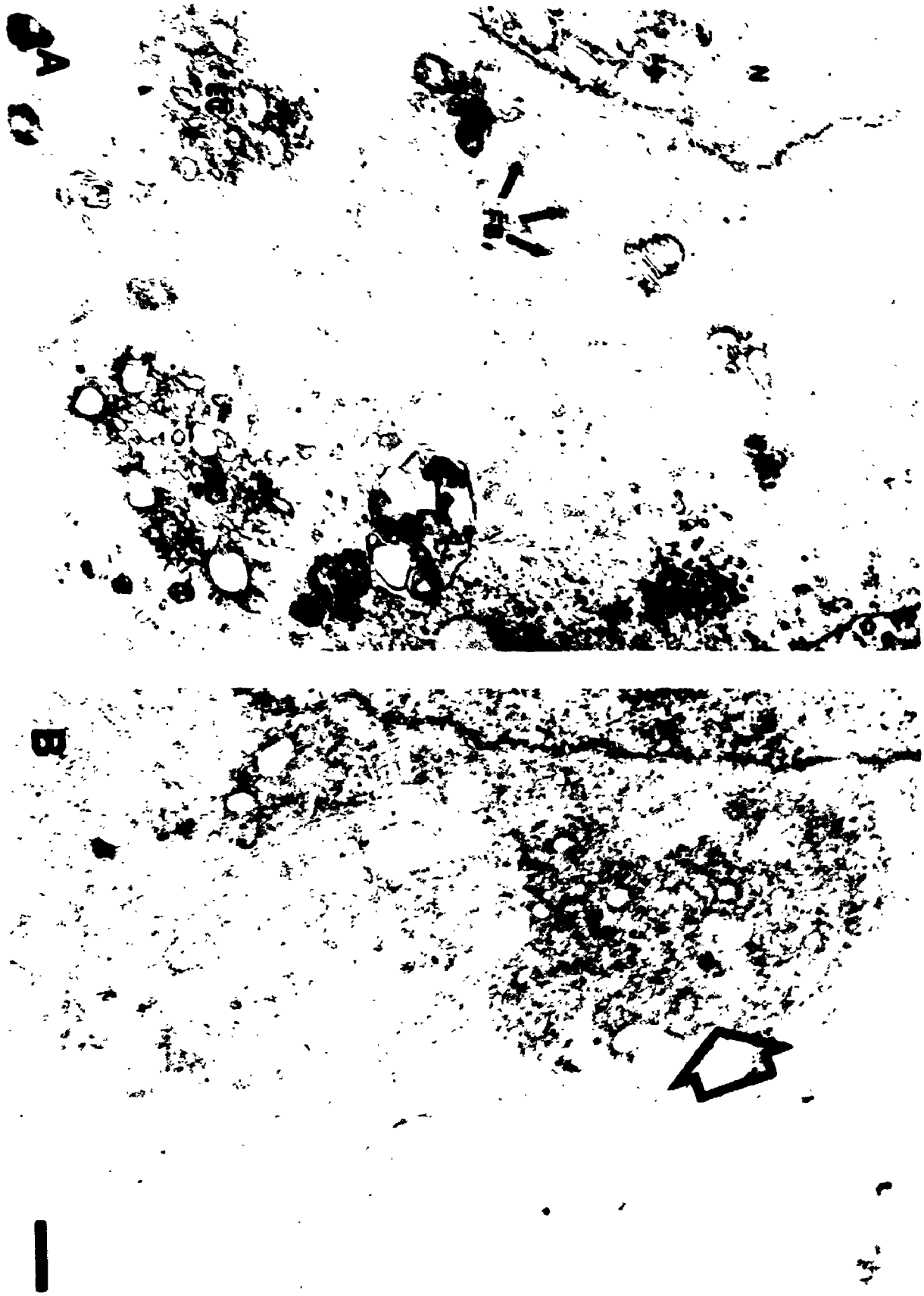
A
N
B

Figure 3.6. BFA-induced membrane clusters contain recognizable organelles. In addition to an abundance of tubular and vesicular membranes, membranous complexes in BFA-treated morulae (C,D) contained endosomes (E), lysosomes (Ls), and mitochondria (M). In SECM cultured morulae (A,B), smooth tubular and vesicular membranes (SM) appeared as smaller clusters. Also evident in the cytoplasm of control morulae were single, short, flattened cisternae studded with electron dense particles, reminiscent of rough endoplasmic reticulum (RER). Nuclei (N).
Scale bars 500 nm.

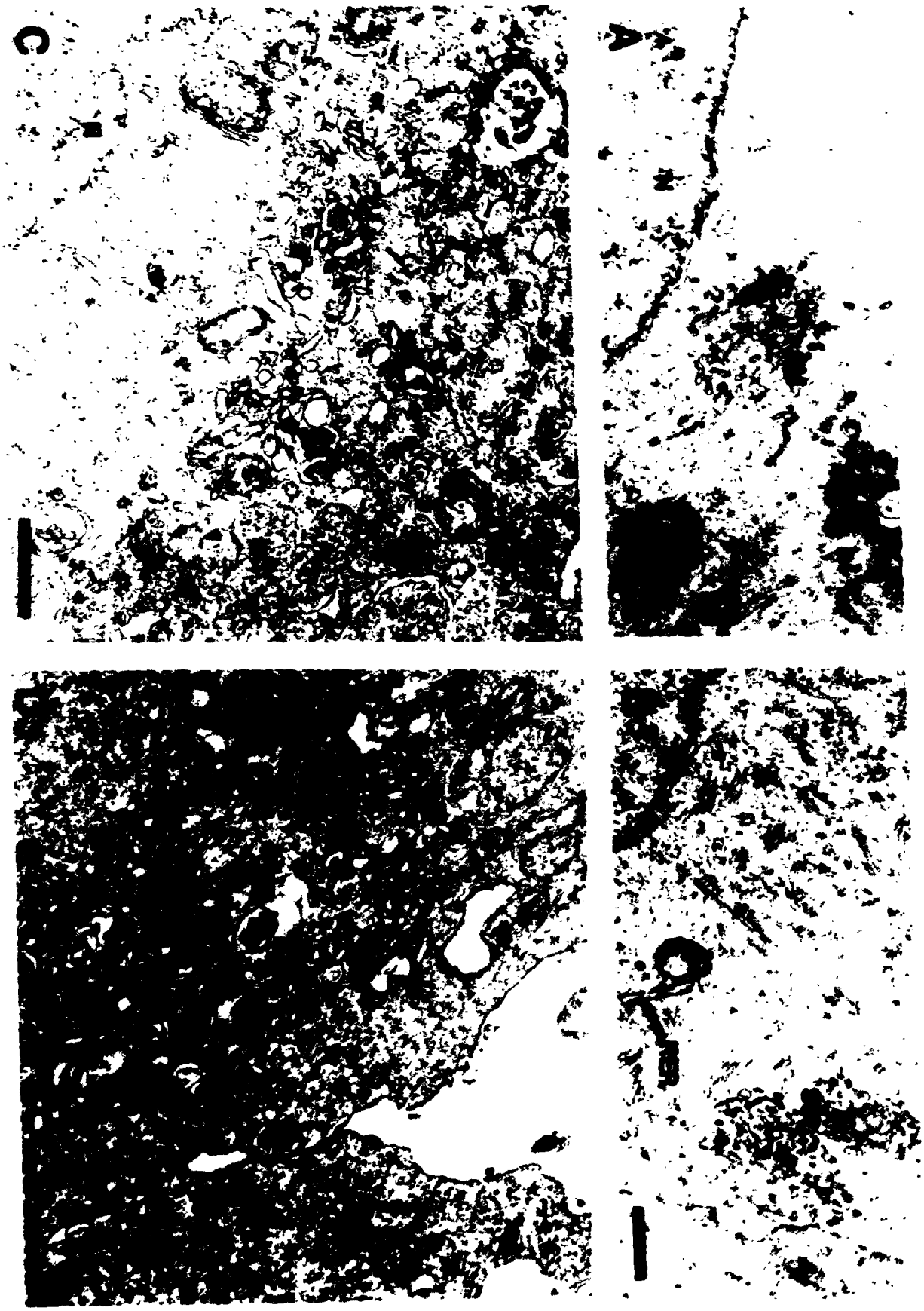
C
A

Figure 3.7. Monensin alters the morphology of membranous organelles in morulae. Culturing morulae for 4 hr in SECM containing 5 μg/ml monensin (A,B,C) had multiple effects on the structure of membranous organelles including, increasing the electron density of matrices within mitochondria (M), increasing the size and internal complexity of lysosomes (Ls), disrupting plasma membranes along basolateral domains (B, between small arrows), and inducing the swelling of membranous compartments possibly derived from Golgi complexes (arrow in A, C). Visualized at a similar magnification, Golgi complexes (GC) and endosome clusters (EC) in morulae cultured in SECM alone (D,E), appeared smaller than putative swollen Golgi cisternae in monensin-treated morulae (C). Also evident in monensin-treated morulae (A) were lipid droplets (L) whose size and distribution appeared unaltered by the drug compared with controls. Nuclei (N). Scale bars = 500 nm.

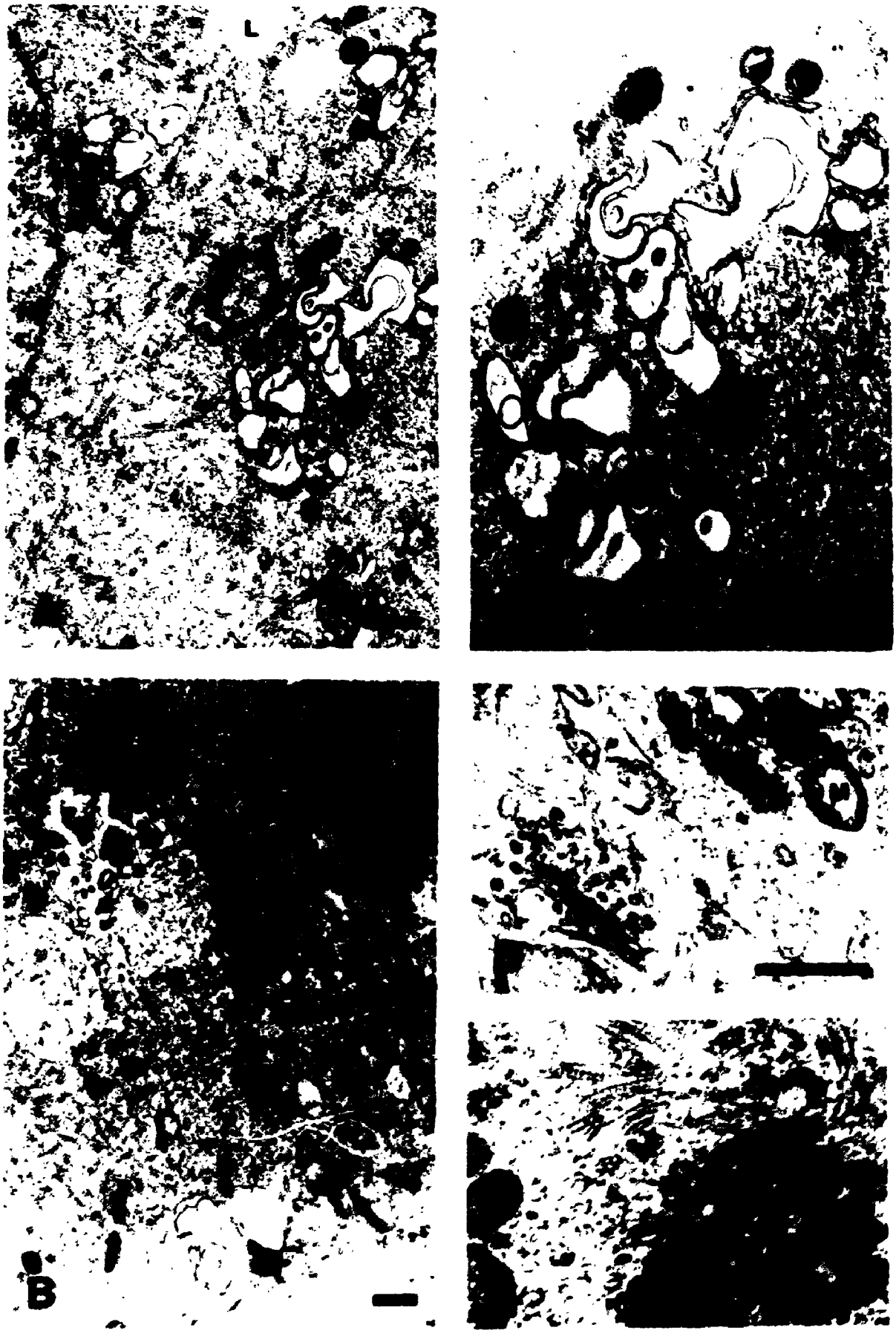
L
B

slightly oval or round. Nucleoli were approximately 2-5 μm in diameter and consisted of a reticulated area surrounding one or more electron dense areas (Fig. 3.3 A). Chromatin in nuclei was mostly euchromatic, with occasional small condensations, and was enclosed by a nuclear envelope consisting of a double membrane (Fig. 3.5 A; Fig. 3.6 A). Also apparent in the cytoplasm of control morulae were crystalloid inclusions (Fig. 3.4 C), found singly or in loose association with other organelles. Crystalloid inclusions appeared as cross-striated crystaline structures not bound by a membrane (Fig. 3.4 C). These structures are a characteristic feature of the cytoplasm of cleaving mouse embryos, thought to represent a stored form of cytokeratin (Capco *et al.*, 1993).

Treatment of morulae for 4 hrs with 5 μg/ml BFA profoundly altered the distribution, but not the structure, of many cytoplasmic organelles. In contrast to control embryos, where organelles were dispersed singly and in small clusters throughout the cytoplasm, most organelles in BFA-treated embryos had coalesced into large, heterogeneous clusters (Fig. 3.3 B). Clusters numbered 1 or 2 per cell and could be found in proximity to either the nucleus or the plasma membrane. Clusters were rich in smooth tubular and vesicular membrane compartments (Fig. 3.5 B), but also contained a variety of recognizable organelles including mitochondria, endosomes, and lysosomes (Fig. 3.6 C,D). Although no morphometric analysis was performed, no Golgi complexes were observed in BFA-treated embryos, either within or outside of the heterogeneous organelle clusters created by the drug. Binucleate blastomeres were also evident in BFA-treated embryos, although no distinguishable

effects were apparent on nuclear morphology, including the nucleolus, chromatin, and nuclear envelope (Fig. 3.3 B; 3.5 B; 3.6 C). BFA-treatment also had no reproducible effect on the distribution or structure of fibrillar bodies, crystalloid inclusions, or lipid droplets.

Treatment of morulae for 4 hrs with 5 μg/ml monensin had multiple structural effects distinct from BFA, confirming that each drug possesses unique sites of action. Treatment with monensin dramatically altered the structure of many membranous organelles including the plasma membrane (Fig. 3.3 C, Fig. 3.7 B). Within cells, monensin increased the electron density of mitochondrial matrices (Fig. 3.7 A,B,C; Fig. 3.8), induced swelling of membranous compartments possibly derived from Golgi complexes, as judged by their close association with flattened cisternae (Fig. 3.7 A,C), and increased the apparent size of lysosomes, which now also appeared to contain a medium electron dense material similar to ground cytoplasm (Fig. 3.7 B). Lastly, monensin also exhibited a profound effect on the plasma membrane of apposed membrane regions which became highly involuted (Fig. 3.8).

No morphometric analysis was performed to determine the frequency of gap junctions under the different treatment conditions. However, examining comparable numbers of embryos, only one gap junction was seen in monensin-treated embryos, no gap junctions were seen in BFA-treated embryos, whereas 9 gap junctions were observed in control embryos.

Figure 3.8. Apposed basolateral membranes (between arrows) in morulae are disrupted following treatment with monensin. Extensive involution of apposed membrane regions was apparent in morulae cultured for 4 hr in SECM containing 5 μg/ml monensin (A,B). Mitochondria (M). Nuclei (N). Scale bars 500 nm.

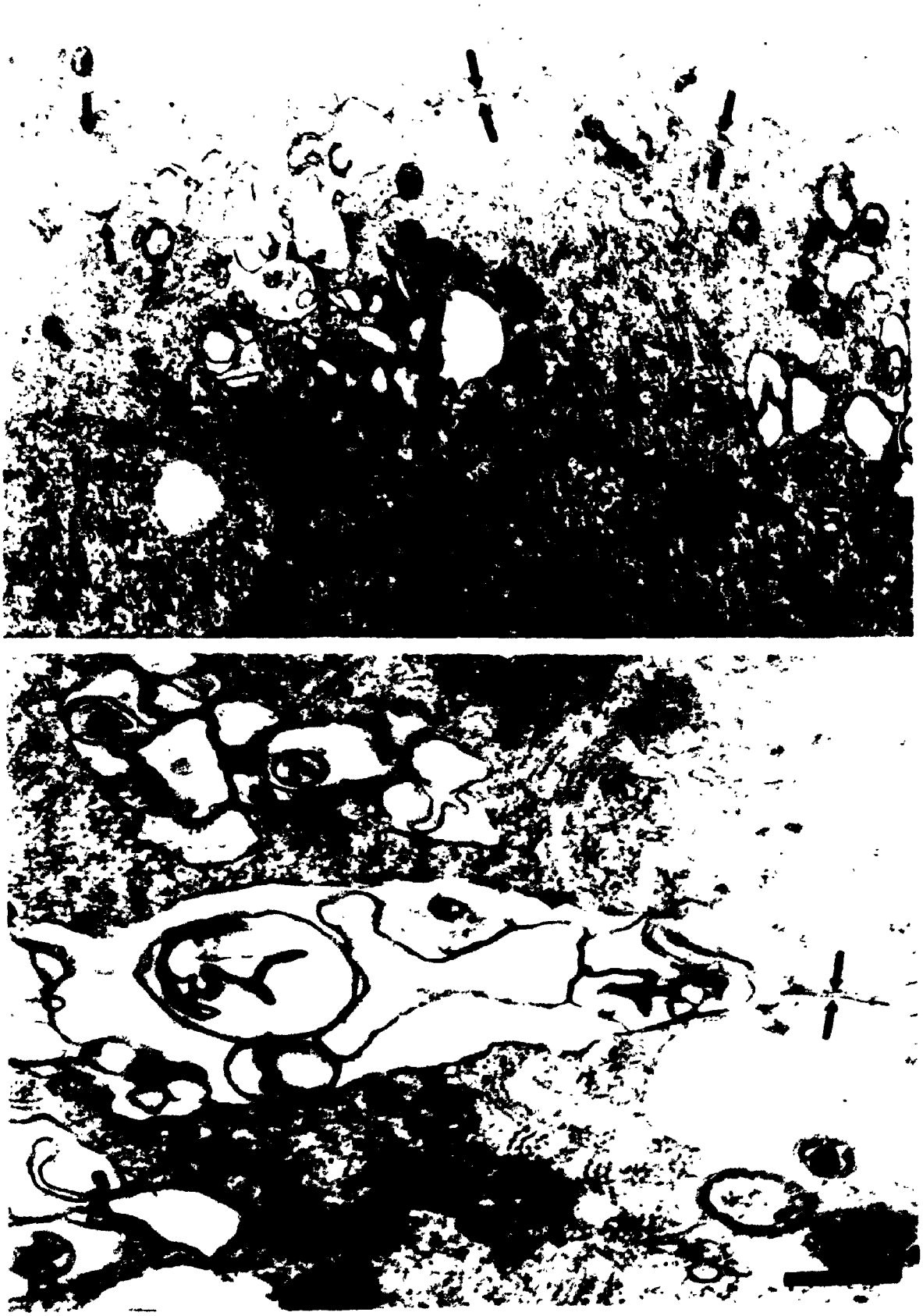

3.4 Discussion.

3.41 Putative targets of monensin and brefeldin-A in the preimplantation embryo.

In the present study, monensin and BFA each exhibited characteristic disturbances of membranous organelles, revealing each had unique sites of action. A summary of the effects of these agents on intracellular organelle structure and function as described in the literature is presented in Fig. 3.9. Secretory and integral membrane proteins are normally translocated within cells through common organelles and compartments which include the endoplasmic reticulum (ER), Golgi complexes, trans-Golgi network (TGN), an endosomal compartment, a prelysosomal compartment, and lysosomes. Movement of membrane and proteins between these compartments and to the plasma membrane occurs by budding and fusion of transport vesicles (reviewed by Melancon *et al.*, 1991; Sztul *et al.*, 1992). Individual transport steps which have been documented or proposed are depicted by dashed arrows in Fig. 3.9 (Untreated; Lippincott-Schwartz, 1993; Duden *et al.*, 1991; Pelham, 1991; Wood *et al.*, 1991; Gruenberg and Howell, 1989).

The most cited effect of BFA is to cause collapse of Golgi complexes and their reabsorption into the ER (reviewed by Klausner *et al.*, 1992). Trafficking from the ER to the Golgi and between Golgi cisternae is mediated by non-clathrin-coated vesicles (reviewed by Rothman and Orci, 1992). Vesicle formation is dependent on

Figure 3.9. Summary of reported effects of trafficking inhibitors on organelle structure and function. Secretory and integral membrane proteins are normally translocated within cells between common organelles which include the endoplasmic reticulum (ER), Golgi complex (GC), trans-Golgi Network (TGN), an endosomal compartment (EC), a prelysosomal compartment (PLC), and lysosomes (L). Movement of membrane and proteins between these compartments and to the plasma membrane occurs by budding and fusion of transport vesicles. Individual transport steps which have been documented or proposed are depicted in the figure by dashed arrows (Untreated). BFA is best known for its ability to inhibit anterograde, and enhance retrograde, membrane traffic between the ER and GC to create a hybrid (ER/GC) compartment. Other cell line specific effects of BFA include induction of fusion of the TGN with the EC, tubulation of lysosomes, and alterations in transcytosis and endocytosis, although no effects on trafficking to lysosomes and lysosomal function have been observed. Due to its activity as a Na^+ ionophore, monensin is believed to interfere with the function of acidic organelle compartments including acidic endosomes (*i.e.* PLC), lysosomes, and the cisternae of the TGN (indicated in the figure by cross-hatching). TGN disfunction is accompanied by swelling of this compartment possibly as an artifact of fixation. Membrane trafficking is arrested in monensin-treated cells at the TGN. In some cells monensin also inhibits trafficking to lysosomes and inhibits endocytosis.

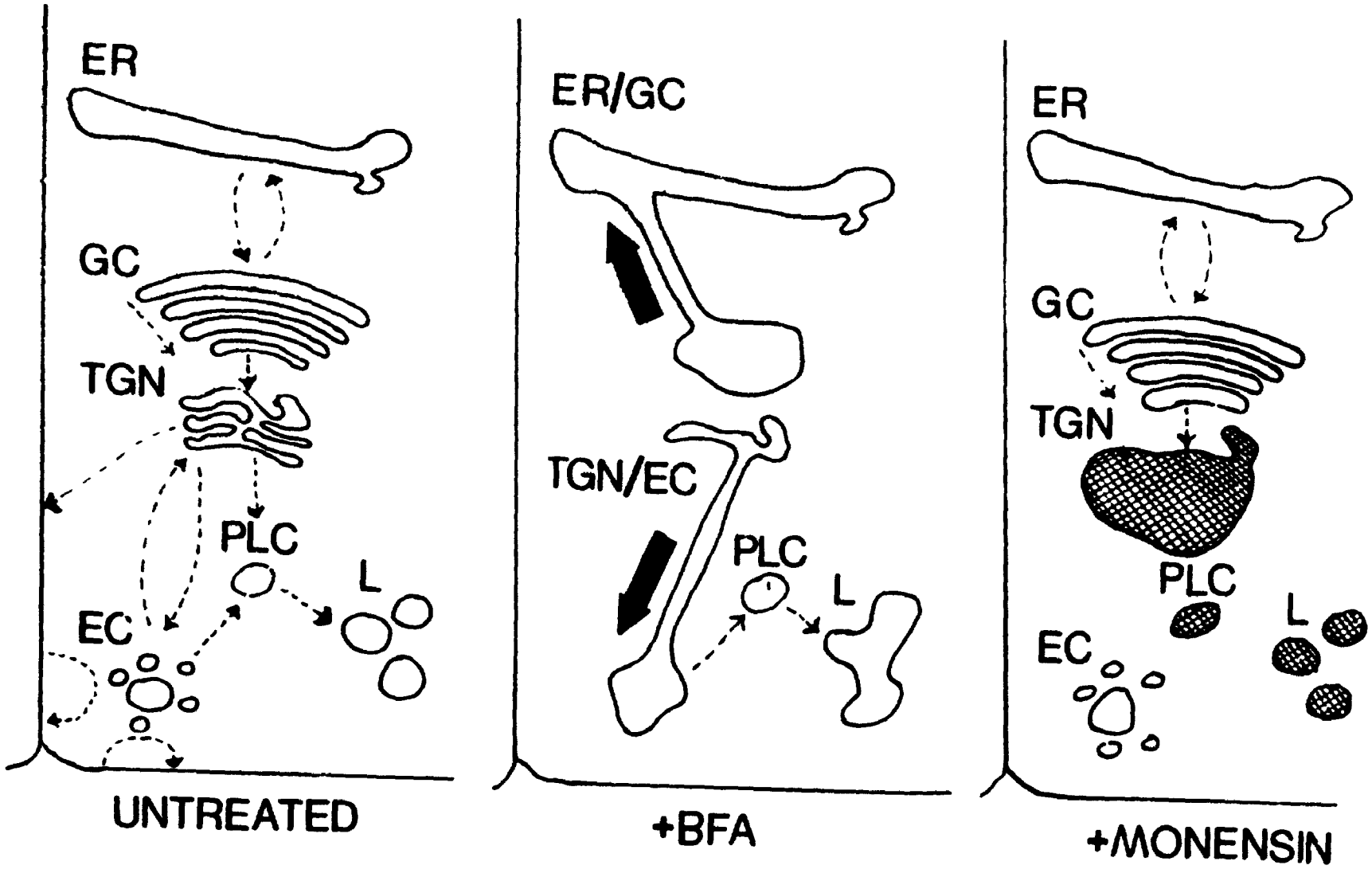
ER
GC
TGN
PLC
L
EC
UNTREATED
ER/GC
TGN/EC
PLC
L
+BFA
ER
GC
TGN
PLC
L
EC
+MONENSIN

the recruitment of a set of proteins from the cytoplasm to the budding membrane, the most well-studied member of which is ß-cop . In the presence of BFA, ß-cop is redistributed to the cytosol and vesicle formation is inhibited (Donaldson, 1990; Orci *et al.*, 1991). When this occurs, Golgi cisternae tend to form tubules which are elongated along microtubules, and rapidly fuse with the ER (Lippincott-Schwartz *et al.*, 1989, 1990). As a result, proteins normally resident in the Golgi are redistributed into a mixed Golgi/ER compartment (Wood and Brown, 1992).

In NRK and PtK_1 cells, BFA has been found to induce tubulation and fusing of the TGN and early endosomes, as well as tubulation of lysosomes, the former suggesting the existence of a transport pathway linking these organelles (Lippincott-Schwartz *et al.*, 1991; Wood and Brown, 1992). BFA-treatment of polarized MDCK cells selectively alters the degree and directionality of endocytosis and transcytosis of vesicles (Prydz *et al.*, 1992; Low *et al.*, 1992; Hunziker *et al.*, 1991). However, no effects on vesicular trafficking to lysosomes and lysosomal function have been observed. The effects of BFA on the structure of the Golgi, TGN, and endosomes support the existence of a general mechanism for regulating organelle structure and membrane traffic, which likely involves microtubules (Kelly, 1990).

In contrast to BFA, the effects of monensin are likely due to its activity as a Na^+ ionophore, and its capacity to collapse Na^+ and H^+ gradients by facilitating the passage of Na^+ across biological membranes. Na^+/H^+ gradients are created through the activity of H^+-translocating, ATP-hydrolyzing enzymes (H^+-ATPases). In coated

vesicles, acidic endosomes, lysosomes, and the cisternae of the TGN, these enzymes create acidic intracellular compartments through the inward transport of H^+ (Maxfield, 1985). Since one H^+ is exchanged for every Na^+ ion transported, monensin effectively neutralizes acidic compartments, which subsequently cease to function. In this manner, monensin is reported to inhibit degradation in lysosomes, and the processing and trafficking of proteins at the TGN (reviewed by Mollenhauer *et al.*, 1990). In some cells monensin inhibits endocytosis, presumably as a result of interference with membrane recycling steming from the neutralization of acidic endosomes (Wilcox *et al.*, 1982). Monensin has also been reported to inhibit trafficking of receptor-mediated endocytosed ligand to lysosomes (Merion and Sly, 1983). In the case of the TGN, loss of function is also accompanied by swelling of its cisternae, although all cisternae of the Golgi complex may swell in response to monensin (Morre *et al.*, 1983). Swelling is presumably due to the flow of water in the direction of osmotically active Na^+. Little is known about the swelling response, if any, of lysosomes, coated vesicles, or endosomes (Mollenhauer *et al.*, 1990). In bovine mammary epithelial cells examined using enhanced video microscopy, the swelling of the TGN was only observed upon fixation (Morre *et al.*, 1992).

The effects of BFA and monensin on embryos are summarized in Fig. 3.10. In BFA-treated embryos, no Golgi complexes were apparent. In addition, BFA altered organelle distribution creating large, heterogenous organelle clusters rich in tubular and vesicular membranes. Although several different types of organelles were evident within these clusters including mitochondria, lysosomes and endosomes, no effects on

Figure 3.10. Summary of effects of trafficking inhibitors on embryo organelle structure. Normally, cytoplasmic organelles in embryos are dispersed throughout the cell (Untreated). Readily identifiable organelles include the nucleus (N), mitochondria (M), the endoplasmic reticulum (ER), Golgi complex (GC), the trans-Golgi network (TGN), endosome clusters (EC) and lysosomes (L). Treatment of morulae for 4 hr with BFA resulted in the creation of large heterogenous organelle clusters (HOC), which consisted of an abundance of smooth tubular and vesicular membrane in addition to readily identifiable organelles including endosomes, lysosomes, and mitochondria. In contrast, treatment with monensin caused swelling of putative Golgi cisternae, an increase in the size and complexity of lysosomes, an increase in the electron density of mitochondrial matrices, and perturbation of apposed plasma membrane regions.

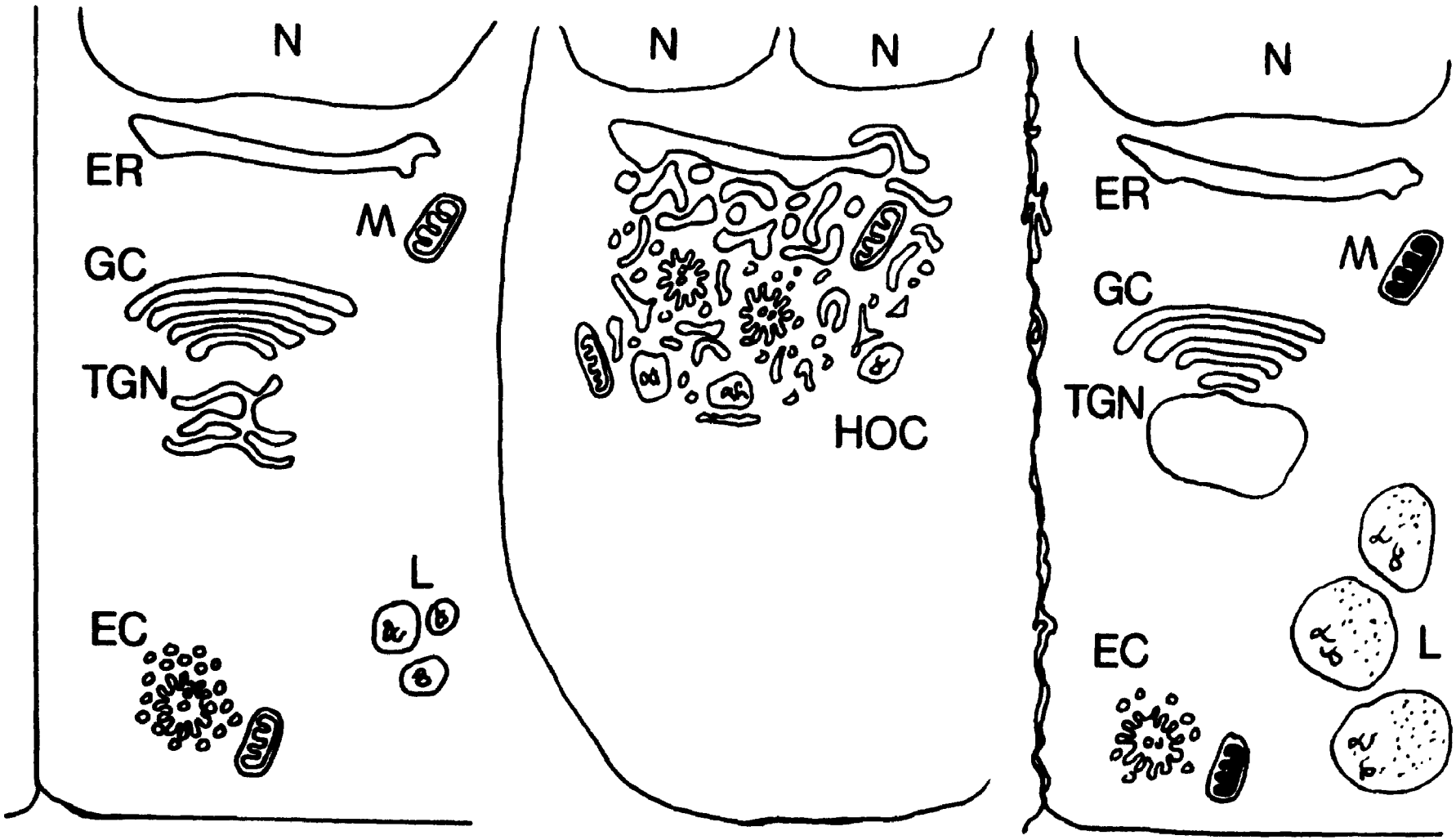
N
ER
M
GC
TGN
L
EC
UNTREATED
N
N
HOC
+BFA
N
ER
M
GC
TGN
EC
L
+MONENSIN

their morphology were apparent.

The lack of Golgi and the preponderance of smooth tubular and vesicular membranes observed in BFA-treated embryos are consistent with the noted ability of this drug to cause collapse of Golgi complexes and their reabsorption into the ER. Both the disruption of organelle distribution and the inhibition of cytokinesis in the embryo in response to BFA may have been achieved through interference with the ability of all membranous organelles including the plasma membrane to be organized by microtubules. As in most cells, microtubules in the embryo influence cell shape and organization, and are necessary for cell division (Maro and Pickering, 1984; Goodall and Maro, 1986). The distribution of those organelles not directly associated with microtubules, could also have been affected indirectly if these organelles were associated with microtubule-dependent structures. In human fibroblasts, mitochondrial distributions are determined by their association with endoplasmic reticulum, whose distribution is dependent on microtubules (Soltys and Gupta, 1992).

At the level of the electron microscope, monensin was found to have several effects on embryo organelle structure, including swelling of cisternae likely belonging to Golgi complexes, increasing the apparent size and vacuolar complexity of lysosomes, perturbing the plasma membrane, and increasing the electron density of mitochondrial matrices. The effect on Golgi-like compartments suggest that in embryos, monensin may interfere with the trafficking of nascent proteins at this organelle. The preponderance of swollen membranous compartments in relation to

flattened cisternae in putative Golgi complexes affected by monensin, suggest that the effects of this agent may not be confined to just the cisternae of the TGN. Although lysosomes in monensin-treated embryos also showed an apparent increase in size, the increased vacuolar complexity suggests that this may have been achieved through inhibition of lysosomal function rather than any osmotic effects arising from disruption of Na^+ ions. Inhibition of lysosomal function without a concurrent inhibition in vesicular trafficking to lysosomes would have resulted in an accretion of material targeted for degradation. In contrast to the Golgi and lysosomes, the matrices of mitochondria appeared condensed in the presence of monensin. This is consistent with the findings of others (reviewed in Mollenhauer *et al.*, 1990), and likely due to the fact that in these structures, H^+ are normally pumped in an outward direction (Darnell *et al.*, 1990). The reason apposed plasma membrane regions in monensin-treated embryos were so grossly altered remains unclear. Unfixed monensin-treated embryos were virtually indistinguishable from control embryos under the phase contrast microscope. Given the likely disruption of Na^+/H^+ gradients in monensin-treated embryos, it is possible that membrane perturbations arose artifactually as a result of induced hypersensitivity to slight osmotic shocks associated with the fixation and embedding protocol.

3.42 Trafficking of nascent connexin43 in morulae.

Cx43 distribution in the cytoplasm of morulae visualized by anti-Cx43/302 was found to be sensitive to cycloheximide. To my knowledge this is the first experimental evidence identifying cytoplasmic immunoreactivity for Cx43 as nascent protein. Similar cytoplasmic staining for Cx43 was also observed with the two other peptide antibodies used in this study, confirming the specificity of this pattern for Cx43. In cardiac cells as well as several fibroblast cell lines, no cytoplasmic staining with anti-Cx43/302 has been seen (B.J. Nicholson, unpublished observations) indicating that this is not a consistent property of either that antibody or most types of cell.

In morulae, treatment with BFA or monensin was found to redistribute nascent Cx43 in the cytoplasm. No quantifiable effect of these agents on punctate and zonular staining of apposed membranes was evident, although in some embryos these staining patterns appeared reduced in frequency. Fewer gap junctions were evident in trafficking inhibitor-treated embryos although these data were not morphometrically quantified. A reduction in plasma membrane staining patterns over time would be consistent with the interupted delivery of Cx43 to the plasma membrane, as well as the rapid turnover rate observed for this protein in cultured cells ($t_{1/2}$ ranging from 1-2.5 hrs; Laird *et al.*, 1991; Musil *et al.*, 1990). Similar turnover rates have been observed for Cx32 and Cx26 in cultured hepatocytes (Traub *et al.*, 1989). However, the turnover rate for Cx43 in preimplantation mouse embryos is unknown. In addition, gap junctions in trafficking inhibitor-treated embryos could also have been stabilized

in surface plasma membranes by alterations in endocytotic and transcytotic activity (Mollenhauer *et al.*, 1990; Hunziker *et al.*, 1991).

BFA and monensin had qualitatively different effects on the distribution of nascent Cx43 in the cytoplasm, reaffirming the structural evidence that each had unique sites of action. BFA, but not monensin, abolished the small, diffuse cytoplasmic foci, and in their place appeared reticular staining, possibly indicative of Cx43 being concentrated in the tubular and vesicular membranes found within the large heterogeneous organelle clusters observed with the electron microscope. Although monensin may have had multiple sites of action, the large juxtanuclear clouds observed following treatment with this inhibitor are consistent with accumulation of Cx43 in swollen Golgi cisternae. However, based on the known effect of monensin on lysosome function, accretion of Cx43 in this organelle in embryos also cannot be ruled out. Since BFA and monensin have opposite effects on the cisternae of Golgi (abolishment vs embellishment) and the small diffuse cytoplasmic foci for Cx43 were only completely abolished in the presence of the former, this staining pattern in control embryos may represent Cx43 in Golgi or Golgi-derived vesicles. However, it is unlikely that this staining pattern represents nascent Cx43 in the ER since the same antibody failed to detect Cx43 in the cytoplasm of 4-cell embryos, when translation of Cx43 transcripts has already begun (De Sousa *et al.*, 1993; see chapter 4).

Monensin has also been shown to alter Cx43 distribution in neonatal cardiac myocytes (Puranam et al, 1993). Treatment for 7 hrs redistributed cytoplasmic Cx43 from small diffuse foci into larger intracellular structures, and reduced the frequency of plaque-like structures at apposed membrane regions, as depicted by immunofluorescence with anti-Cx43/360. In this study, monensin also redistributed a medial Golgi sialoglycoprotein (MG-160), into swollen cytoplasmic structures which frequently, but not always, colocalized with Cx43. Co-localization of Cx43 with other Golgi-specific antigens has also recently been demonstrated in rat myometrium during labor (Hendrix *et al.*, 1992).

My results, combined with those of others (Hendrix *et al.*, 1992; Puranam *et al.*, 1993; Laird *et al.*, 1993), provide the first immunocytochemical evidence in a diversity of cell types that Cx43 enters the Golgi apparatus, where it may be post-translationally modified en route to the plasma membrane. These results are also in agreement with the biochemical detection of Cx32 in Golgi membrane fractions (Rahman *et al.*, 1993).

Chapter 4

The control of *de novo* gap junction assembly in the 8-cell stage

4.1 Introduction.

In the preimplantation mouse embryo inhibition of transcription and translation from the early 4-cell stage onward does not interfere with the assembly of functional gap junctions at their normal time, although compared to control embryos the extent of coupling is significantly reduced (McLachlin *et al.*, 1983; McLachlin and Kidder, 1986). Thus there is enough connexin protein by the 4-cell stage to permit some coupling once gap junctions are assembled. My ability to detect Cx43 in gap junctions with compaction, and in the cytoplasm but not the plasma membrane prior to compaction, suggested that this protein was one of the members of the connexin gene family which could contribute to this coupling.

The objective of the present chapter was to determine the limiting factor regulating assembly of gap junctions during compaction in the 8-cell stage. Although mRNA for Cx43 is present by the 4-cell stage (Valdimarsson *et al.*, 1991), it remained unclear whether the cytoplasmic immunoreactivity for Cx43 detected in precompaction embryos represented newly synthesized protein or stored protein awaiting a signal to be mobilized to the plasma membrane, or both. In addition, although I could not detect Cx43 in the plasma membrane prior to compaction, the

possibility remained that gap junction assembly at compaction might involve recruitment of either masked Cx43 or other connexins stored in the plasma membrane. Thus, in the present chapter two questions were posed: First, is Cx43 mRNA translated as soon as it becomes available in the 4-cell stage, and secondly, is *de novo* gap junction assembly dependent on trafficking of Cx43 to the plasma membrane during compaction? Since at the time these experiments were conducted there was no supply of the anti-Cx43 antibodies (anti-Cx43/252 and anti-Cx43/360) which could detect Cx43 in the cytoplasm of precompaction embryos, the sensitivity of that Cx43 staining to cycloheximide was not examined. To determine if Cx43 is translated prior to compaction, I examined if Cx43 mRNA is found in polyribosomes in the 4-cell stage. Given the ability of trafficking-inhibitors to alter trafficking organelles and redistribute nascent Cx43 in morulae (chapter 3), the requirement of *de novo* gap junction assembly for trafficking of proteins, including Cx43, to the plasma membrane, was examined by treating uncompacted 8-cell embryos continually with trafficking inhibitors until control embryos had acquired functional gap junction channels.

4.2 Materials and methods.

4.21 Embryo ribonucleoprotein fractionation and RNA isolation.

In order to investigate the utilization of Cx43 mRNA for protein synthesis in the 4-cell stage (the earliest stage in which it had been detected by Northern blotting) a microscale ribonucleoprotein (RNP) fractionation technique known to effectively separate subribosomal (*i.e.* less than 80S) and polyribosomal (*i.e.* 80S and greater) RNP fractions was used (Naus *et al.*, 1992). The mRNA content of these fractions was then assayed by reverse transcription coupled with the polymerase chain reaction (RT-PCR). Approximately 500 embryos were collected for each RNP fractionation. Embryos were washed five times through ice cold CMF-PBS containing 0.3% PVP, and deposited in a 10-20 μl volume of the last wash in the bottom of a mini-Dounce homogenizer on ice. Embryos were homogenized using the "A" pestle in 300 μl of a solution containing 1% NP-40, 0.4% sodium deoxycholate, 500 units/ml RNasin (Promega, Madison, WI), 10 μg/ml cycloheximide, and 20 μg *E. coli* rRNA in TSM/EGTA buffer (40 mM Tris-HCl, 150 mM NaCl, 20 mM magnesium acetate, 10 mM EGTA, 10 mM dithiothreitol, Ph 7.5; Kidder and Conlon, 1985). The homogenate was centrifuged for 3 min at 24,000 rpm (22,000 x g), 4°C, in the TLA-100 rotor of a Beckman tabletop ultracentrifuge to pellet nuclei and mitochondria. The post-mitochondrial supernatant was divided into two equal portions and each was layered over 50 μl of 40% sucrose in TSM/EGTA and centrifuged in the same rotor for 40 min at 50,000 rpm (100,000 x g), 4°C, forming a polyribosomal

pellet and a subribosomal supernatant.

The subribosomal supernatants were carefully withdrawn and transferred to microfuge tubes. Twenty μl of 3 M sodium acetate and 440 μl of absolute ethanol were added to each and the RNPs allowed to precipitate overnight at -20°C. Each polyribosomal pellet was dissolved in 8 μl of solubilization solution (10 mM Tris-HCl, 1 mM EDTA, pH 8.0, 100 units/ml RNasin, 10 mM dithiothreitol) containing 10 μg *E. coli* rRNA, and then the two pellet fractions were combined. Eighty-five μl of solution D were added [solution D is 4 M guanidinium thiocyanate (GIBCO/BRL, Burlington, Ont.), 25 mM sodium citrate pH 7.0, containing 0.5% Sarkosyl and 100 mM ß-mercaptoethanol; Chomczynski and Sacchi, 1987] and the sample was stored at -20°C overnight. After removal from ethanol by centrifugation, the subribosomal precipitates were likewise each dissolved in 8 μl of solubilization solution, combined, and then diluted with 85 μl of solution D. The two fractions in solution D were then layered over 100 μl of 5.7 M CsCl in 0.1 M EDTA, pH 7.5 and centrifuged in the Beckman TLA-100 rotor at 80,000 rpm (250,000 g) for 4 hr at 20°C to pellet RNA. The pellets were dissolved at room temperature in 100 μl of 2.5 M ammonium acetate and ethanol precipitated overnight at -20°C.

4.22 Reverse transcription-polymerase chain reaction.

After centrifugation to remove the ethanol, the RNA pellets were rinsed twice with cold 70% ethanol before air drying. Reverse transcription (RT) and

amplification of cDNA by polymerase chain reaction (PCR) was based on the method of Rappolee *et al.* (1989). RNA from each RNP fraction was reverse transcribed into cDNA by incubation at 42°C for 90 min with a mixture of 30 U of AMV-RT (Boehringer Mannheim, Laval, Québec) and the following reagents: 0.4 μg oligo-dT primer, 10 mM $MgCl_2$, 100 mM Tris-HCl buffer, pH 8.3, 10 mM dithiothreitol, 1 mM each dNTP, and 40 U of RNAsin (Promega) in a 20 μl volume. Reactions were stopped by boiling for 10 min followed by flash cooling on ice, and divided into suitable aliquots (20-25 embryo equivalents/μl) which were stored at -20°C or used immediately for PCR. Reverse transcriptions were also performed on 2 μg of mouse brain and liver RNA.

PCR was performed on 50-75 embryo equivalents of cDNA using 2.5 U of *Taq* DNA polymerase (GIBCO/BRL) in a solution consisting of 1 μM oligonucleotide 5' and 3' sequence-specific primers, 200 μM dNTP, 10 mM Tris-HCl, pH 8.8, 3.5 mM $MgCl_2$, 50 mM KCl, and 0.1% Triton X-100, in a 50 μl volume. Amplification reactions were carried out for 30 cycles using a Perkin Elmer Cetus DNA Thermal Cycler (1 min at 94°C, 1 min at 65°C, and 2 min at 72°C). Oligonucleotide primers for mouse Cx43 amplified a 332 bp segment spanning nucleotides 807-1138 (corresponding to a.a 203-312) of mouse Cx43. This segment contains a diagnostic restriction site for Hpa II producing 162 and 170 bp fragments. The mouse Cx43 primers were (5'-primer) 5'-TGGCTGCTCCTCACCAACGGC-3', and (3'-primer) 3'-CGTCTGGAGCCGGACTACTGG-5'. Primers for ß-actin were also used; these amplify a 243 bp segment of the cDNA spanning an intron (87 bp) in the genomic

sequence. The mouse ß-actin primers were (5'-primer) 5'-CGTGGGCCGCCC-TAGGCAACCA-3, and (3'-primer) 3-'GGGGGGACTTGGGATTCCGGTT-5' (Tokunaga *et al.*, 1986). Restriction enzyme digestion of the 332 bp Cx43 amplified fragment was performed on PCR products which had been precipitated overnight at -20°C with 3 M ammonium acetate and ethanol, pelleted, washed with 70% ethanol, and air dried. Reactions were performed with 10 units of Hpa II (BRL, Burlington, Ont.) in 1X One Phor All Buffer Plus (Pharmacia LKB Biotechnology, Que.) for 1 hour at 37°C.

4.23 Southern analysis.

PCR products were separated by electrophoresis in an 80-V constant voltage field in a 4% agarose gel (NuSieve 3:1, FMC BioProducts, Rockland, ME) containing 40 mM Tris-acetate, 1 mM EDTA and 0.75 µg/ml ethidium bromide. Prior to Southern transfer of gel contents, a transparent acetate template denoting the position of the PCR amplification products was prepared whilst viewing the gel on a UV transilluminator, and the orientation of the gel was marked by notching the bottom right corner. Gel separated PCR products were then denatured by soaking gels for 45 min in 1.5 M NaCl, O.5 N NaOH. Gels were next rinsed in ddH_2O, and soaked for 30 min and then 15 min in two changes of neutralizing buffer (1 M Tris, 1.5 M NaCl, pH 7.4). Neutralizing buffer was removed by rinsing three times in ddH_2O. PCR products were transferred to Hybond-N (Amersham, Oakville, Ont.) by capillary blotting overnight (16-20 hr) in 10X SSC (1.5 M NaCl, 150 mM tri-sodium citrate,

pH 7.0) as described in Sambrook *et al.* (1989).

Blots were probed with cDNAs labeled by the random primer method (Feinberg and Vogelstein, 1983) using reagents from a BRL Random Primers DNA Labeling System (Bethesda Research Laboratories Life Technologies, Inc., Burlington, Ont.). Each labeling reaction in a 50 μl volume contained 25 ng of insert DNA, previously excised from its respective vector and isolated by electrophoresis in low melting point agarose (Valdimarsson, 1993), and 50 μCi of ^{32}P-dCTP (3000 Ci/mmole, NEN-Dupont, Markham, Ont.). Reactions were carried out at room temperature for 5 hr from the addition of Klenow fragment, and were stopped by the addition of 5 μl of stop buffer (0.2 M Na_2EDTA, pH 7.5). To determine the total and incorporated radioactivity in each labeling reaction, a 1 μl aliquot was first diluted with 500 μl of distilled water, which in turn was spotted six times as 5 μl aliquots on GF/C or GF/F filters (Whatman). Three of these dried filters were placed directly in scintillation vials with Omnifluor (NEN-Dupont) to measure total label. The remaining three were precipitated for 2-3 min in two volumes of ice cold 10% trichloroacetic acid, followed by a rinse with 70% ethanol, to determine incorporated radioactivity. Probe mixes were eluted through a Nick column (Pharmacia) in Tris-EDTA buffer (TE buffer, Sambrook *et al.*, 1989) to separate labeled cDNA probe from unincorporated nucleotides. The total radioactivity in the recovered probe was measured by spotting a 1 μl sample of the eluted probe. The specific activity of labeled cDNA probes ranged from 1-2 X 10^9 cpm/μg DNA.

Blots were probed with labeled cDNAs in a Robbins Hybridization Incubator (Model 310). Blots were first prehybridized for 4 hr at 42°C in prehybridization solution [5X SSPE, 50% deionized formamide, 5X Denhardt's, 10% dextran sulfate, and 100 μg/ml denatured salmon sperm DNA (Sambrook et al, 1989) and then hybridized overnight at the same temperature in prehybridization solution containing 1-3 ng/ml of ^{32}P-labeled probe, boiled for 10 min immediately before use. Following hybridization, blots were rinsed briefly, and then for 30 min with 2X SSC, 0.5% SDS at 42°C, and then with the same buffer for 30 min at 65°C. Following this, blots were washed once for 30 min and twice for an hour each, at 65°C with 0.5X SSC, 0.5% SDS. Blots were drained, wrapped tightly in Saran Wrap® to prevent drying, and exposed to Kodak X-Omat XRP-1 film in autoradiographic folders containing a Dupont Cronex Xtra-life intensifying screen (Dupont, Wilmington, DE). Blots were exposed at -80°C from 1.5 to 22 hr. Hybridization signals were quantified using an LKB Ultroscan XL laser densitometer.

4.24 cDNA probes.

Cx43-specific PCR amplification products were detected by hybridization with a previously characterized 1.4 kb cDNA, representing the entire coding sequence for rat Cx43, which was cloned into a Bluescript M13 + plasmid vector. This cDNA was isolated from a heart library and hybridizes to a 3.0 kb RNA present in several adult tissues and in mouse blastocysts (Beyer *et al.*, 1987; Barron *et al.*, 1989). ß-actin specific PCR amplification products were detected by hybridization with a previously

characterized 2.0 kb embryonic chick brain cDNA, which had been cloned into the pBR322 plasmid vector (Cleveland *et al.*, 1980).

4.25 Embryo manipulation and dye coupling.

To determine if the *de novo* gap junction assembly during compaction is dependent on mobilization of connexins to the plasma membrane, uncompacted 8-cell embryos (68-70 hr pHCG) were isolated and placed in SECM at 37°C, 5% CO_2 containing either 0.01-0.05% ethanol (carrier control), 5 μg/ml monensin, or 1-5 μg/ml brefeldin A until carrier control embryos had compacted and established functional gap junction channels. Since monensin is unstable at high temperatures embryos were transferred to fresh pre-equilibrated culture medium every 4-6 hours. To test for functional channels a single blastomere of an embryo would be injected iontophoretically with the fluorescent dye 6-carboxyfluorescein (10 mM in distilled water; Kodak, Rochester, NY) using a continuous train of hyperpolarizing current pulses of 17 nA (200 millisecond duration, one pulse per second). Dye delivery was terminated 1 minute after impalement, and the electrode was maintained in the injected cell for the duration of each observation. Non-injected sister embryos were rescued from either monensin or brefeldin A treatments by passage through three changes of carrier control SECM, followed by collection and incubation in a fourth wash at 37°C, 5% CO_2 until 120 hrs post-hCG.

Microelectrodes for dye injection were prepared from glass capillary tubing (WP instruments Inc., New Haven, CT; No.1B100F) using a vertical microelectrode puller (Narashige), and backfilled with dye for approximately 10 hours before use. Injections were performed at room temperature (28-30°C) on a Zeiss Axiovert 35 inverted microscope fitted with phase epifluorescence optics, and a narrow-band FITC excitation filter (BP 485/20) and barrier filter (BP 520-560) in the light path. Embryos were held for microinjection by suction using a fire polished glass holding pipette with an opening of 30-50 μm. Microelectrode and holding pipettes were attached to DeFonbrune micromanipulators (Beaudouin, Paris). The bathing solution (FM-1) was grounded through a KCl-agar bridge (4% agarose in 3 M KCl in a 1 mm glass capillary). Membrane potentials were recorded on a Brush 220 chart recorder. Embryos were photographed using Kodak T-Max 35 mm film (ISO 400) which was developed in Kodak T-Max developer for 6.5 min at 22 °C.

4.3 Results.

4.31 Cx43 mRNA is on polyribosomes in the 4-cell stage.

To determine whether Cx43 mRNA is recruited into polyribosomes for translation as soon as it becomes available in the 4-cell stage, embryo ribonucleoproteins (RNPs) were separated into subribosomal (S) and polyribosomal (P) fractions. This fractionation technique, developed using 10 mg samples of mouse liver and tested with cultured rat glioma cells exhibiting a high level of Cx43 expression, results in an almost complete separation of subribosomal and polyribosomal RNPs, with 80S monosomes being split between the two fractions (Naus *et al.*, 1992). Preliminary sedimentation profiles of embryo ribonucleoprotein revealed that they were similar to that seen in mouse liver (Pape and Kidder, personal communication).

RNA isolated from 4-cell stage S and P RNP fractions prepared using the microscale fractionation technique was reverse transcribed to cDNA and subjected to DNA amplification using oligonucleotide primers designed to amplify a 332 bp segment of mouse Cx43. Amplification products were separated on a 1% ethidium bromide-containing agarose gel and probed with radiolabeled cDNA after Southern blotting. In cDNA prepared from three separate RNA extractions, the Cx43 primers selectively amplified only the expected 332 bp fragment from both the S and P RNP fractions of 4-cell embryos, with most of the amplification product being contributed

by the P fraction (Fig. 4.1 Ai). A similar fragment was always amplified from brain cDNA, the positive control. *Hpa*II digestion of this fragment generated a poorly-resolved doublet at the approximate location expected for the diagnostic restriction fragments (162 and 170 bp). In addition, hybridization with the 1.4 kb Cx43 cDNA detected only the single 332 bp band in brain and embryo fractions (Fig. 4.1 Bi). Although faint in this figure, longer autoradiographic exposures also detected the faster migrating restriction fragments produced by *Hpa*II digestion. The faintness of these restriction fragments in relation to the undigested amplification product may be related to their smaller size. The smaller a DNA fragment is, the more likely it will diffuse laterally during blotting and hybridize inefficiently (Selden, 1989).

One problem with the use of RT-PCR to detect Cx43 mRNA is the absence of introns from the genomic coding sequence (Willecke *et al.*, 1991a). Since the amplified segment obtained from genomic DNA is the same size as that from cDNA, precautions were taken to ensure the absence of contaminating DNA, including the isolation of embryo RNA by pelleting through CsCl. To check that the 332 bp Cx43 fragment obtained from the S and P fraction cDNA did not arise from contamination, an oligonucleotide primer set for ß-actin was used with the same RT preparations. This primer set amplifies a 243 bp segment from cDNA but, because the primers bracket an 87 bp intron, amplifies a 330 bp segment from genomic DNA. When this primer set was used for PCR with genomic DNA both 243 and 330 bp fragments could be detected on ethidium bromide-stained gels, although using the more stringent criterion of hybridization with the cloned cDNA, only the larger (intron containing)

Figure 4.1. Cx43 mRNA is recruited into polyribosomes in the 4-cell stage. (A) Ethidium bromide-stained agarose gel containing PCR products obtained with primer sets which amplify a 332 bp segment of Cx43 cDNA (i), or a 243 bp segment of ß-actin cDNA (ii); the 330 bp ß-actin segment derived from amplification of genomic DNA (Genom.) is also shown. (B) Southern blot of the gel in (A) probed with ^{32}P-labeled cDNA for Cx43 (i) or ß-actin (ii). The 332 bp Cx43 fragment from mouse brain cDNA (Br), included as a positive control, was digested with Hpa II to reveal the presence of a diagnostic restriction site indicated by the doublet at 162-170 bp. This doublet appears faintly in the present figure and required longer autoradiographic exposures to be visualized clearly. Liver cDNA (L) served as positive control for the ß-actin amplification. Absence of the 330 bp intron-containing ß-actin amplification product in the 4-cell embryo subribosomal (S) and polyribosomal (P) RNP fraction cDNAs demonstrates that these are free of genomic DNA contamination. The cDNA in embryo lanes are derived from 25 embryo equivalents each. In three separate experiments Cx43 mRNA was found predominately in the P fraction. No amplification products were obtained from E. coli rRNA (-), the carrier RNA used during RNA purification, using either of the two primer sets.

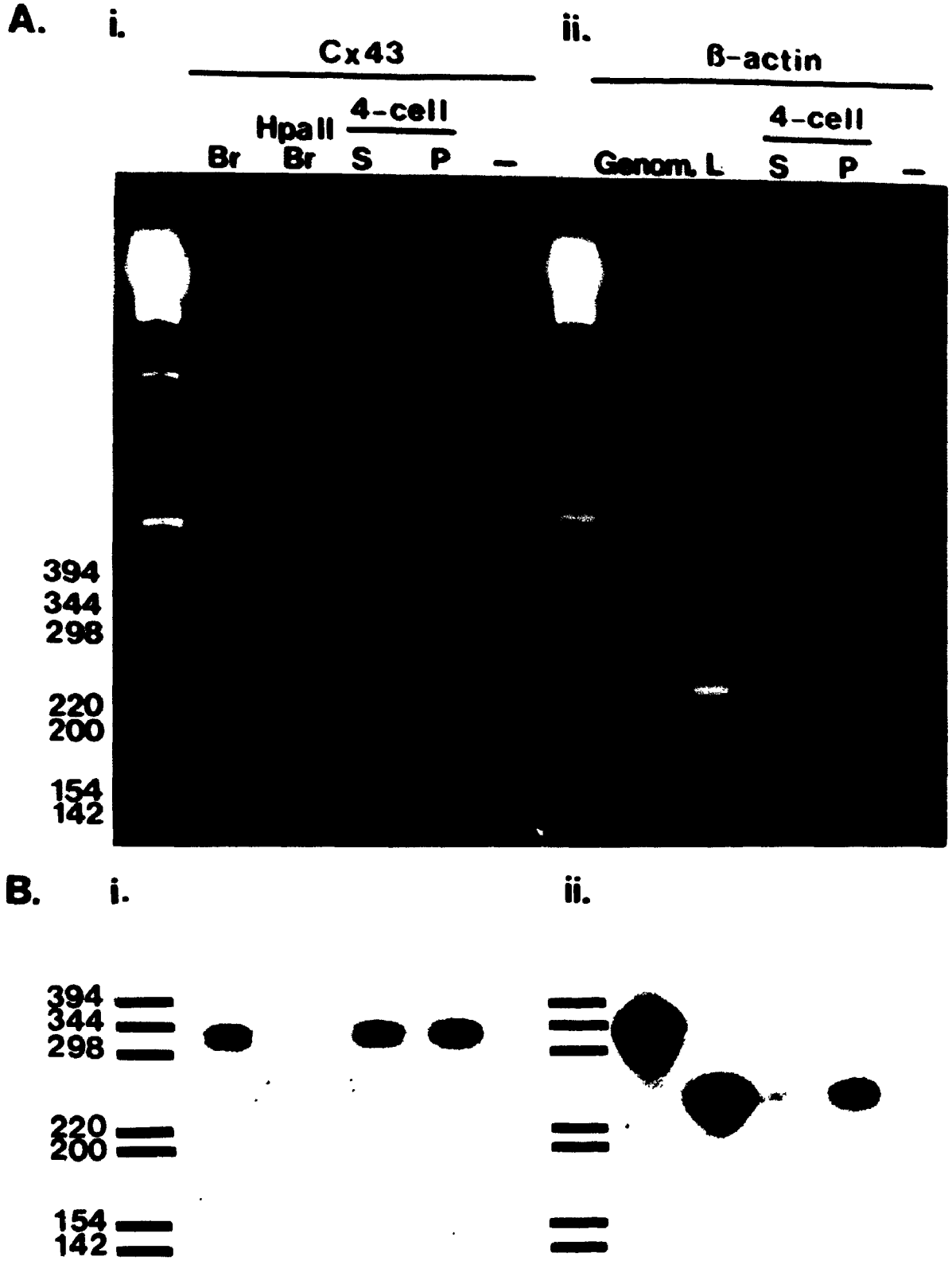
A.
i.
Cx43
ii.
ß-actin
HpaII
4-cell
4-cell
Br
Br
S
P
–
Genom. L
S
P
–
394
344
298
220
200
154
142
B.
i.
ii.
394
344
298
220
200
154
142

fragment could be confirmed as ß-actin (Fig. 4.1 Aii, Bii). This larger fragment could not be detected in the embryo RNP fractions on either the gel or the Southern blot, even upon longer autoradiographic exposures, confirming the absence of genomic DNA from these preparations. No amplification products were evident when either Cx43 or ß-actin primers were used to amplify cDNA prepared from E. coli rRNA, the carrier RNA used during embryo fractionation and RNA purification. Thus, the amplification product detected in the 4-cell P RNP fractions was specific for Cx43 mRNA, suggesting that this message is translated at this stage. At least a portion of the cytoplasmic Cx43 immunoreactivity in 4-cell embryos must therefore be nascent Cx43.

4.32 Monensin and brefeldin-A inhibit the acquisition of dye coupling in the 8-cell stage.

Given that Golgi complexes are also present in uncompacted embryos (Fig. 2.13), and the evidence from chapter 3 that these organelles and nascent Cx43 distribution in morulae could be affected by the trafficking inhibitors monensin and BFA, the ability of these agents to prevent the *de novo* assembly of gap junctions and delay the onset of intercellular coupling at compaction was examined. Intercellular communication via gap junctions was assayed by dye coupling, wherein the intercellular transfer of microinjected carboxyfluorescein was monitored. Uncompacted 8-cell embryos were cultured in the continued presence of either 5 μg/ml monensin or 1-5 μg/ml BFA until control embryos treated with carrier solvent (0.01-0.05%

ethanol) began exhibiting rapid dye transfer to all blastomeres. To guard against the inactivation of inhibitors during the culture period, embryos (control and treatment groups) were transferred to fresh culture drops every 4-5 hours. Embryos exhibiting no dye transfer or transfer to only a single blastomere were designated as not coupled, the latter situation presumably arising from transfer of dye through remnant cytoplasmic bridges connecting sister blastomeres (Kidder *et al.*, 1988). Conversely, embryos exhibiting transfer to more than one blastomere were considered coupled. The extent of coupling was further categorized based on the rate of dye transfer, defined as the time necessary for dye to enter all the cells in the focal plane of the injected cell, up to 30 minutes. Dye transfer times of ≤ 10 min, 10-20 min, or 20-30 min were considered rapid, moderate, and slow, respectively. Coupling in embryos with incomplete dye transfer after 30 minutes was considered very slow.

Both monensin and BFA markedly reduced both the incidence of dye coupling and extent of coupling where it occurred (Fig. 4.2). Virtually all of the control embryos were coupled, with close to 75% of these embryos showing rapid dye transfer. In contrast, no dye coupling was detected in over 50% of embryos treated with either monensin or BFA. Similarly, coupling in over half of inhibitor-treated embryos classified as coupled was very slow (*i.e.* incomplete after 30 minutes) (Table 4.1). Although the effects of monensin and BFA on dye coupling were virtually identical, BFA appeared to be slightly less effective. Twenty-two percent of coupled BFA-treated embryos exhibited rapid dye transfer compared with 9% of coupled monensin-treated embryos. However, this still only amounted to approximately 11%

Figure 4.2. Monensin or BFA interfere with the acquisition of dye coupling during compaction. Precompaction 8 cell embryos were cultured in SECM containing 0.01-0.05% ethanol (control; A,D,G,J), 5 μg/ml monensin (B,E,H,K), or 1-5 μg/ml BFA (C,F,I,L) for 10 to 18 hours before being injected with 6-carboxyfluorescein and monitored for dye transfer. Virtually all control embryos exhibited rapid dye transfer to all cells within 30 minutes (A,D,G,J). Greater than 50% of both monensin- and BFA-treated embryos showed either no dye transfer (C,F,I,L), or transfer to a single, adjacent blastomere. Remaining embryos exhibited either a reduced rate of dye transfer (B,E,H,K), or transfer to only a subset of cells (Table 4.1). Although the embryos in all treatment groups initially underwent cell flattening during culture, BFA-treated embryos later showed decompaction of one or more blastomeres. There was no correlation between the incidence of decompaction and the extent of dye coupling in these embryos. Scale bar equals 20 μm.

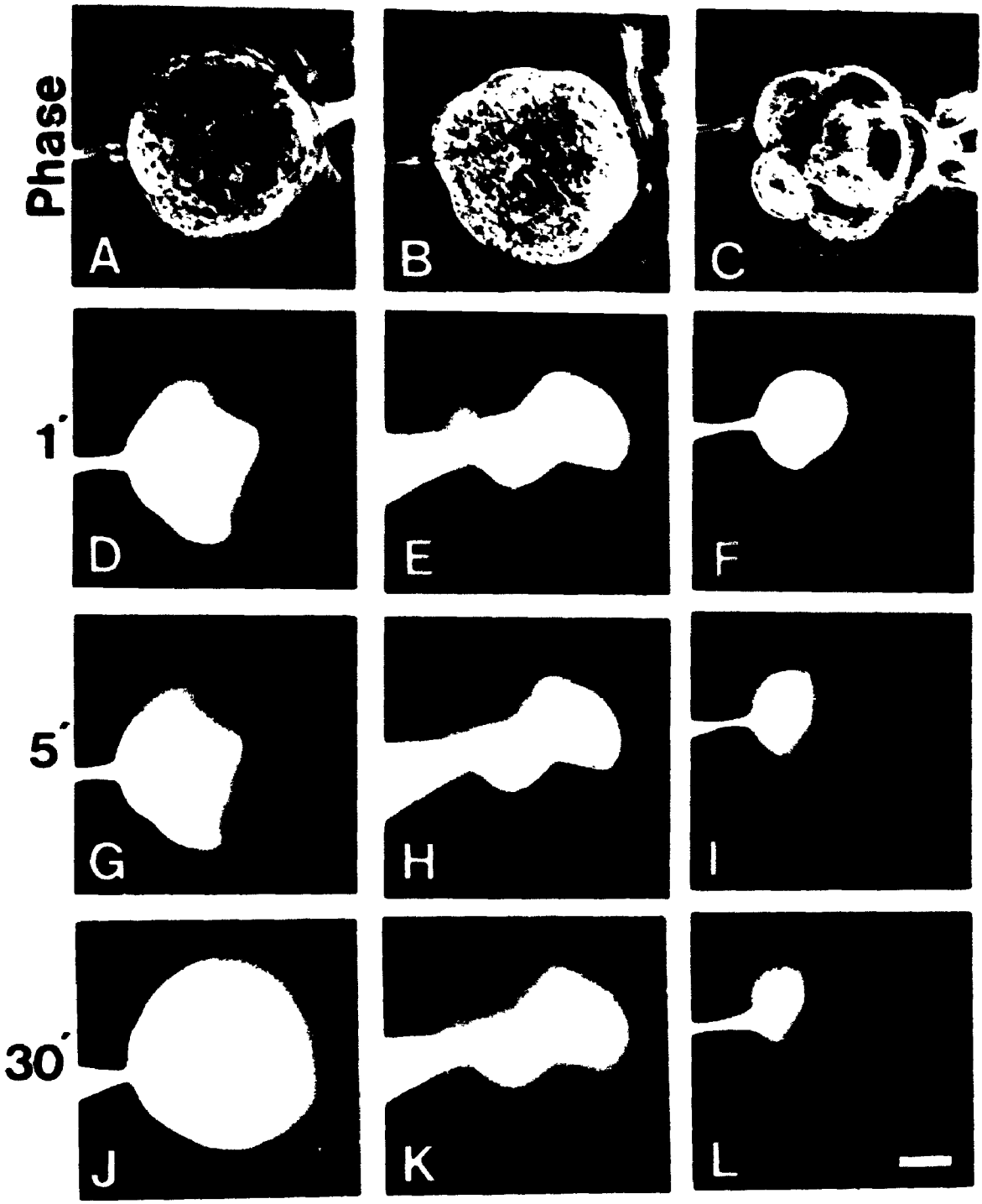
Phase
A
B
C
1'
D
E
F
5'
G
H
I
30'
J
K
L

Table 4.1

Treatment of uncompacted 8-cell embryos with monensin or BFA reduces the frequency and limits the extent of dye coupling

Treatment[a]	Number Scored	% Embryos Coupled[b]	% of Coupled Embryos: Dye Transfer Time (min)[c] Rapid ≤ 10	Moderate 10-20	Slow 20-30	Very Slow ∅[d]
Control	28	96	74	15	7	4
5 μg/ml Monensin	23	48	9	18	18	55
5 μg/ml BFA	22	41	22	0	22	56

[a] Embryos were cultured from 10 to 18 hours in SECM containing either 0.01-0.05% ethanol (control) or inhibitor, prior to being injected with 6-carboxyfluorescein.

[b] Defined as embryos exhibiting transfer of dye from an injected blastomere to more than one adjacent blastomere. Transfer to a single blastomere was assumed to be due to cytoplasmic bridges connecting mitotic sisters.

[c] Defined as the time taken for dye to enter all the cells in the focal plane of injection, up to 30 minutes.

[d] Although embryos were coupled, dye had not entered all cells in the focal plane of injection by the end of the 30 minute observation period.

of all BFA-treated embryos, and 5% of all monensin-treated embryos tested for dye coupling. Despite BFA's ability to induce decompaction of one or more blastomeres, there was no correlation between the state of compaction of a treated embryo and its ability to transfer dye. Most importantly, the inhibitory effect of monensin or BFA on the establishment of dye coupling was reversible. Non-injected embryos treated for up to 18 hours with either drug were washed free of inhibitor by passage through several drops of control culture medium and then observed for their ability to form blastocysts. Gap junctional communication between embryonic blastomeres is an essential requirement for blastocyst development (Buehr *et al.*, 1987). After 10 hours of recovery, only 40% of either monensin-treated (n 63) or BFA-treated (n 25) embryos had formed a blastocoel cavity, compared to 80% of controls (n 64). By 34 hours, however, there was virtually no difference between these groups with 96% of controls (n =82), 97% of monensin-treated (n 63), and 90% of BFA-treated embryos (n =38) having cavitated (Fig. 4.3). Thus, although blastocyst formation was delayed, neither monensin nor BFA irreversibly damaged the ability of embryos to resume normal development.

4.33 Monensin and brefeldin-A prevent the formation of gap junctions containing connexin43.

Finally, to confirm that monensin and BFA delayed the acquisition of gap junctional communication by interfering with the *de novo* assembly of gap junctions, embryos treated with inhibitors from prior to compaction (68 hr post hCG) until the

Figure 4.3. Embryos rescued from monensin and BFA can still cavitate. Embryos were cultured from the early 8-cell stage, prior to compaction, for up to 18 hr in SECM containing either 0.01% ethanol (A), 5 μg/ml monensin (B), or 1-5 μg/ml BFA, before being washed and transferred to carrier control culture medium. Although cavitation was delayed in inhibitor-treated embryos, after 34 hr of recovery virtually all of embryos in each treatment group had formed blastocysts.

Scale bar 50 μm.

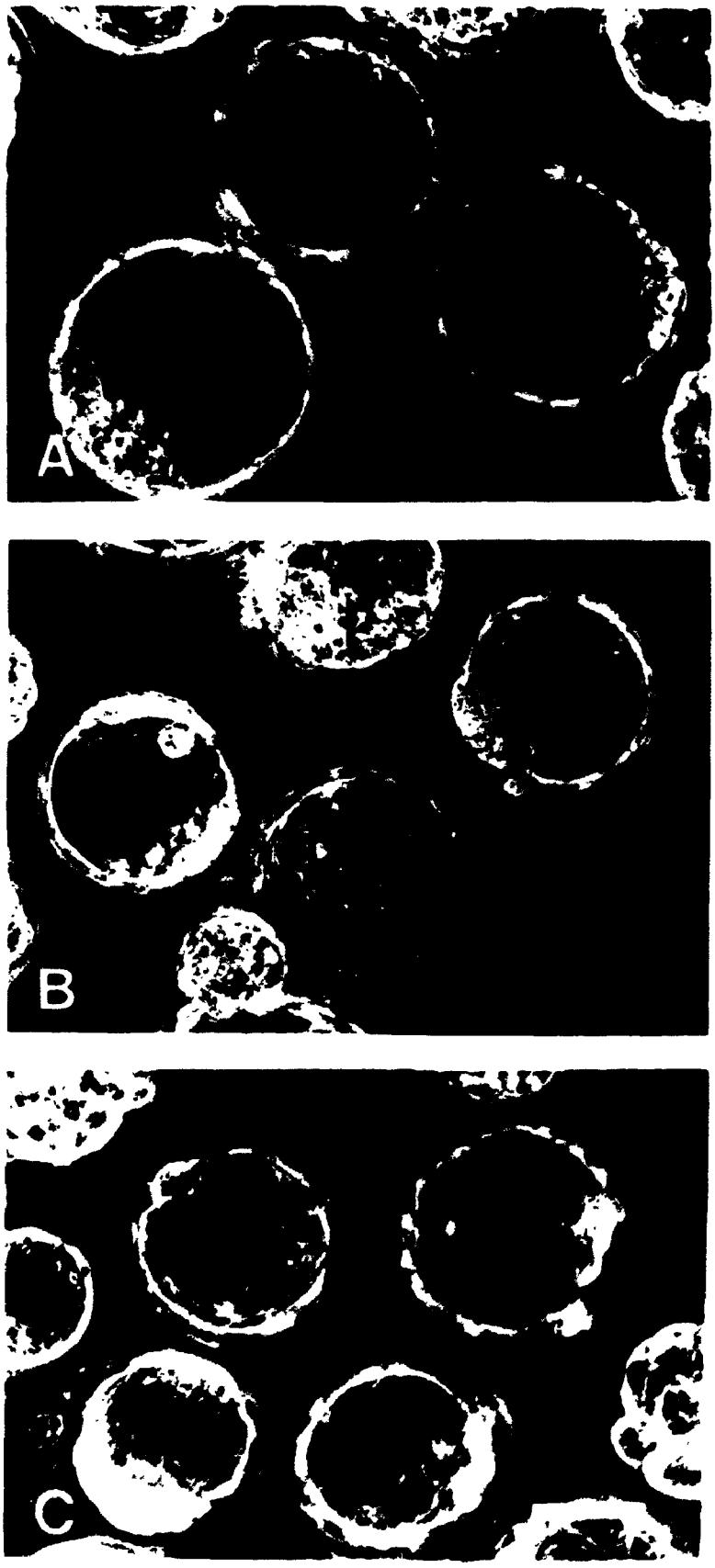
A
B
C

acquisition of rapid dye coupling by controls 12 hours later, were stained for immunofluorescence with anti-Cx43/302. In three separate, blind experiments both monensin and BFA consistently reduced the frequency and size of gap junction-like structures within treated embryos (Fig. 4.4). This effect was especially pronounced in BFA-treated embryos, which during the treatment period first compacted and then decompacted as observed with morulae. Anti-Cx43/302 did recognize cytoplasmic structures in both monensin- and BFA-treated embryos, and the staining patterns were very similar to those exhibited by compacted morulae treated with the same inhibitors (Fig. 3.2).

Figure 4.4. Treatment with monensin or BFA beginning prior to compaction reduces the size and frequency of gap junction-like structures. Uncompacted 8-cell embryos were cultured in the presence of either 0.05% ethanol (A), 5 μg/ml monensin (B), or 1 μg/ml BFA (C), as described for the dye coupling experiments. In three separate, blind experiments, monensin and BFA consistently reduced the size and frequency of gap junction-like structures (arrowheads) within most treated embryos. Effects ranged from complete abolishment of identifiable gap junctions, mostly seen in BFA-treated embryos (C), to partial abolishment wherein embryos exhibited either a uniform or regional reduction in plaque size and frequency (B). These treatments induced the same cytoplasmic staining patterns seen in post-compaction embryos treated for 4 hr (Fig. 3.2). Small diffuse foci (open arrows) seen in controls (A) were augmented by large juxtanuclear clouds (curved arrows) in the presence of monensin (B), and replaced by a reticulated network of immunoreactivity (solid arrows) with BFA (C). Scale bar = 32 μm.

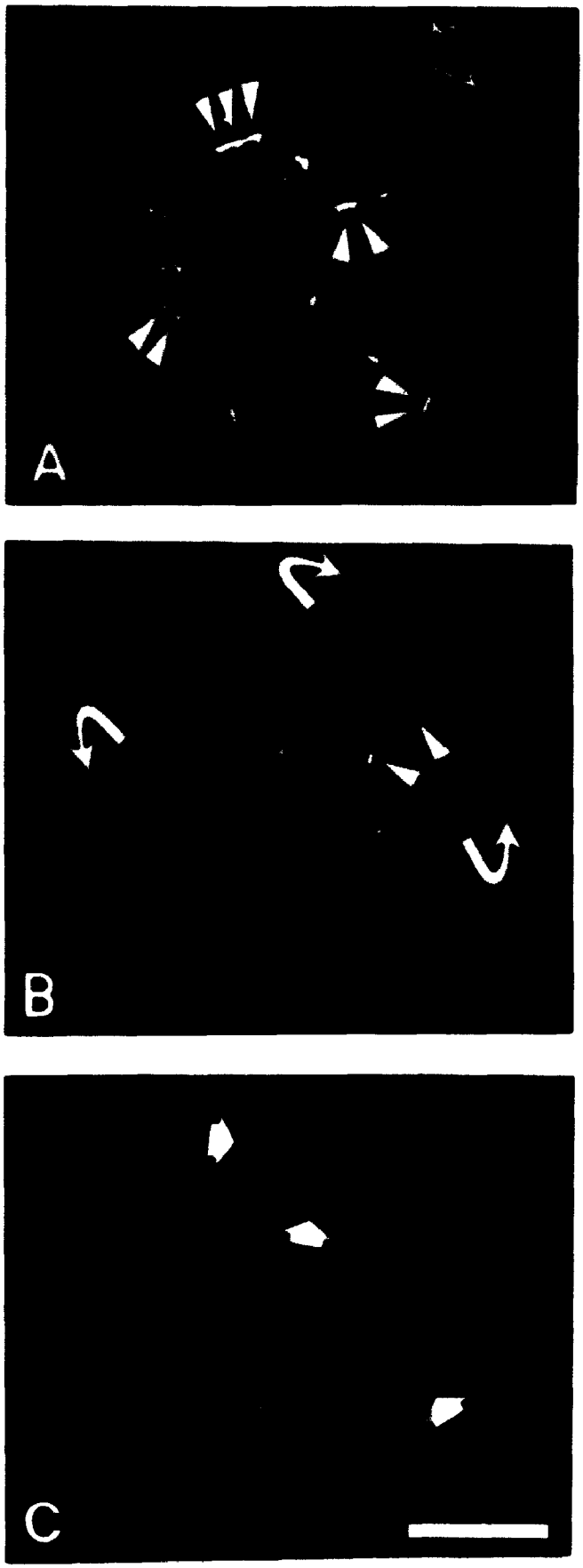
A
B
C

4.4 Discussion.

4.41 Regulation of *de novo* gap junction assembly in the mouse preimplantation embryo.

Treatment of precompaction embryos with monensin or BFA reversibly interfered with the onset of dye coupling, and the formation of gap junction-like structures during compaction. These results suggest that gap junction channels assembled at that time are dependent on one or more intracellular protein trafficking steps. Translation of Cx43 mRNA during preimplantation development begins at least as early as the 4-cell stage, at least 12 hours (one cell cycle) in advance of when gap junctions first form. For this reason, it is unlikely the onset of gap junction assembly in the 8-cell stage is triggered by the onset of Cx43 translation.

Based on these results and those described in preceding chapters, in addition to previously established information, it is possible to construct a model to describe the regulation of *de novo* gap junction assembly in the mouse preimplantation embryo. This model is summarized in Fig. 4.5, and consists of 4 major tenets, which are described and justified below:

(1) **Prior to compaction in the 8-cell stage, connexins are unlikely to reside in the plasma membrane.** Using antibodies raised against four different C-terminal domains of Cx43, this protein could not be detected at the surface prior to signs of

Figure 4.5. Model for the regulation of *de novo* gap junction assembly in relation to Cx43 trafficking. In the figure, Cx43 is depicted as an integral membrane protein with its "extracellular" loops directed in towards the lumen of cytoplasmic organelles. Prior to compaction (top), Cx43 is absent from the plasma membrane, although oogenetically derived stored protein may reside in endosome clusters (EC) in the cortical cytoplasm. Since translation of Cx43 mRNA has already begun by this time it is also likely that nascent Cx43 resides in the endoplasmic reticulum (ER), although it is unclear whether it can be immunocytochemically localized to this organelle at this stage. Immediately prior to or during compaction (bottom) Cx43 is translocated to the plasma membrane, presumably to apposed membrane regions, where it is inserted into gap junctions. Both nascent Cx43, delivered via the Golgi complex (GC), and stored Cx43, which may be delivered to the plasma membrane via the trans-Golgi network (TGN) or independently thereof, may be used for *de novo* gap junction assembly. Trafficking of Cx43, and presumably other connexins, can be inhibited by BFA and monensin, possibly acting on GC cisternae. Delaying the second round of DNA replication in the 2-cell stage also inhibits *de novo* gap junction assembly, presumably by acting distal to the GC by interfering with the trafficking of Golgi-derived vesicles (V). Although Cx43 is depicted in cytoplasmic organelles as an integral membrane protein, the point at which this protein is oligomerized into connexons remains unknown. Nuclei (N).

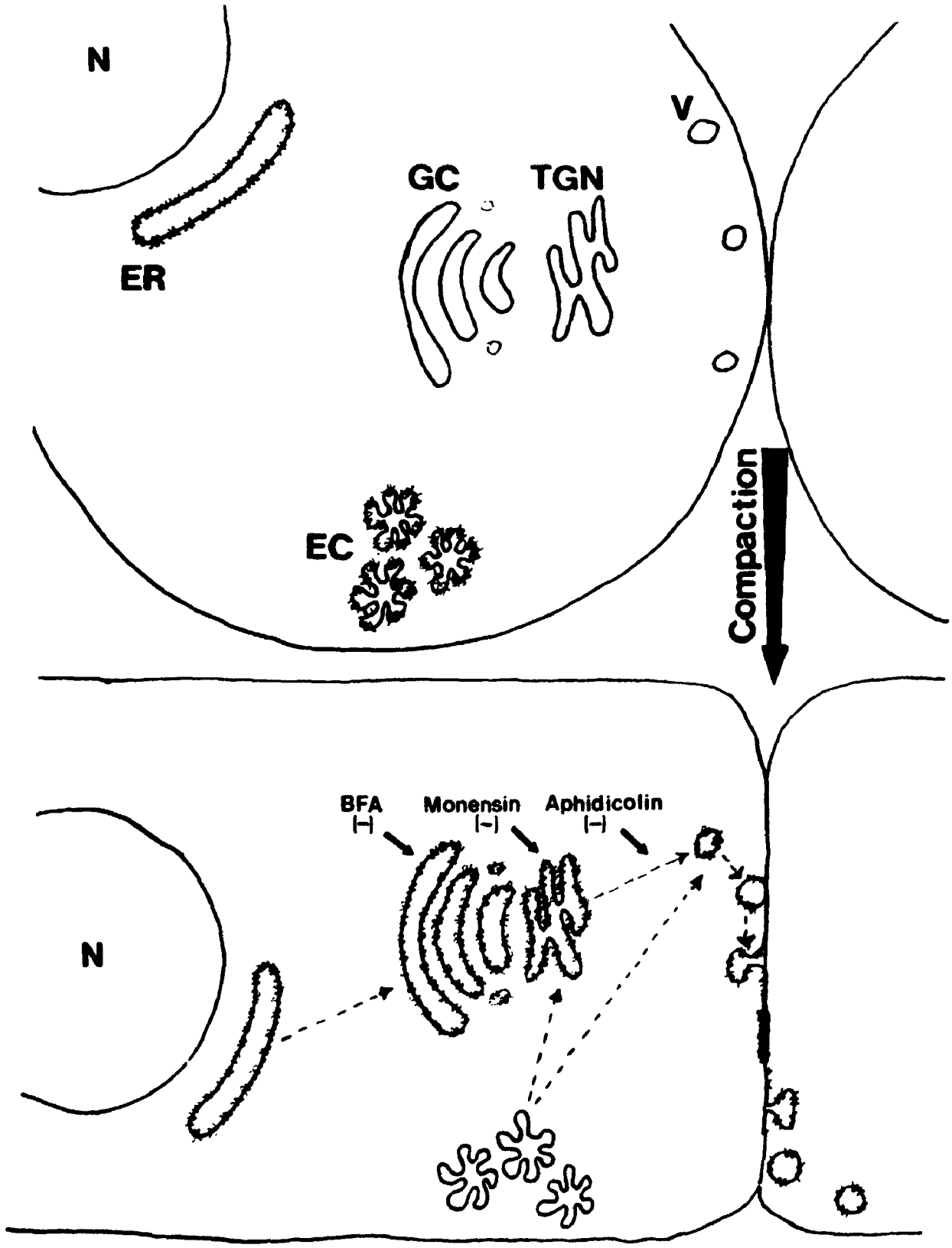
N
ER
GC
TGN
V
EC
Compaction
BFA
[–]
Monensin
[–]
Aphidicolin
[–]
N

cell flattening in the 8-cell stage using immunofluorescence (present study section 2.32; Valdimarsson *et al.*, 1991; Nishi *et al.*, 1991). Cx32 is similarly absent in precompaction embryos, not to mention postcompaction embryos as well (section 2.31). In addition, 4-cell embryos or their isolated blastomeres are unable to form gap junctions when paired with each other or with communication-competent 8-cell embryos (Goodall and Johnson, 1982; McLachlin *et al.*, 1983). These results suggest that it is unlikely that any utilizable connexins are in the surface membranes of embryos prior to gap junction assembly. However, as discussed for Cx32 (section 2.41), the presence of masked connexins in surface membranes still cannot be ruled out altogether. Our ability to detect connexins in the surface membranes of both pre- and postcompaction embryos may also have been influenced by the permeabilization of surface membranes with non-ionic detergents for wholemount immunofluorescence.

(2) **Precompaction embryos contain both nascent and stored connexins, both of which can contribute to the *de novo* assembly of gap junctions.** Inhibition of transcription or translation from the 4-cell stage onward significantly reduces but does not completely abolish the acquisition of functional gap junctions in the 8-cell stage (McLachlin and Kidder, 1986). Thus, although continued embryonic gene expression is required to provide the full complement of gap junctional communication, sufficient gap junction precursors (*i.e.* connexins) are already available at the 4-cell stage to permit some coupling later in development. In the present chapter, evidence supporting the translation of Cx43 in the 4-cell stage was provided by the detection of Cx43 mRNA in polyribosomes. Although we cannot preclude the possibility that the

initiation of translation of connexin transcripts begins earlier in development (*i.e.* as soon as new message becomes available with the activation of embryonic transcription), it is also possible that oogenetically derived Cx43 may contribute to embryonic gap junctions. Cx43 is utilized by the oocyte to mediate gap junctional communication with surrounding cumulus cells in the ovary (section 2.33). Cumulus-oocyte gap junctions are assumed to disassemble by lateral dispersion of subunits in the plane of surface membranes (Larsen *et al.*, 1987). Given the apparent absence of connexins from the surface of precompaction embryos, these proteins are presumably internalized into endosome-like structures in the cortical cytoplasm (section 2.42), which could then be recycled to the surface at the appropriate time (see tenet #4 below).

(3) **Prior to compaction, connexins are in either the endoplasmic reticulum or in endosomes, but absent from the Golgi complex.** In chapter 2, the detection of Cx43 in endosome-like structures was a distinctive feature of precompaction embryos, absent from later stages (Fig. 2.8). Conversely, the small diffuse cytoplasmic foci in compacted embryos, were absent from earlier stages. This cytoplasmic staining in morulae is likely to represent nascent protein in Golgi or Golgi-derived vesicles, since it was sensitive to cycloheximide and could be redistributed by BFA or monensin (section 3.42). The detection of Cx43 mRNA in polyribosomes in the 4 cell stage, also suggests that nascent Cx43 resides in the ER of these embryos. However, it is unclear whether one would be able to detect it with the antibodies which provided the endosome-like staining (anti-Cx43/252 and anti-Cx43/360), since the antibody which

detected nascent Cx43 in morulae could not do so in earlier stages. It is also conceivable that Cx43 cannot be detected in the ER by immunofluorescence since it may be too diffusely distributed within this organelle.

(4) **The *de novo* assembly of gap junctions is regulated post-translationally and involves the temporally restricted mobilization of connexins into the plasma membrane immediately prior to or during compaction.** In the present chapter, treatment of uncompacted 8-cell embryos with BFA or monensin immediately prior to gap junction assembly, inhibited both the acquisition of cell coupling, and the formation of gap junction plaque-like structures. In morulae, both of these agents altered the distribution of nascent Cx43 and affected the existence/morphology of Golgi complexes (sections 3.32, 3.33). Thus, the *de novo* assembly of gap junctions is likely dependent upon trafficking of connexins to the plasma membrane through the Golgi, immediately prior to or during compaction. Since both BFA and monensin are general protein trafficking inhibitors, it is also possible that other important auxiliary factors necessary for gap junction assembly are also recruited at this time. *De novo* assembly of functional gap junctions can also be inhibited by delaying the second round of DNA replication (in the 2-cell stage) for 10 hrs with aphidicolin (Valdimarsson and Kidder, manuscript in preparation). This treatment was originally found by Smith and Johnson (1985) to result in embryos which completely failed to compact. These results suggest that interfering with the timing of DNA synthesis can interfere with the normal trafficking of connexins two cell cycles later, and argues that this trafficking is a temporally regulated event. Although the effect of aphidicolin

together with the effects of BFA and monensin argue strongly that the control of connexin trafficking is a significant event in the regulation of *de novo* gap junction assembly during preimplantation development, these results do not preclude the existence of other regulatory sites. In cultured somatic cells for example, the regulated step in gap junction assembly appears to be the formation of plaques after nascent connexin has arrived at the plasma membrane (Musil and Goodenough, 1991).

The overlapping effects of BFA and monensin on the cisternae of the Golgi argue strongly that this organelle plays a role in the trafficking of nascent connexins. The fact that these agents were not 100% effective in preventing all coupling suggests either that the treatment conditions used were "leaky", or that trafficking of connexins via the Golgi can be bypassed. One explanation consistent with the latter would be if the putative recycling of Cx43 in endosomes to the cell surface were independent of the Golgi or its associated elements. In fact, recycling of endosomes to the surface can occur directly or via the TGN (Gruenberg and Howell, 1989). Interestingly, compared with monensin twice as many of the coupled embryos treated with BFA exhibited a rapid rate of dye transfer similar to controls. In BFA treated embryos, direct recycling of putative Cx43 in endosomes could have been supplemented by recycling via the TGN, whose sorting function would have been unhindered by BFA even if its cellular distribution had been altered (Wood *et al.*, 1991). This would not have been the case in embryos treated with monensin which, based on the reported effects of this inhibitor (Mollenhauer *et al.*, 1990), would have impaired TGN function.

It also remains possible that some of the intercellular communication acquired despite treatment with monensin or BFA, resulted from the recruitment of cryptic connexins already at the embryo surface prior to the initition of inhibitor treatment. In such a case the unmasking of these connexins into a utilizable form might depend upon the recruitment of a regulatory factor lying distal to, or independent of, the sites of action for these inhibitors. However, the results presented in my study argue that the *de novo* assembly of gap junctions at compaction could not be achieved by this mechanism alone. This is substantiated by the fact that interembryonic gap junctional communication requires protein synthesis (McLachlin *et al.*, 1983).

4.42 Post-translational modification of connexin43's C-terminal region in relation to its distribution.

As discussed previously (chapter 2), the Cx43 antibodies used in the present study and by others (Nishi *et al.*, 1991) provided both unique and overlapping staining patterns in preimplantation embryos which underwent both temporal and organelle specific changes. Since all antibodies were directed against epitopes within C-terminal specific sequences, it follows that these changes were accompanied by post-translational modifications in the C-terminal domain of Cx43.

Prior to compaction, Cx43 was visualized in endosome-like structures with only two antibodies, anti-Cx43/252 and anti-Cx43/360, which recognized epitopes within the peptide regions spanning a.a. 252-271 and 360-382 of Cx43, respectively.

Similar structures were not observed by Nishi *et al.* (1991) with their antibody against the Cx43 sequence spanning a.a. 370-382. With signs of cell flattening at compaction, the epitopes recognized by the above three antibodies, as well as anti-Cx43/302, directed against epitope(s) within a.a. 302-319 of Cx43, were all detectable in the cytoplasm and in gap junction-like structures in apposed membranes. However, only the anti-Cx43/252 and anti-Cx43/302 epitopes were detectable in apposed membrane regions outside of gap junctions in the outward facing cells of morulae and trophectoderm of blastocysts. In morulae, detection of anti-Cx43/302 epitope(s) was correlated with the appearance of nascent Cx43 protein in the Golgi since this detection was sensitive to cycloheximide and could be morphologically altered by treatment with monensin or BFA (chapter 3).

Despite inhibiting the delivery of Cx43 to the plasma membrane in compacting embryos, neither BFA or monensin interfered with the temporal maturation of Cx43 so that the anti-Cx43/302 epitope(s) became visible. The distribution of Cx43 visualized by the detection of these epitope(s) was similar to that previously seen in morulae treated with each inhibitor, suggesting that Cx43 was redistributed to similar structures (Compare Fig. 4.4 with Fig. 3.2). Inhibition of functional gap junction assembly with aphidicolin also does not inhibit the temporal maturation of the anti-Cx43/302 epitope(s) which become abundantly detectable in the cytoplasm of treated embryos (Valdimarsson and Kidder, manuscript in preparation). Thus, the maturation step that renders the anti-Cx43/302 epitope(s) visible must occur prior to plasma membrane insertion, presumably in the Golgi.

Recognition of Cx43 epitopes, maturation of Cx43 in trafficking organelles, and/or the assembly of Cx43 into gap junctions may depend on changes in phosphorylation. Western blotting of lysates of late 4-cell embryos and morulae with the anti-Cx43/302 antibody, reveals that Cx43 is phosphorylated sometime in the period leading to or following *de novo* gap junction assembly (Valdimarsson, 1993). In cardiomyocytes, entrance and trapping of Cx43 in the Golgi complex with monensin, is biochemically correlated with 40 and 41 kD forms of Cx43, the latter representing a phosphorylated form of the protein. Further phosphorylation of Cx43, to 42 and 44 kD forms, is believed to occur distal to the site of monensin blockage (Puranam *et al.*, 1993; Laird *et al.*, 1993). In contrast, Musil and Goodenough (1991) reported in NRK cells that phosphorylation of Cx43 to forms similar to that found in cardiomyocytes, is not necessary for the protein to translocate to the plasma membrane.

Chapter 5

Conclusions and future directions

In summary, the results of the present study support the following conclusions:

(1) Cx43 is one member of the connexin gene family which contributes to gap junctions in the preimplantation mouse embryo.

(2) Although the evidence makes it unlikely that Cx32 contributes to gap junctions in the early embryo, the contribution of other members of the connexin gene family cannot be ruled out.

(3) Cx43 contributes to gap junctions in the ovarian follicle between cumulus cells and between these cells and the oocyte.

(4) Prior to *de novo* assembly of gap junctions in the 8-cell stage, it is unlikely that Cx43 is present in the plasma membranes of embryonic blastomeres.

(5) Cx43 mRNA is in polyribosomes at least as early as the 4-cell stage. Thus, the onset of Cx43 translation is unlikely to play a role in regulating the timing of gap junction assembly.

(6) The *de novo* assembly of gap junctions is dependent upon mobilization of nascent Cx43 and possibly other connexins to the plasma membrane, immediately prior to or during compaction.

(7) Cx43 in embryonic gap junctions may consist of both embryonically expressed, nascent protein translocated to the plasma membrane via the Golgi complex, and oogenetically stored protein residing in endosomes and delivered to the membrane independently of the Golgi and its associated structures.

(8) The distribution of Cx43 within cytoplasmic organelles, and in and out of gap junctions in the plasma membrane, may be accompanied by post-translational modifications of its C-terminal domain.

(9) Once established, the reported cell cycle associated down-regulation of gap junctional communication (Goodall and Maro, 1986), must be achieved by gating of existing channels rather than plaque disassembly.

These conclusions further our understanding of how and when intercellular communication may be modulated through the control of gap junction formation. However, several questions still remain which will need to be addressed in future experiments.

One set of experiments is related to the regulation of gap junction assembly at compaction. First, it remains to be determined if other members of the connexin gene family contribute subunits for embryonic gap junctions, and if their distribution is regulated in a manner similar to Cx43. These experiments await the availability of immunochemical probes for the connexins whose mRNAs have been detected during preimplantation development, namely Cx30.3, 31, 31.1, 40, and 45. However, previous studies demonstrating the inability of precompaction embryos to support interembryonic dye coupling, suggest that these other connexins are also absent from the plasma membrane prior to compaction (McLachlin *et al.*, 1983; Kidder *et al.*, 1987).

Secondly, it remains necessary to confirm the identity of the cytoplasmic organelles involved in connexin trafficking, and the timing of their involvement. Double immunocytochemistry could be used to co-localize connexins with organelle specific antigens, and initially at least, these experiments could be done at an immunofluorescent level. Immunochemical probes for clathrin (in coated vesicles), and antigens associated with the endoplasmic reticulum, Golgi, and lysosomes have been used previously in the preimplantation mouse embryo (Maro *et al.*, 1985). FITC or rhodamine conjugated to dextran could also be used as an immunofluorescent marker for fluid-phase endocytosis (Fleming *et al.*, 1993). Incubation of ovulated oocytes with this marker might confirm the existence of Cx43 in endosomes in precompaction embryos. The ability of trafficking inhibitors to alter the immunofluorescent distribution of organelle-specific antigens would also help to

identify the targets of these drugs in the embryo, and their effects on connexin trafficking. Multiple targets of action for each drug would be suggested by their ability to redistribute more than one organelle-specific antigen. Providing the redistribution of these antigens could be matched with that seen for Cx43, the need for immunocytochemical localization at the level of the electron microscope could be obviated.

Thirdly, although the present study identifies the events (connexin trafficking and maturation) which appear to be regulated during *de novo* gap junction assembly, it remains unclear how the timing of these events is controlled. Since a 10 hour delay in DNA replication at the 2-cell stage interferes with the ability of embryos to later compact as well as form gap junctions (Smith and Johnson, 1985; Valdimarsson and Kidder, manuscript in preparation), it is likely that this timing is established early in development, and involves a cascade of regulatory events.

Like transcriptional activation in the 2-cell stage, the *de novo* assembly of gap junctions may be regulated post-translationally by phosphorylation (Poueymirou and Schultz, 1989; Manejwala *et al.*, 1991). By Western blot analysis, phosphatase-sensitive Cx43 specific bands could be detected in morulae but not 4-cell embryos (Valdimarsson, 1993). However, given the large time interval between these stages, it is unclear from these data when Cx43 is phosphorylated (*i.e.* once it reaches the Golgi, enters the plasma membrane, is assembled into gap junctions, or all three). To determine if the phosphorylation resulting in this mobility shift in Cx43 is dependent

on passage through the Golgi or insertion into the plasma membrane. Western blot analysis for Cx43 could be performed on compacting embryos treated with trafficking inhibitors (see Puranam *et al.*, 1993). The nature and general location of phosphorylated Cx43 amino acid residues could hypothetically also be mapped by phosphoamino acid analysis in conjunction with tryptic digestion of the protein (Crow *et al.*, 1990; Milks *et al.*, 1988). However, these latter experiments would be complicated by the limited amount of biological material available in embryos.

Protein kinase C (PKC) may play a role in the observed phosphorylation of Cx43 in morulae, as well as possibly in the control of *de novo* gap junction assembly. In cultured bovine lens cells, activation of PKC with 12-*O*-tetradecanoylphorbol 13 acetate (TPA), results in inhibition of dye coupling and increased phosphorylation of Cx43 (Reynhout *et al.*, 1992). Compacted embryos treated with another activator of PKC, the diacylglycerol analog diC_8, also exhibit reduced dye coupling, although the effects of this treatment on the relative mobility of Cx43 on a gel, or its distribution in cells, has not been examined (Valdimarsson and Kidder, manuscript in preparation).

As discussed previously in chapter 2, activation of PKC in the 4-cell stage prematurely induces compaction but not intercellular communication (Winkel *et al.* 1990; Valdimarsson and Kidder, manuscript in preparation). However, if a cascade of regulatory events controls the initiation of gap junction assembly in the 8 cell stage, then one explanation for the inability of PKC to prematurely induce coupling in the 4-cell stage is that the substrate upon which it acts is absent or inaccessible at this

time. If that substrate were Cx43, and if its interaction with Cx43 specifically involved phosphorylation of serine and/or threonine residues in the C-terminal domain of this protein, then the effectiveness of PKC as an inducer of intercellular communication might be dependent upon the temporal maturation of this region of Cx43, observed in the present study. Given that aphidicolin treatment in the 2-cell stage does not interfere with the temporal maturation of the C-terminal tail of Cx43 (discussed in section 4.42), it would be interesting to test if gap junctional communication (as well as compaction) in aphidicolin-treated embryos could be rescued by treating them with activators of PKC by the time age-matched controls had reached the 8-cell stage.

Lastly, the detection of Cx43 in plaque-like structures at mitotic boundaries raises interesting questions concerning how and why intercellular communication is modulated at mitosis. It is unclear what phenotype would result by interference in this process. If cells normally uncouple from their neighbours in order to prevent transmission of mitosis inducing signals, then interfering with this process would presumably be reflected by an increase in the mitotic synchronicity of cells in the embryo. Conversely, if cells uncouple to be free from mitosis-suppressing signals, interference with this process would ultimately lead to arrest at interphase of affected cells.

According to the model proposed in chapter 2.43, mitotic regulation of coupling might involve cell cycle controlled activation of the *src*-oncogene product,

which would then down-regulate channel activity through phosphorylation of a specific Cx43 tyrosine residue. If the *src*-oncogene product is involved in this putative signal transduction pathway, then there are likely functional overlaps with other tyrosine kinases which can compensate for its absence. Targeted disruption of the *src*-oncogene does not interfere with cell viability in mice, although within weeks after birth, mice that are homozygous for the disrupted gene show a deficiency in osteoclast formation, leading to osteopetrosis (Soriano *et al.*, 1991).

Given that other tyrosine kinases could be involved in regulating channel activity, a more appropriate starting point for these experiments would be Cx43 itself. As described by Swenson *et al.* (1990), site-directed mutagenesis could be used to create point mutations in specific tyrosine residues in Cx43, suspected to be involved in the regulation of channel activity. The same technique could also be used to create deletion mutations to assess the importance of specific protein domains. To assess the impact of mutations, *in vitro* transcribed mRNAs encoding mutated forms of Cx43 would be injected into embryos. Hypothetically, coupling via endogenous connexins might then be disrupted by either direct competition with mutant connexins for translation, or by the formation of hybrid channels.

In summary, the results of the present study support the conclusion that *de novo* assembly of gap junctions in the preimplantation mouse embryo is dependent upon the temporally regulated mobilization of at least one (Cx43), and possibly other connexins to the plasma membrane, immediately prior to or during compaction. This

mobilization is accompanied by the temporal maturation of Cx43 within cytoplasmic organelles. In the future, it will be necessary to identify the mechanisms involved in regulating the timing and execution of these events.

References

Allen, F., Tickle, C., Warner, A. (1990) The role of gap junctions in patterning of the chick limb bud. *Development* **108**, 623-634.

Anderson, E., and Albertini, D. (1976) Gap junctions between the oocyte and companion follicle cells in the mammalian ovary. *J. Cell Biol.* **71**, 680 89.

Atkinson, M.M., Menko, A.S., Johnson, R.G., Sheppard, J.R., Sheridan, J.D (1981) Rapid and reversible reduction of junctional permeability in cells infected with a temperature sensitive mutant of avian sarcoma virus. *J. Cell Biol.* **91**, 573-578.

Azarnia, R., Reddy, S. Kmiecik, T.E., Shalloway, D., Loewenstein, W.R. (1988) The cellular *src*-gene product regulates junctional cell to cell communication. *Science* **239**, 398-401.

Barron, D.J., Valdimarsson, G., Paul, D.L., Kidder, G.M. (1989) Connexin32, a gap junction protein, is a persistent oogenetic product through preimplantation development of the mouse. *Dev. Genet.* **10**, 318-323.

Becker, D.L., LeClerc, D.C., Warner, A. (1992) The relationship of gap junctions and compaction in the preimplantation mouse embryo. *Development* **Supplement**, 113-118.

Bennett, M.V.L., Barrio, L.C., Bargiello, T.A., Spray D.C., Hertzberg, E.C. Saez, J.C. (1991) Gap junctions: New tools, new answers, new questions. *Neuron* **6**, 305-320.

Bevilacqua A., Loch-Caruso, R., Erickson, R.P. (1989) Abnormal development and dye coupling produced by antisense RNA to gap junction protein in mouse preimplantation embryos. *P.N.A.S. (USA)* **86**, 5444-5448.

Beyer, E.C. (1990) Molecular cloning and developmental expression of two chick embryo gap junction proteins. *J. Biol. Chem.* **265**, 14439-14443.

Beyer, E.C., Paul, D.L., Goodenough, D.A. (1987) Connexin43: A protein from rat heart homologous to a gap junction protein from liver. *J. Cell Biol.* **105**, 2621-2629.

Beyer, E.C., Kistler, J., Paul, D.L., Goodenough, D.L. (1989) Antisera directed against connexin43 peptides react with a 43-kD protein localized to gap junctions in myocardium and other tissues. *J. Cell Biol.* **108**, 595 605

Mollenhauer, H.H., Morre, D.J., Rowe, L.D. (1990) Alteration of intracellular traffic by monensin; mechanism, specificity and relationship to toxicity. *Biochim. et Biophys. Acta.* **1031**, 225-246.

Morgan, D.O., Kaplan, J.M., Bishop, J.M., Varmus, H.E. (1989) Mitosis-specific phosphorylation of $p60^{c\text{-}src}$ by $p34^{cdc2}$-associated protein kinase. *Cell* **57**, 775-786.

Morre, D.J., Boss, W.F., Grimes H., Mollenhauer, H.H. (1983) Kinetics of Golgi apparatus membrane flux following monensin treatment of embryogenic carrot cells. *Eur. J. Cell Biol.* **30**, 25-32

Morre, D.J., Mollenhauer, H.H., Spring, H., Trendelenburg, M., Montag, M., Mollenhauer, B.A., Morre, D.M. (1992) Swelling of Golgi apparatus of bovine mammary epithelial cells in response to monensin treatment requires fixation. *Eur. J. Cell Biol.* **57**, 321-324.

Murray, A.W., and Gainer, H.St.C. (1989) Regulation of gap junctional communication by protein kinases. In *Cell interactions and gap junctions, Vol. I*, (Sperelakis N. and Cole W.C. eds.), Boca Raton, Florida, p.p. 97-106.

Musil, L.S., Cunningham, B.A., Edelman, G.A., Goodenough, D.A. (1990) Differential phosphorylation of the gap junction protein connexin43 in junctional communication-competent and -deficient cell lines. *J. Cell Biol.* **111**, 2077-2088.

Musil, L.S. and Goodenough, D.A. (1991) Biochemical analysis of connexin43 intracellular transport, phosphorylation, and assembly into gap-junctional plaques. *J. Cell Biol.* **115**, 1357-1374.

Naus, C.C.G., Elisevich, K., Zhu, D., Belliveau, D.J., Del Maestro, R.F. (1992) In vivo growth of C6 glioma cells transfected with connexin43 cDNA. *Cancer Res.* **52**, 4208-4213.

Naus, C.C.G., Hearn, S., Zhu, D., Nicholson, B.J., Shivers, R.R. (1993) Ultrastructural analysis of gap junctions in C6 Glioma cells transfected with connexin43 cDNA. *Exp. Cell Res.* **206**, 72-84.

Naus, C.C.G., Zhu, D., Todd, S.D.L., Kidder, G.M. (1992) Characteristics of C6 glioma cells overexpressing a gap junction protein. *Cell. Mol. Neurobiol.* **12**, 163-175.

Nicholson, B., Dermietzel, R., Teplow, D., Traub, O., Willecke, K., Revel, J.-P. (1987) Two homologous protein components of hepatic gap junctions. *Nature* **329**, 732-734.

Cleveland, D.W., Lopata, M.A., Macdonald, R.J., Cowan, N.J., Rutter, W.J., Kirschner, M.W. (1980) Number and evoluionary conservation of α- and ß tubulin and cytoplasmic ß- and γ-actin genes using specific cloned cDNA probes. *Cell* **20**, 95-105.

Crow, D.S., Beyer, E.C., Paul, D.L., Kobe, S.S., Lau, A.F. (1990) Phosphorylation of connexin43 gap junction protein in uninfected and Rous Sarcoma virus transformed mammalian fibroblasts. *Mol. Cell. Biol.* **10**, 1754-1763.

Darnell, J., Lodish, H., Baltimore, D. (1990) Molecular cell biology 2nd ed., W.H. Freeman and Company, New York.

De Sousa, P.A., Valdimarsson, G., Nicholson, B., Kidder, G.M. (1993) Connexin trafficking and the control of gap junction assembly in mouse preimplantation embryos. *Development* **117**, 1355-1367.

Donaldson, J.G., Lippincott-Schwartz, J., Bloom, G.S., Kreis, T.E., Klausner, R.D (1990) Dissociation of a 110-kD peripheral membrane protein from the Golgi apparatus is an early event in brefeldin A action. *J. Cell Biol.* **111**, 2295-2306.

Ducibella, T.M., and Anderson, E. (1975) Cell shape and membrane changes in the eight-cell mouse embryo: prerequisite for morphogenesis of the blastocyst. *Dev. Biol.* **47**, 45-58.

Ducibella, T., Albertini, D.F., Anderson, E., Biggers J.D. (1975) The preimplantation mammalian embryo: Characterization of intercellular junctions and their appearance during development. *Dev. Biol.* **45**, 231-250.

Duden, R., Allan, V., Kreis, T. (1991) Involvement of ß-COP in membrane traffic through the Golgi complex. *Trends Cell Biol.* **1**, 14-19.

Dvorak, M., Cech, S., Stastna, J., Tesarik, J., Travnik, P. (1985) The differentiation of preimplantation mouse embryos. Department of Histology and Embryology, Medical faculty, J.E. Purkyne University, Brunensis, Hungary.

Ebihara, L., Beyer, E.C., Swenson, K.I., Paul, D.L., Goodenough, D.A. (1989) Cloning and expression of a *Xenopus* embryonic gap junction protein. *Science* **243**, 1194-1195.

Eghbali, B., Kessler, J.A., Spray, D.C. (1990) Expression of gap junction channels in communication incompetent cells after stable transfection with cDNA encoding connexin32. *P.N.A.S. (USA)* **87**, 1328-1331.

Evans, W.H., Carlile, G., Rahman, S., Torok, K. (1992) Gap junction communication channel: peptides and anti peptide antibodies as structural probes. *Biochem. Soc. Trans.* **20** (4), 856-861.

Feinberg, A.P. and Vogelstein, B. (1983) A technique for radiolabeling DNA restriction endonuclease fragments to high specific activity. *Anal Biochem* **132**, 6-13.

Fishman, G.I. (1992) Connexins and the heart. *Trends Cardiovasc. Med.* **2**, 50-55.

Flagg-Newton, J.L., Dahl, G., Loewenstein, W.R. (1981) Cell junction and cyclic AMP: I. Up regulation of junctional membrane permeability and junctional membrane particles by administration of cyclic nucleotide or phosphodiesterase inhibitors. *J. Memb. Biol.* **63**, 105-121.

Fleming, T.P., Garrod D.R., Elsmore A.J. (1991) Desmosome biogenesis in the mouse preimplantation embryo. *Development* **112**, 527-539.

Fleming, T.P., Hay, M., Javed, Q., Citi, S. (1993) Localisation of tight junction protein cingulin is temporally and spatially regulated during early mouse development. *Development* **117**, 1135-1144.

Fleming, T.P., McConnell, J., Johnson M.H., Stevenson, B.R. (1989) Development of tight junctions de novo in the mouse early embryo: control of assembly of the tight junction-specific protein, ZO-1. *J. Cell Biol.* **108**, 1407-1418.

Fleming, T.P., and Pickering, S.J. (1985) Maturation and polarization of the endocytotic system in outside blastomeres during mouse preimplantation. *J. Embryol. exp. Morph.* **89**, 175-208.

Fraser, S.E., Green, C.R., Bode, H.R., Gilula, N.B. (1987) Selective disruption of gap junctional communication interferes with a patterning process in Hydra. *Science* **237**, 49-55.

Furshpan, E.S., and Potter, D.D. (1959) Transmission at the giant motor synapses of the crayfish *J. Physiol.* **145**, 289-325.

Garfield, R.E., Sims, S., Hannan, M.S., Daniel, E.E. (1977) Gap junctions: their presence and necessity in myometrium during parturition. *Science* **198**, 958-961.

Gilula, N.B., Reeves, O.R., Steinbach, A. (1972) Metabolic coupling, ionic coupling, and cell contacts. *Nature* **235**, 262-265.

Zimlich, R.L., Kumar, N.M., Gilula, N.B. (1988) Sequence and developmental expression of mRNA coding for a gap junction protein in *Xenopus*. *J. Cell Biol.* **107**, 1065-1073.

Goodall, H. (1986) Manipulation of gap junctional communication during compaction of the early mouse embryo. *J. Embryol. exp. Morph.* **91**, 283-296.

Goodall, H. and Johnson, M.H. (1982) Use of carboxyfluorescein diacetate to study formation of permeable channels between mouse blastomeres. *Nature* **295**, 524-526.

Goodall, H., and Maro, B. (1986) Major loss of junctional coupling during mitosis in early mouse embryos. *J. Cell Biol.* **102**, 568-575.

Goodenough, D.A., Paul, D.L., Jesaitis, L. (1988) Topological distribution of two Cx32 antigenic sites in intact and split rodent hepatocyte gap junctions. *J. Cell Biol.* **107**, 1817-1824.

Goodenough, D.A., and Revel, J.-P. (1970) A fine structural analysis of intercellular junctions in the mouse liver. *J. Cell Biol.* **45**, 272-290.

Gruenberg, J., and Howell, K. (1989) Membrane traffic in endocytosis: insights from cell-free assays. *Annu. Rev. Cell Biol.* **5**, 453-481.

Haefliger, J-A., Bruzzone, R., Jenkins, N.A., Gilbert, D.A., Copeland, N.G., Paul, D.L. (1992) Four novel members of the connexin family of gap junction proteins. *J. Biol. Chem.* **267**, 2057-2064.

Helenius, A., Mellman, I., Wall, D., Hubbard, A. (1983) Endosomes. *Trends Biochem. Sci.* **8**, 245-250.

Hendrix, E.M., Mao, S.J.T., Everson, W., Larsen, W.J. (1992) Myometrial connexin43 trafficking and gap junction assembly at term and in preterm labor. *Mol. Reprod. Dev.* **33**, 27-38.

Hennemann, H., Schwarz, H.-J., Willecke, K. (1992a) Characterization of gap junction genes expressed in F9 embryonic carcinoma cells: molecular cloning of mouse connexin31 and -45 cDNAs. *Eur. J. Cell Biol.* **57**, 51-58.

Hennemann, H., Suchyna, T., Lichtenberg-Frate, H., Jungbluth S., Dahl, E., Schwarz, J., Nicholson, J., Willecke, K. (1992b) Molecular cloning and functional expression of mouse connexin40, a second gap junction gene preferentially expressed in lung. *J. Cell Biol.* **117**, 1299-1310.

Hoh, J.H., John, S.A., Revel, J.-P. (1991) Molecular cloning and characterization of a new member of the gap junction gene family, connexin 31. *J. Biol. Chem.* **266**, 6524-6531.

Howlett, S.K. (1986) The effect of inhibiting DNA replication in the one cell mouse embryo. *Roux's Arch. Dev. Biol.* **195**, 499-505.

Hunziker W., Whitney, J.A., Mellman, I. (1991) Selective inhibition of transcytosis by brefeldin A in MDCK cells. *Cell* **67**, 617-627.

Johnson, M.H., and Maro, B. (1986) Time and space in the mouse early embryo: a cell biological approach to cell diversification. In *Experimental approaches to mammalian embryonic development*. (Rossant J. and Pedersen R.A., eds.) New York, Cambridge University Press, p.p. 35-65.

Johnson, R., Meyer, R., Lampe, P. (1989) Gap junction formation: A "self-assembly" model involving membrane domains of lipid and protein. In *Cell interactions and Gap junctions, Vol. I*, (Sperelakis N. and Cole W.C., eds.), Boca Raton, Florida, p.p. 159-179.

Johnson, R., and Sheridan, J.D. (1971) Junctions between cancer cells in culture, Ultrastructure and permeability. *Science* **174**, 717-719

Kalimi, G.H., and Lo, C.W. (1988) Communication compartments in the gastrulating mouse embryo. *J. Cell Biol.* **107**, 241-255.

Kalimi, G.H., and Lo, C.W. (1989) Gap junctional communication in the extraembryonic tissues of the gastrulating mouse embryo. *J. Cell Biol.* **109**,, 3015-3026.

Kelly, R.B. (1990) Microtubules, membrane traffic, and cell organization. *Cell* **61**, 5-7.

Kidder, G.M. (1992) The genetic program for preimplantation development. *Dev. Genetics* **13**, 319-325.

Kidder, G.M. (1993) Genes involved in cleavage, compaction, and blastocyst formation. In *Genes in mammalian reproduction*. Wiley-Liss, Inc., p.p. 45-71.

Kidder, G.M., Barron, D.J., Olmsted, J.M. (1988) Contribution of midbody channels to embryogenesis in the mouse. *Roux's Arch. Dev. Biol.* **197**, 110-114.

Kidder, G.M. and Conlon, R.A. (1985) Utilization of cytoplasmic poly(A)$^+$RNA for protein synthesis in preimplantation mouse embryos. *J. Embryol. Exp. Morph.* **89**, 223-234.

Kidder, G.M., and McLachlin, J.R. (1985) Timing of transcription and protein synthesis underlying morphogenesis in preimplantation mouse embryos. *Dev. Biol.* **112**, 265 275.

Kidder, G.M., Rains, J. McKeon, J. (1987) Gap junction assembly in the preimplantation mouse conceptus is independent of microtubules, microfilaments, cell flattening, and cytokinesis. *P.N.A.S. (USA)* **84**, 3718 3722.

Klausner, R.D., Donaldson, J.G., Lippincott-Schwartz, J. (1992) Brefeldin A: Insights into the control of membrane traffic and organelle structure. *J. Cell Biol.* **116**, 1071-1080.

Kohen, E., Kohen, C., Thorell, B., Mintz, D.H., Rabinovitch, A. (1979) Intercellular communication in pancreatic islet monolayer cultures: a microfluorometric study. *Science* **204**, 862-865.

Laird, D.W., Puranam, L., Revel, J.-P. (1991) Turnover and phosphorylation dynamics of connexin43 gap junction protein in cultured cardiac myocytes. *Biochem. J.* **273**, 67-72.

Laird, D.W., Puranam, K.L., Revel, J.-P. (1993) Identification of intermediate forms of connexin43 in rat cardiac myocytes. (*in press*).

Laird, D.W., Yancey, S.B., Bugga, L., Revel, J.P. (1992) Connexin expression and gap junction communication compartments in the developing mouse limb. *Dev. Dynamics* **195**, 153-161.

Lal, R., Laird, D.W., Revel, J.-P (1993) Antibody perturbation analysis of gap junction permeability in rat cardiac myocytes. *Pflugers Archiv.* (in press).

Larsen, W.J., Tung, H.N., Polking, C. (1981) Response of granulosa cell gap junctions to human chorionic gonadotropin (hCG) at ovulation. *Biol. of Reprod.* **25**, 1119-1134.

Larsen,W.J., and Wert, S.E. (1988) Roles of cell junctions in gametogenesis and in early embryonic development. *Tissue & Cell* **20** (6), 809 848.

Larsen, W.J., Wert, S.E., Brunner, G.D. (1987) Differential modulation of rat follicle cell gap junction populations at ovulation. *Dev. Biol.* **122**, 61 71.

Latham, K.E., Garrels, J.I., Chang, C., Solter, D. (1991) Quantitative analysis of protein synthesis in mouse embryos. I. Extensive reprogramming at the one and two-cell stages. *Development* **112**, 921 932.

Latham, K.E., Solter, D., Schultz, R.M. (1992) Acquisition of a transcriptionally permissive state during the 1-cell stage of mouse embryogenesis. *Dev. Biol.* **149**, 457-462.

Lau, A.F., Kanemitsu, M.Y., Kuvata, W.E., Danesh, S., Boynton, A.L. (1992) Epidermal growth factor disrupts gap junctional communication and induces phosphorylation of Cx43 on serine. *Mol. Biol. of the Cell* **3**, 865-874.

Lawrence, T.S., Beers, W.H., Gilula N.B. (1978) Transmission of hormonal stimulation by cell to cell communication. *Nature* **272**, 501-506.

Lee, S., Gilula, N.B. and Warner, A.E. (1987). Gap junctional communication and compaction during preimplantation stages of mouse development. *Cell* **51**, 851-860.

Levine, E., Werner, R., Neuhaus, I., Dahl, G. (1993) Asymmetry of gap junction formation along the animal-vegetal axis of *Xenopus* oocytes. *Dev. Biol.* **156**, 490-499.

Lippincott-Schwartz, J. (1993) Bidirectional membrane traffic between the endoplasmic reticulum and Golgi apparatus. *Trends Cell Biol.* **3**, 81-88.

Lippincott-Schwartz, J., Donaldson, J.G., Schweizer, A., Berger, E.G., Hauri, H.-P., Yuan, L.C., Klausner, R.D. (1990) Microtubule-dependent retrograde transport of proteins into the ER in the presence of brefeldin A suggests an ER recycling pathway. *Cell* **60**, 821-836.

Lippincott-Schwartz, J., Yuan, L.C., Bonafacio, J.S., Klausner, R.D. (1989) Rapid redistribution of Golgi proteins into the ER in cells treated with brefeldin A: evidence for membrane cycling from Golgi to ER. *Cell* **56**, 801-813.

Lippincott-Schwartz, J., Yuan, L., Tipper, C., Amherdt, M., Orci, L., Klausner, R.D. (1991) Brefeldin A's effects on endosomes, lysosomes, and the TGN suggest a general mechanism for regulating organelle structure and membrane traffic. *Cell* **67**, 601-616.

Lo, C.W., and Gilula, N.B. (1979) Gap junctional communication in the preimplantation mouse embryo. *Cell* **18**, 399-409.

Loewenstein, W.R. (1981) Junctional intercellular communication: the cell to cell membrane channel. *Physiol. Rev.* **61**, 829-913.

Low, S.H., Tang, B.L., Wong, S.H., Hong, W. (1992) Selective inhibition of protein targeting to the apical domain of MDCK cells by brefeldin A. *J. Cell Biol.* **118**, 51-62.

Magnuson, T., Demsey, A., Stackpole, C.W. (1977) Characterization of the intercellular junctions in the preimplantation mouse embryo by freeze-fracture and thin section electron microscopy. *Dev. Biol.* **61**, 252-261.

Makowski, L., Caspar, D.L., Phillips, W.C., Goodenough, D.A. (1977) Gap junction structures. II Analysis of the x-ray diffraction data. *J. Cell Biol.* **74**, 629-645.

Manejwala, F., Logan, C.Y., Schultz, R.M. (1991) Regulation of hsp70 mRNA levels during oocyte maturation and zygotic gene activation in the mouse. *Dev. Biol.* **144**, 301-308.

Maro, B., and Pickering, S.J. (1984) Microtubules influence compaction in preimplantation mouse embryos. *J. Embryol. Exp. Morph.* **84**, 217 232

Maro, B., Johnson, M.H., Pickering, S., Louvard, D. (1985) Changes in the distribution of membranous organelles during mouse early development. *J. Embryol. exp. Morph.* **90**, 287-309.

Maxfield, F.R. (1985) Acidification of endocytotic vesicles and lysosomes. In *Endocytosis* (Paston, I. and Willingham, M.C. eds.), Plenum Press. New York, p.p. 235-257.

McLachlin, J.R., Caveney, S., Kidder, G.M. (1983) Control of gap junction formation in early mouse embryos. *Dev. Biol.* **98**, 155-164.

McLachlin, J.R. and Kidder, G.M. (1986) Intercellular junctional coupling in preimplantation mouse embryos: Effect of blocking transcription or translation. *Dev. Biol.* **117**, 146-155.

Mehta, P.P., Yamamoto, M., Rose, B. (1992) Transcription of the gene for the gap junctional protein Cx43 and expression of functional cell cell channels are regulated by cAMP. *Mol. Biol. of the Cell*, **3**, 839-850.

Melancon, P., Franzusoff, A., Howell, K.E. (1991) Vesicle budding: insights from cell-free assays. *Trends Cell Biol.* **1**, 165-171.

Merion, M., and Sly, W.S. (1983) The role of intermediate vesicles in the absorptive endocytosis and transport of ligand to lysosomes by Human fibroblasts. *J. Cell Biol.* **96**, 644-650.

Meyer, R.A., Laird, D.W., Revel, J.-P., Johnson, R.G. (1992) Inhibition of gap junction and adherens junction assembly by connexin and A CAM antibodies. *J. Cell Biol.* **119**, 179-189.

Milks, L.C., Kumar, N.M., Houghten, R., Unwin, N., Gilula, N.B. (1988) Topology of the 32 kd liver gap junction protein determined by site directed antibody localization. *EMBO J.* **7**, 2967 2975.

Mollenhauer, H.H., Morre, D.J., Rowe, L.D. (1990) Alteration of intracellular traffic by monensin; mechanism, specificity and relationship to toxicity. *Biochim. et Biophys. Acta.* **1031**, 225-246.

Morgan, D.O., Kaplan, J.M., Bishop, J.M., Varmus, H.E. (1989) Mitosis-specific phosphorylation of $p60^{c\text{-}src}$ by $p34^{cdc2}$-associated protein kinase. *Cell* **57**, 775-786.

Morre, D.J., Boss, W.F., Grimes H., Mollenhauer, H.H. (1983) Kinetics of Golgi apparatus membrane flux following monensin treatment of embryogenic carrot cells. *Eur. J. Cell Biol.* **30**, 25-32

Morre, D.J., Mollenhauer, H.H., Spring, H., Trendelenburg, M., Montag, M., Mollenhauer, B.A., Morre, D.M. (1992) Swelling of Golgi apparatus of bovine mammary epithelial cells in response to monensin treatment requires fixation. *Eur. J. Cell Biol.* **57**, 321-324.

Murray, A.W., and Gainer, H.St.C. (1989) Regulation of gap junctional communication by protein kinases. In *Cell interactions and gap junctions, Vol. I*, (Sperelakis N. and Cole W.C. eds.), Boca Raton, Florida, p.p. 97-106.

Musil, L.S., Cunningham, B.A., Edelman, G.A., Goodenough, D.A. (1990) Differential phosphorylation of the gap junction protein connexin43 in junctional communication-competent and -deficient cell lines. *J. Cell Biol.* **111**, 2077-2088.

Musil, L.S. and Goodenough, D.A. (1991) Biochemical analysis of connexin43 intracellular transport, phosphorylation, and assembly into gap-junctional plaques. *J. Cell Biol.* **115**, 1357-1374.

Naus, C.C.G., Elisevich, K., Zhu, D., Belliveau, D.J., Del Maestro, R.F. (1992) In vivo growth of C6 glioma cells transfected with connexin43 cDNA. *Cancer Res.* **52**, 4208-4213.

Naus, C.C.G., Hearn, S., Zhu, D., Nicholson, B.J., Shivers, R.R. (1993) Ultrastructural analysis of gap junctions in C6 Glioma cells transfected with connexin43 cDNA. *Exp. Cell Res.* **206**, 72-84.

Naus, C.C.G., Zhu, D., Todd, S.D.L., Kidder, G.M. (1992) Characteristics of C6 glioma cells overexpressing a gap junction protein. *Cell. Mol. Neurobiol.* **12**, 163-175.

Nicholson, B., Dermietzel, R., Teplow, D., Traub, O., Willecke, K., Revel, J.-P. (1987) Two homologous protein components of hepatic gap junctions. *Nature* **329**, 732-734.

Nishi, M., Kumar, N.M., Gilula, N.B. (1991). Developmental regulation of gap junction gene expression during mouse embryonic development. *Dev. Biol.* **146**, 117-130.

Orci, L., Tagaya, M. Amherdt, M., Perrelet, A., Donnaldson, J.G., Lippincott-Schwartz, J., Klausner, R.D., Rothman, J.E. (1991) Brefeldin A, a drug that blocks secretion, prevents the assembly of non-clathrin-coated buds on Golgi cisternae. *Cell* **64**, 1183-1195.

Paul, D.L. (1986) Molecular cloning of cDNA for rat liver gap junction protein. *J. Cell Biol.* **103**, 123-134.

Paul, D.L., Ebihara, L., Takemoto, L.J., Swenson, K.I., Goodenough, D.A. (1991) Connexin46, a novel lens gap junction protein, induces voltage-gated currents in nonjunctional plasma membrane of *Xenopus* oocytes. *J. Cell Biol.* **115**, 1077-1089.

Pelham, H.R.B. (1991) Muliple targets for brefeldin-A. *Cell* **67**, 449-451.

Pepper, M.S., and Meda, P. (1992) Basic fibroblast growth factor increases junctional communication and Cx43 expression in microvascular endothelial cells. *J. Cell Physiol.* **153**, 196-205.

Peracchia, C. (1989) Control of gap junction permeability and calmodulin-like proteins. In *Cell interactions and gap junctions, Vol. I*, (Sperelakis N. and Cole W.C., eds.), Boca Raton, FL: CRC Press, p.p. 125-142.

Petzoldt, U. (1984) Regulation of stage-specific gene expression during early mouse development: Effect of cytochalasin B and aphidocolin on stage specific protein synthesis in mouse eggs. *Cell Diffn.* **15**, 163-167.

Petzoldt, U. and Muggleton-Harris, A. (1987) The effect of the nucleocytoplasmic ratio on protein sythesis and expression of stage-specific antigen in early cleaving mouse embryos. *Development* **99**, 481-491.

Picton, C., Klee, C.B., Cohen, P. (1980) Phosphorylase kinase from rabbit skeletal muscle: identification of the calmodulin binding subunits. *Eur. J. Biochem.* **111**, 553-561.

Poucymirou, W.T., and Schultz, R.M. (1989) Regulation of the mouse preimplantion development: inhibition of synthesis of proteins in the two cell embryo that require transcription by inhibitors of cAMP-dependent protein kinase. *Dev. Biol* **133**, 588-599.

Prydz, P., Hansen, S.H., Sandvig, K., van Deurs, B. (1992) Effects of brefeldin A on endocytosis, transcytosis and transport to the Golgi complex in polarized MDCK cells. *J. Cell Biol.* **119**, 259-272.

Puranam, K.L., Laird, D.W., Revel, J.-P. (1993) Trapping an intermediate form of connexin43 in the Golgi. *Exp. Cell Biol.* **206**, 85-92.

Rahman, S., Carlile, G., Evans, H. (1993) Assembly of hepatic gap junctions. *J. Biol. Chem.* **268**, 1260-1265.

Rappolee, D.A., Wang, A., Mark, D., Werb, Z. (1989) Novel method for studying mRNA phenotypes in single or small numbers of cells. *J. Cell. Biochem.* **39**, 1-11.

Reeve, W.J.D. (1981) Cytoplasmic polarity develops at compaction in rat and mouse embryos. *J. Embryol. exp. Morph.* **62**, 351-367.

Revel, J.P., Karnovsky, M.I. (1967) Hexagonal array of subunits in intercellular junctions of the mouse heart and liver. *J. Cell Biol* **33**, C7-C12.

Reynhout, J.K., Lampe, P.D., Johnson, R.G. (1992) An activator of protein kinase C inhibits gap junction communication between cultured bovine lens cells. *Exp. Cell Res.* **198**, 337-342.

Rieske, E., Schubert, P., Kreutzberg, G.M. (1975) Transfer of radioactive material between electrically coupled neurons of the Leech central nervous system. *Brain Res.* **84**, 365-382.

Risek, B., Guthrie, S., Kumar, N.B., Gilula, N.B. (1990) Modulation of gap junction transcript and protein expression during pregnancy in the rat. *J. Cell Biol.* **110**, 269-282.

Robertson, J.D. (1963) The occurance of a subunit pattern in the unit membranes of club endings in mauthner cell synapses of the Gold fish brain. *J. Cell Biol.* **19**, 201-221.

Rossant, J. (1986) Development of extraembryonic cell lineages in the mouse embryo. In *Experimental approaches to mammalian embryonic development.* (Rossant J. and Pedersen R.A., eds.), New York, Cambridge University Press, pp. 97-120.

Rothman, J.E., and Orci, L. (1992) Molecular dissection of the secretory pathway. *Nature* **355**, 409-415.

Saez, J.C., Connor, J.A., Spray, D.C., Bennett, M.V.L. (1989) Hepatocyte gap junctions are permeable to the second messenger inositol 1,4,5-trisphosphate and to calcium ions. *PNAS (USA)* **86**, 2708-2712.

Saez, J.C., Nairn, A.C., Czernik, A.J., Spray, D.C., Hertzberg E.L., Greengard, P., Bennett, M.V.L. (1990) Phosphorylation of connexin32, a hepatocyte gap-junction protein, by cAMP-dependent protein kinase C and Ca^{2+}/calmodulin-dependent protein kinase II. *Eur. J. Biochem.* **192**, 263-273.

Sambrook, J., Fritsch, E.F., Maniatis, T. (1989) Molecular cloning: A laboratory manual. 2nd ed., Cold Spring Harbor Laboratory Press, New York.

Saunders, J.W., and Grasseling, M.T. (1968) Ectodermal-mesenchymal interactions in the origin of limb symmetry. In *Epithelial-mesenchymal interaction* (Fleischmayer R. and Billingham R.E., eds.), Williams and Wilkins, Baltimore, p.p. 78-97.

Schliwa, M., and Van Blerkom, J. (1981) Structural interaction of cytoskeletal components. *J. Cell Biol.* **90**, 222-235.

Schultz, G.A. (1986) Utilization of genetic information in the preimplantation mouse embryo. In *Experimental approaches to mammalian embryonic development.* (Rossant J. and Pedersen R.A., eds.), New York, Cambridge University Press., p.p. 239-265.

Schwarzmann, G., Weigardt, H., Rose, B., Zimmerman, A., Ben-Hairn, D., Loewenstein, W.R. (1981) Diameter of the cell-to-cell junctional channels as probed with neutral molecules. *Science* **213**, 551-553.

Sefton, M., Johnson, M.H., Clayton, L. (1992) Synthesis and phosphorylation of uvomorulin during mouse early development. *Development* **115**, 313-318.

Selden, R.F. (1989) Analysis of DNA sequences by blotting and hybridization. In *Current protocols in molecular biology*, (Ausubel F.M., Brent R., Kingston R.E., Moore D.D., Smith J.D., Seidman J.G., Struhl D., eds.), Cold Spring Harbour, Supplement 6, p.p. 2.9.1-2.9.17.

Shenoy, S., Choi, J.-K., Bagrodia, S., Copeland, T.D., Maller, J.L., Shalloway, D. (1989) Purified maturation promoting factor phosphorylates $pp60^{c\text{-}src}$ at the sites phosphorylated during fibroblast mitosis. *Cell* **57**, 761-772.

Shirayoshi, Y., Okada, T.S., Takeichi, M. (1983) The calcium dependent cell cell adhesion system regulates inner cell mass formation and cell surface polarization in early mouse development. *Cell* **35**, 631-638.

Simpson, I., Rose, B., Loewenstein, W.R. (1977) Size limit of molecules permeating the junctional membrane channels *Science* **195**, 294-296.

Smith, R.K., and Johnson, M.H. (1985) DNA replication and compaction in the cleaving embryo of the mouse. *J. Embryol. exp. Morph.* **89**, 133-148.

Soltys, B.J., Gupta, R.S. (1992) Interrelationships of endoplasmic reticulum, mitochondria, intermediate filaments, and microtubules- a quadruple fluorescence labeling study. *Biochem. and Cell Biol.* **70** (10-11), 1174-1186.

Soriano, P., Montgomery, C., Geske, R., Bradley, A. (1991) Targeted disruption of the c-*src* proto-oncogene leads to osteopetrosis in mice. *Cell* **64**, 693-702

Spindle, A.I. (1980). An improved culture medium for mouse blastocysts. *In Vitro* **16**, 669-674.

Spray, D.C., Stern, J.H., Harris, A.L., Bennett, M.V.L. (1982) Gap junctional conductance: comparison of sensitivities to H^+ and Ca^{2+} ions. *P.N.A.S. (USA)* **79**, 441-445.

Subak-Sharpe, H., Burk, R.R., Pitts, J.D. (1969) Metabolic co-operation between biochemically marked mammalian cells in tissue culture. *J. Cell Science* **4**, 353-382.

Swerson, K.I., Piwnica-Worms, H., McNamee, H., Paul, D.L. (1990) Tyrosine phosphorylation of the gap junction protein connexin43 is required for the $pp60^{v\text{-}src}$-induced inhibition of communication. *Cell Regulation* **1**, 989-1002.

Sztul, E.S., Melancon, P., Howell, K.E. (1992) Targeting and fusion of vesicular transport. *Trends Cell Biol.* **2**, 381-386.

Taylor, K.D., and Piko, L. (1987) Patterns of mRNA prevalence and expression of B1 and B2 transcripts in early mouse embryos. *Development* **101**, 877-892.

Tickle, C., Alberts, B., Wolpert, L., Lee, J. (1982) Local application of retinoic acid to the limb bud mimics the action of the polarising region. *Nature* **296**, 564-566.

Tokunaga, K., Taniguchi, H., Yoda, K., Shimizu, M., Sakiyama, S. (1986) Nucleotide sequence of a full-length cDNA for mouse cytoskeletal ß-actin mRNA. *Nucl. Acids Res.* **14**, 2829.

Traub, O., Look, J., Dermietzel, R., Brummer, F., Hulser, D., Willecke, K. (1989) Comparative characterization of the 21-kD and 26 kD gap junction proteins in murine liver and cultured hepatocytes. *J. Cell Biol.* **108**, 1039-1051.

Valdimarsson, G. (1993) Connexin gene expression and gap junction assembly. Ph.D. Thesis, University of Western Ontario, London, Ontario, Canada.

Valdimarsson, G., De Sousa, P.A., Beyer, E.C., Paul, D.L., Kidder, G.M. (1991) Zygotic expression of the connexin43 gene supplies subunits for gap junction assembly during mouse preimplantation development. *Mol. Reprod. Dev.* **30**, 18-26.

Valdimarsson, G., De Sousa, P.A., Kidder, G.M. (1993) Coexpression of gap junction proteins in the cumulus-oocyte complex. *Mol. Reprod. Dev.* **36**, 7-15.

Vestweber, D., Gossler, A., Boller, K., Kemler, R. (1987) Expression and distribution of cell adhesion molecule uvomorulin in mouse preimplantation embryos. *Dev. Biol.* **124**, 451-456.

Warner, A.E., Guthrie, S.C., Gilula, N.B. (1984) Antibodies to gap junctional protein selectively disrupt junctional communication in the early amphibian embryo. *Nature* **311**, 127-131.

Watson, A.J., Damsky, C.H., Kidder, G.M. (1990) Differentiation of an epithelium: factors affecting the polarized distribution of Na^+,K^+-ATPase during mouse embryogenesis. *Dev. Biol.* **141**, 104-114.

Watson, A.J., and Kidder, G.M. (1988) Immunofluorescence assessment of the timing of appearance and cellular distribution of Na^+, K^+ ATPase during mouse embryogenesis. *Dev. Biol.* **126**, 80-90.

Weir, M.P., and Lo, C.W. (1984) Gap junctional communication compartments in the Drosophila wing imaginal disc. *Dev. Biol.* **103**, 102-46.

White, T.W., Bruzzone, R., Goodenough, D.A., Paul, D.L. (1992) Mouse Cx50, a functional member of the connexin family of gap junction proteins, is the lens fiber protein MP70. *Mol. Biol. Cell* **3**, 711-720.

Wilcox, D.K., Kitson, R.P., Widnell, C.C. (1982) Inhibition of pinocytosis in rat embryo fibroblasts treated with monensin. *J. Cell Biol.* **92**, 859-864

Wiley, L.M., Kidder, G.M., Watson, A.J. (1990) Cell polarity and development of the first epithelium. *BioEssays* **12**, 67-73.

Willecke, K., Hennemann, H., Dahl, E., Jungbluth, S., Heynkes, R. (1991a) The diversity of connexin genes encoding gap junctional proteins. *Eur. J. Cell Biol.* **56**, 1-7.

Willecke, K., Heynkes, R., Dahl, E., Stutenkemper, R., Hennemann, H., Jungbluth, S., Suchyna T.M., Nicholson, B.J. (1991b) Mouse connexin37:cloning and functional expression of a gap junction gene highly expressed in lung. *J. Cell Biol.* **114**, 1049-1057.

Winkel, G.K., Ferguson, J.E., Takeichi, M., Nuccitelli, R. (1990) Activation of protein kinase C triggers premature compaction in the four-cell stage mouse embryo. *Devel. Biol.* **138**, 1-15.

Winterhager, E., Grummer, R., Jahn, E., Willecke, K., Traub, O. (1993) Spatial and temporal expression of connexin26 and connexin43 in rat endometrium during trophoblast invasion. *Dev. Biol.* **157**, 399-409.

Wood, S.A., and Brown, W.J. (1992) The morphology but not the function of endosomes and lysosomes is altered by brefeldin A. *J. Cell Biol.* **119**, 273-285.

Wood, S.A., Park, J.E., Brown, W.J. (1991) Brefeldin A causes a microtubule-mediated fusion of the trans-Golgi network and early endosomes. *Cell* **67**, 591-600.

Yancey, S.B., John, S.A., Lal, R., Austin, B.J., Revel., J.-P. (1989) The 43-kD polypeptide of heart gap junctions: immunolocalization, topology, and functional domains. *J. Cell Biol.* **108**, 2241-2254.

Zhang, J.T., and Nicholson, B.J. (1989) Sequence and tissue distribution of a second protein of hepatic gap junctions, Cx26, as deduced from its cDNA. *J. Cell Biol.* **109**, 3391-3401.

Zhu, D., Caveney, S., Kidder, G.M., Naus, C.C.G. (1991) Transfection of C6 glioma cells with connexin43 cDNA: analysis of expression, intercellular coupling and cell proliferation. *P.N.A.S. (USA)* **88**, 1883-1887.

Zhu, D., Kidder, G.M., Caveney, S., Naus, C.C.G. (1992) Growth retardation in glioma cells cocultured with cells overexpressing a gap junction protein. *P.N.A.S. (USA)* **89**, 10218-10221.

Zimmer, D.B., Greens, C.R., Evans, W.H., Gilula, N.B. (1987) Topological analysis of the major protein in isolated intact rat liver gap junctions and gap junction-derived single membrane structures. *J. Biol. Chem.* **262** (16), 7751-7763.